INVESTIGATION OF THE PERFORMANCE OF AN AUTOMATIC ARTERIAL OXYGEN CONTROLLER

A Dissertation Presented to

the Faculty of Graduate School

at the University of Missouri-Columbia

In Partial Fulfillment

of the Requirements for the Degree

Doctor of Philosophy

By

AKRAM AHMAD A. FAQEEH

Dr. Roger Fales, Dissertation Supervisor

Dr. Isabella Zaniletti, Dissertation Co-Supervisor

May 2018

The undersigned, appointed by the dean of the Graduate School, have examined the dissertation entitled

INVESTIGATION OF THE PERFORMANCE OF AN AUTOMATIC ARTERIAL OXYGEN CONTROLLER

Presented by Akram Ahmad Faqeeh,

A candidate for the degree of doctor of philosophy

and hereby certify that, in their opinion, it is worthy of acceptance

_____

Dr. Roger Fales, Associate Professor, Dept. of Mechanical and Aerospace Engineering

_____

Dr. Isabella Zaniletti, Assistant Professor, Dept. of Statistics

_____

Dr. Ahmed Sherif El-Gizawy, Professor, Dept. of Mechanical and Aerospace Engineering

_____

Dr. Noah Manring, Professor, Dept. of Mechanical and Aerospace Engineering

_____

Dr. Craig Kluever, Professor, Dept. of Mechanical and Aerospace Engineering

To my mother: Fatima Bersaly

To my father: Ahmad Faqeeh

To my wife: Jamilah Al-Saraj

To my sisters: Ahlam (Hayat) & Khloud & Modey & Meznah & Ibtsam & Ehssan

To my brothers: Anas & Amjad

To my sons: Ahmad & Aws & Bilal

To all the members of Faqeeh & Bersaly Family

ACKNOWLEDGMENTS

First, praise is to Almighty Allah (God) for his grace and mercy throughout my life. Also, I would like to thank my wife, my parents, my siblings, and my three sons, who always lovingly support me throughout my life.

Sincere gratitude to Dr. Roger Fales (dissertation supervisor) who always be generous with his time, advice, and guidance during my Ph.D. Studies. Throughout the years that I have worked with him, he has always been such a great supervisor with his technical expertise, research skills, flexibility, and patience. Also, I would like to thank Dr. Isabella Zaniletti (dissertation co-supervisor) for her continuous support, guidance, and encouragement. I would also like to thank Dr. Ahmad Sherif El-Gizawy (master thesis supervisor), Dr. Noah Manring, and Dr. Craig Kluever for agreeing to serve on my doctoral committee. I would like to thank Dr. John Pardalos and Dr. Ramak Amjad for their comments on the clinical part of this study. My acknowledgment goes to my research colleague Xuefeng Hou. Also, I would like to thank the University of Missouri Coulter Translational Partnership Program (MU Coulter Program) for funding the current research.

My appreciation to my friends Meshal Al-Farhood, Adel Al-Turki, and Bilal Hussain for every moment that we shared in Columbia-MO. I would like to extend my gratitude to the entire staff of the University of Missouri-Columbia. Also, I would like to thank the entire staff of my sponsor Royal Commission for Jubail & Yanbu. Thanks to my country, Saudi Arabia, for this learning opportunity in the USA. Finally, my appreciation for everyone whom I may not able to mention their names due to the limited space.

TABLE OF CONTENTS

LIST OF TABLES

LIST OF FIGURES

Investigation of the Performance of an Automatic Arterial Oxygen Controller

AKRAM AHMAD A. FAQEEH

Dr. Roger Fales

Dr. Isabella Zaniletti

ABSTRACT

Premature infants often require respiratory support with a varying concentration of the fraction of inspired oxygen (FiO_2) to keep the arterial oxygen saturation (SpO_2) within the desired range to avoid both hypoxemia and hyperoxemia. Currently, manual adjustment of FiO_2 is the common practice in neonatal intensive care units (NICUs). The automation of this adjustment is a topic of interest. The research team, at University of Missouri-Columbia (UMC), has developed a novel automatic arterial oxygen saturation controller. In this study, a systematic approach has been developed to investigate both non-clinical and clinical performance of this device.

The non-clinical investigation of the performance was performed using a neonatal respiratory model (hardware-in-the-loop test). A factorial experimental design was utilized to generate challenging model responses of SpO_2, which were addressed by the controllers. With this study, we demonstrate the stability and ability of the adaptive PI-controller to improve oxygen saturation control over manual control by increasing the proportion of time where SpO_2 of the neonatal respiratory model was within the desired range and by minimizing the variability of the SpO2. In addition, the controller ability to significantly reduce the number of hypoxemic events of the neonatal respiratory model was reported. Results of this investigation show the competence of the controller estimation system for

estimating neonatal respiratory model parameters while the adaptive PI-controller was in use. Also, the functionality of the controller with no mechanical or communication failure was validated non-clinically before heading forward to the clinical trial.

The clinical investigation of the performance was performed by conducting a clinical trial at the NICU of the MU Women's and Children's Hospital. The crossover design was used for the clinical trial to allow within-subject comparison and to eliminate interpatient variability. Two human subjects, with two different target ranges of SpO_2, were enrolled in the study. The adaptive automatic PI-controller shows clinical feasibility to improve the maintenance of SpO_2 within the intended range. With this study, we demonstrate the potential of the automatic controller to minimize the variability of SpO2. In addition, the controller shows the ability to reduce the bradycardia and the hypoxemia. Moreover, the hardware and software of the controller show an ability to transition from manual to automatic mode, and vice versa with no pronounced "bump" or step variation in the control signal, and stability and performance were not adversely affected during the transitions.

Chapter 1 : Introduction

In this chapter, the background and motivation of the current research are first introduced. The literature review is discussed in the second section of this chapter. Then, the research objectives are highlighted and followed by the dissertation outline.

1.1 Background and Motivation

Respiratory support is essential for newborn infants, particularly in those born prematurely. Premature infants commonly experience breathing disorder, which is called respiratory distress syndrome (RDS), formally known as hyaline membrane disease [1]. The tiny air-exchanging sacs of the lungs that is known as alveoli are coated by pulmonary surfactant, which reduces surface tension so that collapse is avoided and the required pressure to re-inflate it with next inspiration becomes less [1-3]. The production of pulmonary surfactant is sufficient in healthy full-term infants so that in rare cases RDS develops in full-term infants [1, 2]. On the other hand, premature infants are prone to RDS due to the inadequacy of surfactant production.

The treatment of the neonatal respiratory disease such as RDS is respiratory support, where the infant is supplied with a mixture of air and oxygen. Regardless of the mode of respiratory delivery (hood, nasal cannula or prongs, endotracheal tube, bag, or mask), the mixture should be humidified, warmed, and has an optimal concentration of fraction of inspired oxygen (FiO_2) [3]. The adjustment of the FiO_2 aims to keep arterial oxygen saturation (SpO_2) within the desired range to avoid both low oxygen saturation (hypoxemia) and high oxygen saturation (hyperoxemia), which are associated with the following risks: mortality, retinopathy of prematurity (ROP), chronic lung disease (CLD), and brain damage [4, 5].

At present, the manual adjustment of FiO_2 is the common approach to maintaining SpO_2 within the prescribed range. A pulse oximeter is used to measure SpO_2 via skin probe so that a nurse applies the appropriate adjustment of FiO_2. It is everyday routine in neonatal care; however, the efficacy of this method is questionable and varies greatly depending on nursing staff and activity in the NICU [6-10]. Reference [9] concluded that maintaining the SpO_2 within the target range manually is a difficult task, as a consequence, a considerable percentage of time spent outside the target range. a contemporary study highlighted that about half of the time spent outside the prescribed range of SpO_2 [9]. A protocol has been developed by the Vermont Oxford Neonatal Network to increase the percentage of time spent within the target range of SpO_2, the percentage increased from 20% to an average of 35% [8]. In contrast, another study shows that the implementation of the developed protocol has no significance at improving the time spent within the SpO_2 target range [10]. It is apparent that the improvement in the manual adjustment of FiO_2 is limited and associated with a high workload [11]. Thus, researchers are moving toward the automation of FiO_2 adjustment.

1.2 Literature Review

The studies towards the automation of FiO_2 were initiated in 1979 [12, 13]. Since that date, multiple studies have been published to automate the adjustment of FiO_2. The automated algorithms simply command adjustments to the FiO_2, which are actuated accordingly, based on the measured deviation of SpO_2 from a selected set point or range. Regarding this subject, some reviews have highlighted the necessity, rationale, benefits, feasibility, effectiveness, limitations, and further improvements [14-22]. These papers emphasized the need for automatic SpO_2 controller, especially, for premature infants who

experience frequent and severe fluctuations in oxygenation. Also, they show evidence of the superiority of the automatic control of FiO_2 over manual care with available clinical studies when applied to premature infants. However, these studies recommended evaluating the effectiveness and safety of using the automatic controllers by employing extensive clinical trials and considering long-term outcomes. The review [21] mainly aims to summarize and classify the used algorithms for automating FiO_2 adjustment in the neonate. In this paper, the control algorithms are classified into four major categories: rule-based (non-fuzzy and fuzzy), proportional-integral-derivative (PID), adaptive, and robust controller. This classification is used to plan the current literature review and is followed by reviewing researching efforts of the research team at University of Missouri-Columbia (UMC); also, the chronology of the studies is considered.

The rule-based controller is simple if-then loop that is developed based on expert's knowledge to control FiO_2 [21]. Collins et al. [12] had developed an apparatus to automate the regulation of the oxygen supply to premature infants based on the measured partial pressure of arterial oxygen (PaO_2). The apparatus is merely a hard-wired servo-system with using umbilical arterial oxygen catheter-tip electrode as sensor and simple rule-based as control algorithm. After setting the target range for PaO_2, the servo-controller adjusted FiO_2 by a single step of 5% increment or decrement at one-minute sampling interval when PaO_2 is out of the predefined limits. Beddis et al. [13] experimentally show that the apparatus successfully minimized the time where the PaO_2 spent outside the prescribed range of twelve preterm infants, receiving supplemental oxygen via head-box, continuous positive airway pressure (CPAP), or intermittent positive pressure ventilation (IPPV), by

more than 15%. However, the paper highlighted the observation that the PaO_2 was above the prescribed target range more frequent while using servo-control than manual-control.

After the general clinical acceptance of the pulse oximeter which is able to monitor oxygenation noninvasively by determining SpO_2 instead of PaO_2 [23, 24], researchers started to considered pulse oximeter as a feedback sensor to FiO_2 auto-control systems. Morozoff et al. [25] developed a state machine controller which is considered as rule-based in 1993. In this study, a pulse oximeter is used as a sensor to measure SpO_2 to be fed into the state machine controller which adjusts FiO_2. The authors used the sign of the magnitude, velocity, and acceleration as inputs into a state machine. Accordingly, the trend of the error can be determined to define the next state of the state machine where each state has an independent adjustment of FiO_2 and delay, and the state machine was updated one time every second. The developed controller was clinically tested on eight patients that were intubated and required assisted ventilation. The study concluded that the automatic controller positively increased the proportion of time when SpO_2 within the target range.

The high volumes of data with high error-rate that is a visible problem in neonatal intensive care units (NICUs) [26]. This problem is produced by the online monitoring such as a high volume of inaccurate SpO_2 values, which might be generated by pulse oximeter because of the small movements of the patient. It directs Miksch et al. [26] to present a time-oriented data-abstraction method which can derive qualitative description, spreads and deducting intervals, from oscillating high-frequency data such as SpO_2 values. The basic three steps of this method are eliminating data errors, clarifying the curve, and qualifying the curve. By applying such a method, better visualization of patients' condition is possible, which lead to a more accurate suggestion to be applied. Seyfang et al. [27]

utilized the time-oriented data-abstraction method to optimize the adjustment of FiO_2 for newborns based on the clinical expert knowledge to keep the SpO_2 within the prescribed range with minimum adjustments. In the more recent paper, additional description of this algorithm had been presented where the clinical test of the automatic control was performed [28]. However, the authors mentioned that the controller was not designed to respond to acute severe hypoxemic events. The algorithm made the FiO_2 adjustment depends on the two analyses of SpO_2: state analysis and trend analysis which are 180 and 60 seconds moving time-window followed by wait mode where no action is applied. There were five qualitative abstraction values of the state analysis (substantially above, above, normal range, below, substantially below), accordingly, one of five possible FiO_2 adjustments were suggested $(-0.02, -0.01, \pm 0, +0.01, +0.02)$. There were three qualitative abstraction values of trend analysis (increasing, stable, decreasing), which is able to postpone suggested FiO_2 adjustment. For the clinical evaluation, twelve preterm infants who are less than 34 weeks of gestational age at birth and receiving supplemental oxygen via nasal continuous positive air pressure considered to be assigned to this study. The study demonstrated statistical conclusions while comparing between closed-loop, routine manual, and dedicated manual control. In short, the closed-loop control significantly increased the percentage of time where SpO_2 within prescribed range comparing to routine manual control only. Further, a more recent and a larger scale of the clinical trial was performed with 34 preterm infants receiving supplemental oxygen through mechanical ventilation or CPAP using the same algorithm [29], and it ends up with a similar conclusion as previous clinical evolution [28].

For fuzzy logic-rule based controller, Fathabadi et al. [21] mentioned that "The application of fuzzy logic controller to neonatal inspired oxygen control was first reported by Sun et al. [30], paralleling the efforts of Morzoff [31]." In addition to what simple rule-based controller can perform; fuzzy logic controller enables a specific set of inputs to be associated with a number of rules with variable range. The advantages of fuzzy logic control over classical control as following: (a) allowable to deal with difficult systems such as non-linear, (b) able to utilize an expert's knowledge about specific problem, (c) capable to build linguistic representation based on continuous variable, (d) less sensitive to noise and (d) parameter change, and faster computation for real-time application [30, 32, 33]. Sun et al. [30] employs a fuzzy logic approach to design a microprocessor-based system to assist controlling FiO_2 to maintain SpO_2 within the desired range. The generated "rules" of the fuzzy logic controller were based on the neonatologists' knowledge and experience. The 35 if-then developed fuzzy rules constructed by using a weighted-mean method of seven ΔSpO_2 and five SpO_2 slope as input parameters. The system is an open-loop system where the suggestions for adjusting FiO_2 were displayed to be executed by the nurse according to his/her best medical judgment. The clinical evaluation of this system designed to be an experimental period of open-loop computer adjustment FiO_2 (2-hour), preceded and followed by a control period of the traditional routine manual control of FiO_2 (2-hour each). In this paper, clinical trials of two patients requiring mechanical ventilation were reported, and the results were promising as the author described it. Further clinical trials implemented on 16 newborns using identical study design and procedure that had been used previously [34]. The study emphasized the less variability of SpO_2 while using

computer-assisted FiO_2 control, and highlighted the potential of automating such a system in the future.

More recently, a fuzzy logic controller integrated with a medical auto-mixer device was presented by Lopez et al. [35]. Unlike the previous study, the 35 if-then developed fuzzy rules constructed by using five ΔSpO_2 and seven SpO_2 slope as input parameters where the output is 11 possible values for an adjustment $(-5\%, -4\%, -3\%, -2\%, -1\%, 0\%, +1\%, +2\%, +3\%, +4\%, +5)$. Three tests performed to evaluate the performance of the developed system: simulation in Matlab, pulse oximeter simulation, and clinical test. A Matlab simulation and pulse oximeter simulation was performed to ensure the functionality of the control system. However, the pulse oximeter was simply sending data every 2 seconds by the serial port simulating SpO_2 received through a pulse oximeter. Subsequently, a clinical trial was performed on 40 preterm newborns requiring supplemental oxygen. They were randomly divided into control and experimental group with 12 hour periods for the manual control and automated control. The study showed that the percentage of the time, where SpO_2 values within the target range, was 58% for automatic controller compared to 33.7% of manual control. However, the SpO_2 was under the prescribed target range more frequent while using automatic control.

PID is a second category controller that is to be discussed in this literature review. PID-control, consist of proportional (K_p), integral (K_i), and derivative (K_d) term. K_p coefficient is responsible for present system error, K_i coefficient for eliminating bias offset by accumulating previous errors over time, and K_d coefficient for future trend error based on the derivative (rate of change) [36]. One of the first attempts of applying PID-controller

to automate oxygen control in preterm infants had been performed by Tehrani et al. [37], and it was updated in 1994 and 2001, respectively [38, 39]. These controllers were tested by using the advantage of computerized simulation of a mathematical model [40, 41]. In the earliest version controller [37], the SpO_2 is fed into a microcomputer controller where the PaO_2 to be computed by using the specific mathematical equation, then the error signal of the set point is calculated. Subsequently, the error signal is applied to a PID controller to apply the proper adjustment of FiO_2. In the later version of the controller [39], a stepwise control loop was integrated to respond faster to very abrupt reduction in SpO_2. The simulated results, which were under different designed conditions, shows stable and acceptable performance for the controllers. In 2009, three closed-loop controller of FiO_2 (state machine, adaptive, and PID) has been evaluated by being applied to seven ventilated low birth weight infants [42]. The developed PID algorithm was required manual tuning of the gain coefficients. The study revealed that the three automatic algorithms improved the oxygen therapy for targeting the desired range and minimizing the need for manual adjustments.

Turn the literature review into the application of adaptive controller. In the case of changeable parameters of the dynamic plant model, adaptive control is able to provide an approach for automatic adjustment of controllers in the real-time [43]. The advantage and applicability of using an adaptive controller to automate the adjustment of FiO_2 was early noticeable by many researchers. As it was described by Fathabadi et al. [21], "One of the earliest and most significant contributions was made by Sano and Kikucki [44]." Since this study was performed before the general clinical acceptance to the pulse oximeter, the transcutaneous oxygen sensor had used to monitor PaO_2 of newborn infants under

incubator oxygen therapy. Their algorithm, a model reference adaptive control, includes two feedback loops: adaptive compensator and digital controller. The optimum digital controller that suggests the optimal adjustment of FiO_2 to control the assumed nominal model output. By using an analytical model of neonatal respiratory systems developed by Grodins et al. [45], the developed adaptive controller was tested. Also, animal experiments' tests were reported by considering dogs under different low-ventilation conditions. Both applied tests show the potential of the automation using the adaptive algorithm.

A multiple-model adaptive controller (MMAC) developed to regulate oxygen saturation by automatic adjustment of FiO_2 [46, 47]. The MMAC controller consists of a model bank (finite number of models) and controller bank (designed number of controllers) where each of the models associated with the designed controller that provides zero steady-state error and reasonable transient response. The controller output adaptively computed according to the corresponding between the plant and the model, which is associated with the controller in the controller bank. The MMAC controller had been tested to control a finite number of plant models as an initial evaluation, and then it was tested on animals. The MMAC was found to be able to regulate oxygen saturation in both simulations and animal experiments effectively. Another group of researchers studied the applicability and effectiveness of adaptive PID controller to control FiO_2 for infants receiving supplemental oxygen by using hood [48-50]. The ratio between PaO_2 and FiO_2 is calculated using mathematical relationship where PaO_2 is found by using measured SpO_2, this ratio used in the specific equation to find the tuning parameters. The validation of these studies was performed by using simulation, animal trials, and human trials. The authors emphasized the feasibility of using such control algorithm for automating FiO_2 adjustment.

Recently, Dargaville et al. [51] designed a PID adaptive controller for automating the control of FiO_2 in NICU. In their study, the error is the numerical difference between the average of prescribed SpO_2 range and the receiving values of SpO_2. The error, its integral, and its derivative with their coefficient are proportional to the signal output. For the accommodation of some peculiarities of the system under control, some modifications were applied to the PID controller (error attenuation within target range at values $< 80\%$, compensation for the nonlinearity of $SpO_2 - PaO_2$ at high values). Because of the observed inverse proportion between gain and severity of dysfunctional lung [52, 53], the adaptive controller was considered to allow the proportional gain to be modified accordingly. Computerized simulation of oxygenation was used as a non-clinical test to assess the performance of the control algorithm. The study shows the developed algorithm performance was promising and deserves clinical evaluation. Thus, a clinical evaluation was carried on twenty preterm infants on non-invasive respiratory support in 2016 [54]. The study procedure was a prospective interventional of 4-hour period of automated oxygen control, which come in between 4-hour periods of manual control (four hours before and after automated control). The study emphasized the effectiveness of the automated oxygen control since it shows better performance in targeting the prescribed range and significantly reduced hypoxemia and hyperoxemia events.

Before discussing the robust controller, it is appropriate to discuss the unique hybrid algorithm of differential feedback and rule-based that has been developed by Claure et al. [55]. This controller designed to automate FiO_2 adjustment in premature infants who are receiving supplemental oxygen through the mechanical ventilator. The hybrid controller is activated to increase or decrease FiO_2 whenever the SpO_2 travel above or below the

prescribed range. The timely adjustment of FiO depends on the value of SpO_2, its derivate (direction and rate of change), and its duration while it is out the target range. The integrated control rules allow the controller to adapt its response to the need for changing conditions in SpO_2. This hybrid algorithm was tested by assigning 14 very low birth weight infants, the finding was that closed-loop hybrid algorithm control more effective than routine care, and it was comparable to dedicated nurse. This algorithm was clinically evaluated by considering a larger number of patients, different modes of respiratory support, and different target range [56-60]. The closed-loop controller shows superiority performance regarding the percentage of time spent while SpO_2 within the target range for every used condition.

A robust controller aims to control a system with uncertainties at some level of control performance within predefined ranges [61]. There were only two used algorithms for controlling oxygen saturation in infants classified as robust control [21]. One of these two studies was published in 1988 [62]. In this early study, the authors used indwelling umbilical artery electrode as the input of PaO_2 to a robust controller. This robust control algorithm required two control parameters: gain (b) and time delay (T). A pilot study of five infants was performed to characterize control parameters for stability purposes. The used control algorithm in this study was proposed by Astrom et al. [63], T was used as sampling interval while the input to the system equal to the previous input plus the ratio of the output error to b. After evaluating the closed-loop controller in seven preterm newborns receiving supplemental oxygen via a head-box, the study highlighted the noticeable improvement of the closed-loop controller over the manual care at spending time within the predefined range. The second robust algorithm was performed by a research team at

UMC [64]. This study is discussed in the following part of this literature review accompanying the other researching efforts that were accomplished at the same university.

The research team at UMC has considered the automation of FiO_2 adjustment as one of the main researching project since their first published works regarding the topic [64-66]. Three graduate students presented their theses, which were at the core of developing a controller for automating the adjustment of FiO_2 in NICU [67-69]. The researching efforts were about modeling the respiratory system of preterm infants, developing proper control algorithm, and constructing an applicable prototype.

Keim [67] contributions were in modeling neonatal respiratory model, finding the relationship between FiO_2 (input) and SpO_2 (output) for estimating purposes, developing control algorithms, and constructing a prototype. Based on the previous modeling studies [41, 70-72], a nonlinear respiratory model was developed by including time-varying parameters. The developed nonlinear and linear model compared using small and large step input, then both compared to the collected clinical data [65, 67]. For the interest of modeling the relationship between FiO_2 and SpO_2 to be used in the area of control design, dynamic fuzzy logic system (DFLS), continuous parameter-estimating extended Kalman filter (CP-EEKF), and discrete parameter-estimating extended Kalman filter (DP-EEKF) were evaluated. A discrete disturbance estimator was utilized to estimate the unknown disturbance, which is then used to modify the control signal to the DP-EEKF. Therefore, the disturbance estimator and DP-EEKF could estimate both disturbances and system parameters. Both the DFLS and DP-EEKF was found to accurately estimate the parameters, yet the DP-EEKF was more efficient at estimation and more applicable to be used in linear control theory.

Robust controller was designed to control automatically FiO_2 adjustments [64, 67]. For robust control, the nominal model and multiplicative uncertainty error model were created. For the performance weights, 5% was an allowable error at low frequency and 300% allowable error at high frequency. A μ-analysis (structured singular value analysis) was used to find the robust performance of the controller. Both robust stability and performance, for a given set of known plant uncertainties, was found for the robust controller with a low bandwidth frequency. Further, adaptive controller based on disturbance and DP-EEKF estimator system was developed [67, 73]. At each iteration, the DP-EEKF estimates the plant gain while the disturbance estimator estimates the disturbance, and they feed into the controller. Both the robust and adaptive controller are compared to a static PI-controller; the adaptive controller was performing the best in the simulation. Subsequently, the first prototype is constructed, which is simply a mechatronic device consisting of electrical and mechanical components, and it is allowable to perform the required FiO_2 adjustments.

Krone [68] investigated the biological system of the infants to model the relationship between SpO_2 and the other measurable parameters: FiO_2, heart rate (HR), and respiratory rate (RR). Fuzzy logic, neural network, and transfer function model were used to develop models that have inputs of FiO_2, HR, and RR. These models were tested, in a simulation environment, to observe which one of those models was performing the best in representing the future SpO_2 (from clinical measurements) for the longest time [66, 68]. After the simulated tests, the transfer function model represents the best future SpO_2.

Linear quadratic regulator PI-controller (LQR-PI) was developed where it controls only FiO_2, and HR and RR were considered as disturbances [68]. Nominal and robust

stability were found in the closed-loop system. The study mentioned that the closed-loop system is stable whenever the gain was positive. A robust controller was designed, where the uncertainty of FiO_2, HR and RR took into the account and found using multiplicative uncertainty. A μ-synthesis controller was developed for six ranges of FiO_2. The nominal stability, nominal performance, robust stability, and robust performance were evaluated to ensure the ability of each controller to perform over the uncertain range successfully. Also, an adaptive controller with feedforward disturbance rejection was developed. This system consisted of a feedback controller for FiO_2 and a feedforward disturbance rejection for HR and RR. The estimated parameters were found by using dynamic transfer function model, and they were updated every 5 seconds. The author highlighted the ability of all developed controllers to reject the disturbances and maintain SpO_2 within the target range in a simulation.

Quigley [69] used a genetic algorithm (GA) to locate the most accurate nominal model at representing SpO_2 based on that appropriate robust controller is selected. The working procedure started with sending model $FiO_2 - SpO_2$ relationship to GA, which selects the proper robust controller based on the estimating parameters. This iterative procedure has a period of 5-seconds. In this study, some modification of the control performance specifications was applied to allow the automatic controller to adjust the FiO_2 as the manual protocol used in NICU. Some additional performance weight was applied to the controller such as the weight used to limit the changing rate of FiO_2 adjustments. The study shows some simulated results of the modified controller. Also, the prototype was modified to be more applicable to perform the automatic adjustment of FiO_2.

Ultimately, many researchers put considerable efforts into studying the automation of FiO_2. However, the automated control has not substituted or reduced the use of manual control yet. It is noticeable that many of the studies included in this literature were following similar studying stages; designing control algorithm or improving existing one, testing the functionality and performance using computer simulation, and finally performing a clinical trial. As mentioned above, several control algorithms have been developed and tested in simulation environment by the research team at UMC. None of these developed control algorithms was experimentally investigated thoroughly. The applicable software of the adaptive controller based on discrete disturbance and DP-EEKF estimator, incorporated with the suitable hardware were structured for automating the adjustment of FiO_2. The experimental non-clinical and clinical, investigation of the performance of the developed controller has not been executed prior to the work that is presented here.

1.3 Research Objectives

In this research, a systematic approach has been developed to investigate both clinical and non-clinical the performance of the automatic SpO_2 controller. In the non-clinical study, the neonatal simulation of oxygenation was used as an input for the adaptive controller (hardware-in-the-loop test). The aim was to assess the performance of the controller in (a) maintaining SpO_2 within a prescribed range and showing the stability of the system's response, (b) estimating neonatal respiratory model parameters, and (c) functioning with no mechanical or communication failure. In the clinical study, the primary objective was demonstrating the clinical feasibility of the controller in a study with two human subjects at two different target ranges of SpO_2. The analyses were applied to the

data that was collected in NICU to show (a) the ability of the device to performs better or at least similar to the manual care at targeting the SpO_2 prescribed range, (b) the stability of the system's response and reducing both hypoxemic and hyperoxaemic episodes, and (c) the ability to transition smoothly from automatic to manual mode and vice versa.

1.4 Dissertation Outline

This dissertation is organized into five chapters as follows:

- Chapter 1 includes background and motivation, literature review, and research objectives of the current study.
- Chapter 2 introduces the neonatal respiratory model, the automatic SpO2 controller, and the utilized statistical analysis.
- Chapter 3 presents the non-clinical study including experiment setup, manual control algorithm, experimental design and procedure, data collection and analysis, results, and discussion.
- Chapter 4 presents the clinical study including experiment setup of the clinical trial, study settings and subjects, study protocol, data collection and analysis, results, and discussion.
- Chapter 5 presents the conclusion and future work.

Chapter 2 : Overview of the Neonatal Respiratory Model, the Automatic Arterial Oxygen Controller, and the Utilized Statistical Analysis

In this chapter, an overview of the neonatal respiratory model is presented. Further details and discussion of this respiratory model can be found in these references [65-68]. Then, an overview of the automatic controller is discussed in three sections. Elaborated details and description of this controller can be found in these references [67, 73]. Finally, the background of the statistical analyses that are used in this research to investigate the performance of the device is introduced.

2.1 Overview Neonatal Respiratory Model

The neonatal respiratory model, to simulate SpO_2 responses due to adjustments of FiO_2, is a first-order transfer function (TF) [65-68]. This TF was developed based on earlier studies [41, 70-72]. The TF was evaluated by using clinical data that was collected in the NICU at MU Women's and Children's Hospital. The study that includes the collection of the clinical data was approved by the local institutional review boards (IRB). It is noted that a lag (time delay) between the FiO_2 and the SpO_2 was indicated and due to the dynamics of the pulse oximeter, transport delay (due to equipment) and the oxygenation time (due to physiology). The lag was not constant; however, a method involving a search window was used to determine the time delay between the FiO_2 and SpO_2. The delay was removed from the data to fit model parameters (for the part of the model that excludes time delay) to maximize the accuracy of FiO_2 event modeling process. The studies confirmed and validated the ability to use the first-order transfer function to model the relationship

between FiO_2 and SpO_2 using clinical data. Also, some other studies obtained similar and supportive results [52, 74]. The first-order transfer function is

$$G(s) = \frac{Y(s)}{U(s)} = \frac{G_{FiO_2}}{\tau_{FiO_2} s + 1}, \tag{2.1}$$

where s is the Laplace variable, $Y(s)$ is the output SpO2, U(s) is the input FiO2, and G_{FiO_2} and τ_{FiO_2} are the gain and time constant associated with the input of FiO_2 and the output SpO_2. Therefore, using different combinations of the two parameters allows the model to have a response that closely resembles the collected clinical data for premature infants. In addition, there is an "unknown" disturbance to the infant response which results in the desaturation events. By unknown, we mean that the cause of the disturbance is not measured directly.

The dynamic response of the infant model is

$$Y(s) = G(S)[(U(s) - u_0) + (D(S) - d_0)] + y_0\,, \tag{2.2}$$

Where $D(s)$ is the disturbance, and the nominal values are denoted by the subscript 0. Fig. 2-1 represents the block diagram of the neonatal respiratory model. In addition, there is a delay included at the input which may cause the instability behavior in model responses.

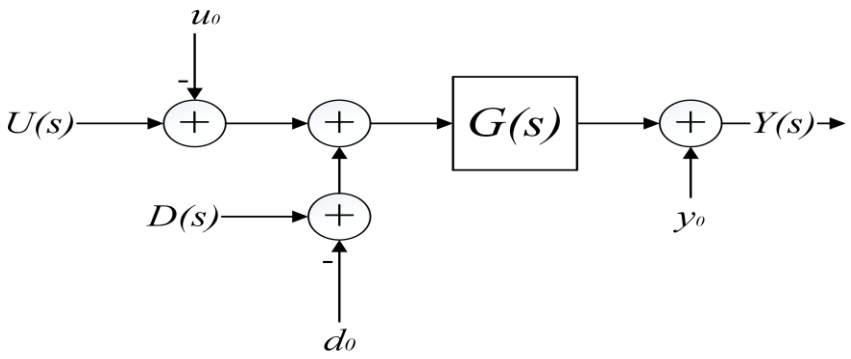

Fig. 2-1 Block diagram of the neonatal respiratory model

2.2 Overview Automatic Arterial Oxygen Controller

The closed-loop control device was developed to automate the control of FiO_2 in premature infants, however, the device can be used for any patient requiring respiratory support [67, 73]. Concisely, the system is a microcontroller that attaches to monitoring devices, such as an oxygen sensor and a pulse oximeter, which send signals of clinical measurements of a patient. Based on the signals that are received, the microcontroller dynamically and adaptively runs its control algorithm to determine the proper percentage of oxygen concentration. Subsequently, the error signal is amplified and used to direct a DC motor that controls the blend (or mixing) valve (connected to oxygen and medical air gas). Then the mixed air is delivered to the infant through a proper respiratory support mode such as heated and humidified high flow nasal cannula. Fig. 2-2 shows the diagram of the automated respiratory support system [67, 73].

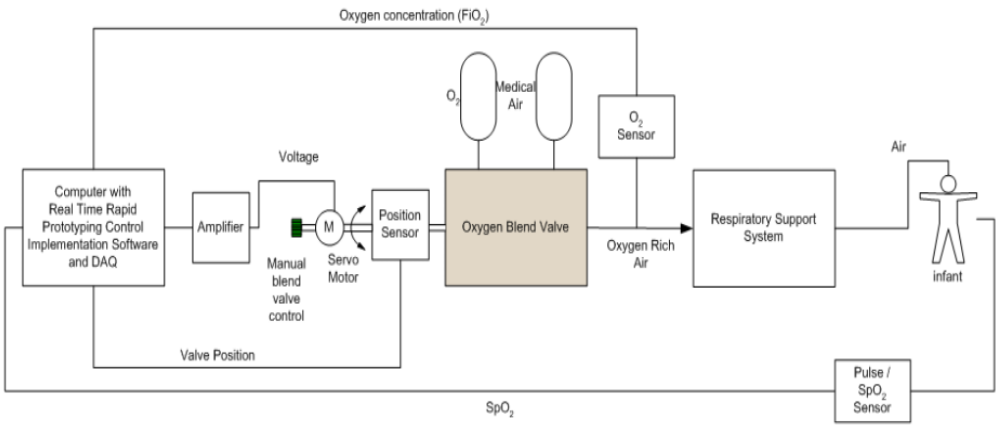

Fig. 2-2: Diagram of the automated respiratory support system [67, 73]

2.2.1 Control Algorithm

The control algorithm is classified as an adaptive, which is based on a discrete disturbance estimator and discrete parameter-estimating extended Kalman filter estimator

(DP-EEKF) [67, 73]. Fig. 2-3 shows the block diagram of the essential elements of the control system. The control algorithm is fundamentally based on estimators, which are the disturbance estimator and the PE-EKF. The estimated parameters are used to determine control gains for the adaptive control which is used to determine the control effort (FiO_2). Unknown disturbances act as a signal which adversely affects the SpO_2. To counteract the disturbance, the feed-forward disturbance compensator is utilized. The total control effort of FiO_2 is the sum of the adaptive control output and the feed-forward disturbance compensator output. The total control effort is sent to the electrical, mechanical, and medical components to produce the proper FiO_2 input to the premature infant. The reference SpO_2 is the average value of the target range that is prescribed.

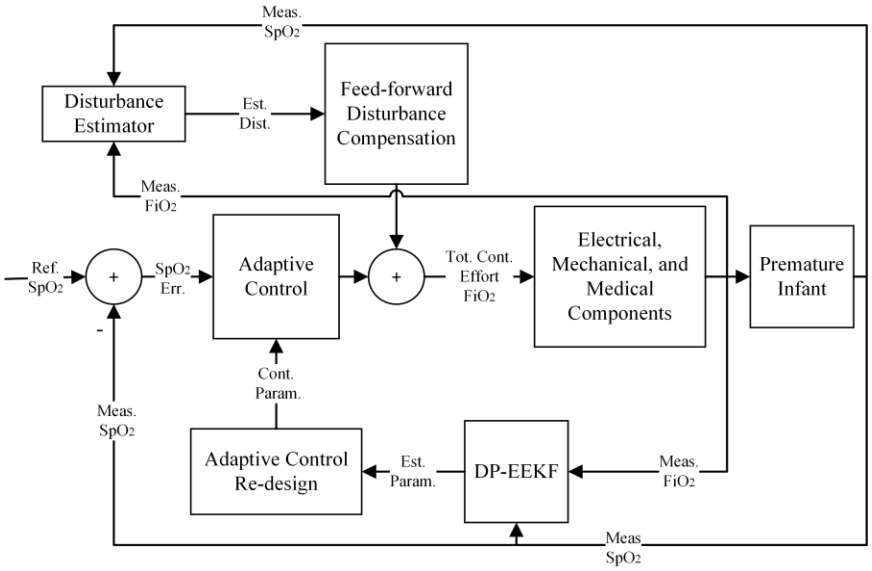

Fig. 2-3: Block diagram of the control system

The adaptive gain for the P-control system is calculated by

$$K_p = \frac{\frac{1}{e_{ss}} - 1}{\hat{x}_3(t)}, \tag{2.3}$$

where e_{ss} is the maximum allowable steady-state error, and $\hat{x}_3(t)$ is the estimated $G_{\mathrm{FiO_2}}$ which is computed by DP-EEKF.

The adaptive gains for the PI-controller are calculated by

$$K_p = \frac{0.4 \times \bar{G}_{\mathrm{FiO_2}}}{\hat{x}_3(t)}, \tag{2.4}$$

$$K_i = \frac{0.01 \times \bar{G}_{\mathrm{FiO_2}}}{\hat{x}_3(t)}. \tag{2.5}$$

The control gains in the case of PI control were designed (using a Ziegler-Nichols method) for a model with a nominal value of $G_{\mathrm{FiO_2}}$, $\bar{G}_{\mathrm{FiO_2}} = 3.5$, and then scaled as shown in Eqs. (2.4) and (2.5). The estimated disturbance $(\hat{d}(t))$, which is computed by disturbance estimator, is multiplied by an additional feed-forward control gain (K_D) to produce the total control effort. Using a trial and error method, K_D is found to be a constant of value 0.4 for stability and good disturbance rejection.

The total control effort for the P-controller with a disturbance canceling feed-forward term is

$$u(t) = \hat{d}(t)K_D + (y_d(t) - y(t))K_p\,, \tag{2.6}$$

where $y_d(t)$ is the average value of the desired target range and $y(t)$ is the feedback value of SpO2. The total control effort PI-control with a disturbance canceling feedforward term is

$$u(t) = \hat{d}(t)K_D + (y_d(t) - y(t))K_p + K_i \int_0^t (y_d(t) - y(t))dt\,. \tag{2.7}$$

The controller is enhanced with anti-integral windup design, to avoid the integral saturation phenomenon while switching from manual to automatic mode and vice versa and while under conditions with extreme disturbance levels, sensor failure, disablement of

the DC motor during manual control, and approaching signal limitations such as the minimum FiO_2 (21% on an absolute scale) and the maximum SpO_2 (100% on an absolute scale). Also, a time-delay compensator is used to compensate for process and transport delays inherent in the equipment and the human subject.

The Kalman filter is used to minimize the estimation error by using a first order model and applying the Kalman gain, *K*. The error covariance matrix, *P*, is the quantification of the error estimation. The state vector, $\hat{x}$, and *P* are updated at each iteration. The authors applied CP-EEKF for estimating SpO_2, G_{FiO_2}, and τ_{FiO_2}. For a better performance of the CP-EEKF, it was converted to DP-EEKF. Fig. 2-4 show the diagram of the process of the DP-EEKF update for each iteration [67, 73].

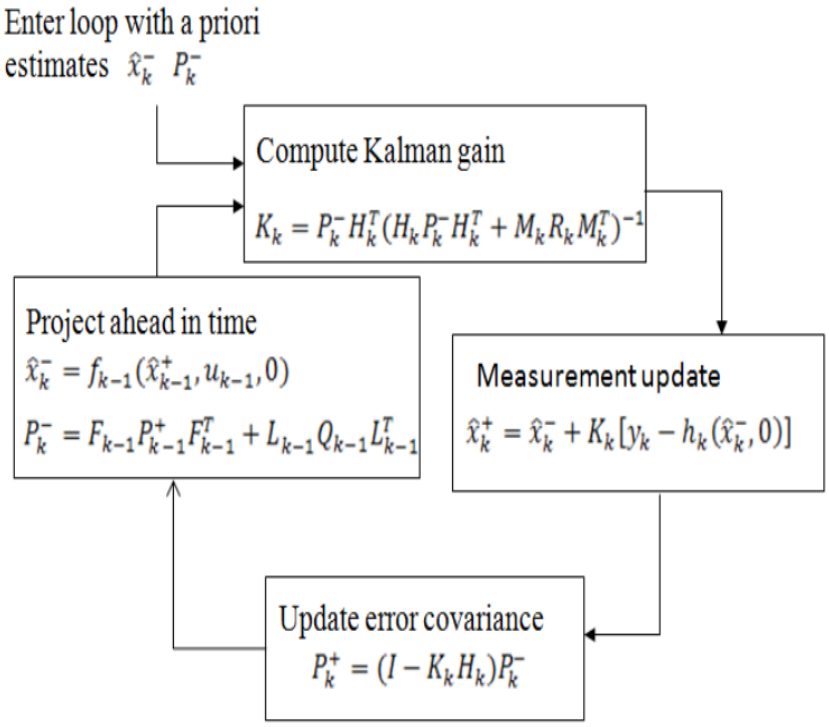

Fig. 2-4: Diagram of the DP-EEKF update process for each iteration [64, 70]

The used *F*, *L*, *H*, and *M* matrices in the controller are given as

$$F_{k-1} = \begin{bmatrix} 1-\hat{\tilde{x}}_2(t)\Delta t & \Delta t(-\hat{x}_1(t)+\hat{x}_3(t)u_{EKF}) & \Delta t\hat{\tilde{x}}_2(t)u_{EKF} \\ 0 & 1-2\hat{\tilde{x}}_2(t)w_p\Delta t & 0 \\ 0 & 0 & 1 \end{bmatrix}\Bigg|_{\hat{x}_k^+},$$

$$L_{k-1} = \begin{bmatrix} \Delta t & 0 & 0 \\ 0 & -\tilde{x}_2^2(t)\Delta t & 0 \\ 0 & 0 & \Delta t \end{bmatrix}\Bigg|_{\hat{x}_k^+}, \tag{2.8}$$

$$H_k = [1\ 0\ 0],$$

$$M_k = 1,$$

where $\hat{x}_1(t)$ is the estimated SpO_2 difference from the average value of the desired target range, $\hat{x}_2$(t) is the estimated τ_{FiO_2}, $\hat{\tilde{x}}_2(t)$ is the inverted value of $\hat{x}_2(t)$, u_{EKF} is the modified control signal, and w_p is an added artificial noise [67, 73]. At each time step, the *F*, *L* matrices are updated with the previous state estimate, as shown in Fig. 2-3, while the *H* and *M* matrices remain constant.

The discrete disturbance estimator is applied to the input FiO_2 and the output $SpO_2$to reject unmodeled dynamics. The used discrete estimator equation is

$$\begin{aligned} \hat{x}_{k+1} &= \left[\Phi - L_p H\right]\hat{x}_k + \left[\Gamma - L_p J, L_p\right]u_k, \\ y_{d_k} &= [I - L_c H]\hat{x}_k + [-L_c J, L_c]u_k, \end{aligned} \tag{2.9}$$

where Φ, Γ, H, and J are the discretized coefficients that are found by using the continuous state space system model [67, 75, 76]. u_k is the combined input of the control signal and measurement. $L_c$is the estimator vector gain, which is determined by

$$L_c = \begin{bmatrix} \dfrac{1-\beta^2}{1-Q} \\ \dfrac{(\beta-1)^2}{\hat{x}_3 Q} \end{bmatrix}, \tag{2.10}$$

$$\beta = e^{-\omega_0 T},$$

$$Q = \frac{\left(T\hat{\hat{x}}_2\right)^3}{6} - \frac{\left(T\hat{\hat{x}}_2\right)^2}{2} + T\hat{\hat{x}}_2 \,,$$

where ω_0 is disturbance estimator pole location in the continuous time domain, β is the discrete time (z-domain) poles of the estimator, and T is the discrete sample time.

Half of the frequency of the discrete time step, T, is used as the upper bound on the pole location. Because of the stability issues, a faster pole is not practical for discrete time implementation. Therefore, the upper bound is $75\, rad/sec$. To avoid the disturbance estimator to be slower than the baby's response, the lower bound chose to be $0.02\, rad/sec$. The gain L_p is given by

$$L_p = \Phi L_c \,. \tag{2.11}$$

A modification of the control signal is taken place by using the output of the disturbance estimator. By using the modified signal, DP-EEKF estimates the system parameter more accurate and remain the system gain in the positive range.

2.2.2 Prototype Hardware and Construction

The porotype consists of both mechanical and electrical components, which is known as mechatronic device [67, 69]. The mechanical components such as blender valve, shaft attached to a heliacal coupler, and miter gears allow transmitting the control signals to the required adjustment of FiO_2. The National Instruments microcontroller which has serial adapters, motor drivers, and a ribbon cable module for analog input and output, receiving the clinical measurements from Spacelabs® patient monitor and the FiO_2 percentage from the oxygen analyzer. This microcontroller sent control signal after being processed by the developed software through a computer. Fig. 2-5 shows the block diagram of the device and connections [67], however, some of these control signals are

possible but not being activated yet in the controller. Fig. 2-6 shows the essential mechanical components of the developed porotype.

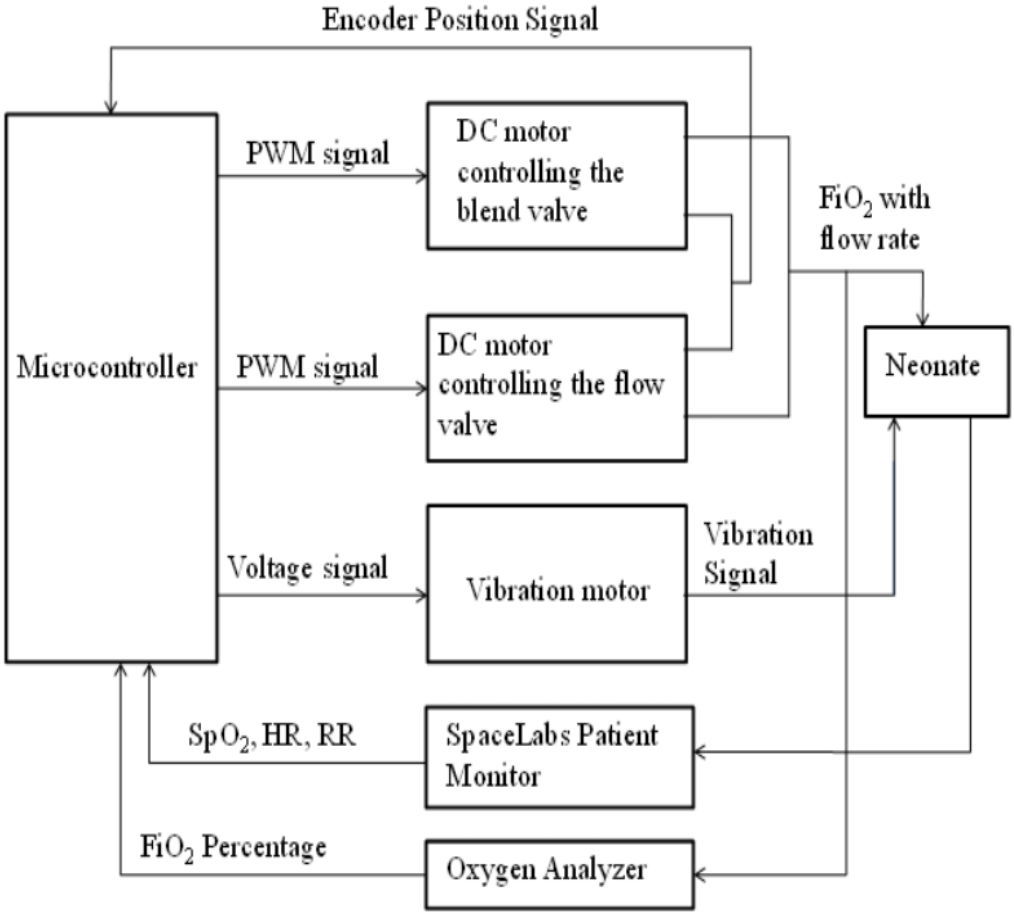

Fig. 2-5: Block diagram of the device and connections [67]

Fig. 2-6: The mechanical component of the porotype [66]

2.2.3 Prototype Software

A graphical programming language (LabVIEW®) was used to develop the software for the current prototype [67]. The software includes Field-Programmable Gate Array module (FPGA) of the microcontroller and Virtual Instrument (VI). In the memory side of the microcontroller, five programs run to treat the received data before sending back the control signal. A block diagram of the process where data flow through the porotype software is shown in Fig. 2-7 [67].

As shown, the SpO_2 and FiO_2 are sent to FPGA VI to be ready for reading by the serial communication VI. Then data processing VI received the serial signal in the form of a string variable. At the point that SpO_2 and FiO_2 percentage is recognized in the string; they sent to data filtering VI. By using discrete low pass filter, the values of SpO_2 is

filtered. Once data filtering is completed, estimation and control VI receives the arrays of SpO_2 and FiO_2 percentage where the estimation system is taken place. Based on this estimation, the control signal of adjusting FiO_2 is sent to another signal communication VI which communicates with FPGA VI. An error signal is created at FPGA VI by subtracting the encoder setpoint from the current encoder position VI. The adjustment of FiO_2 transferred to proper encoder tics and sent back to the mechanical components of the prototype.

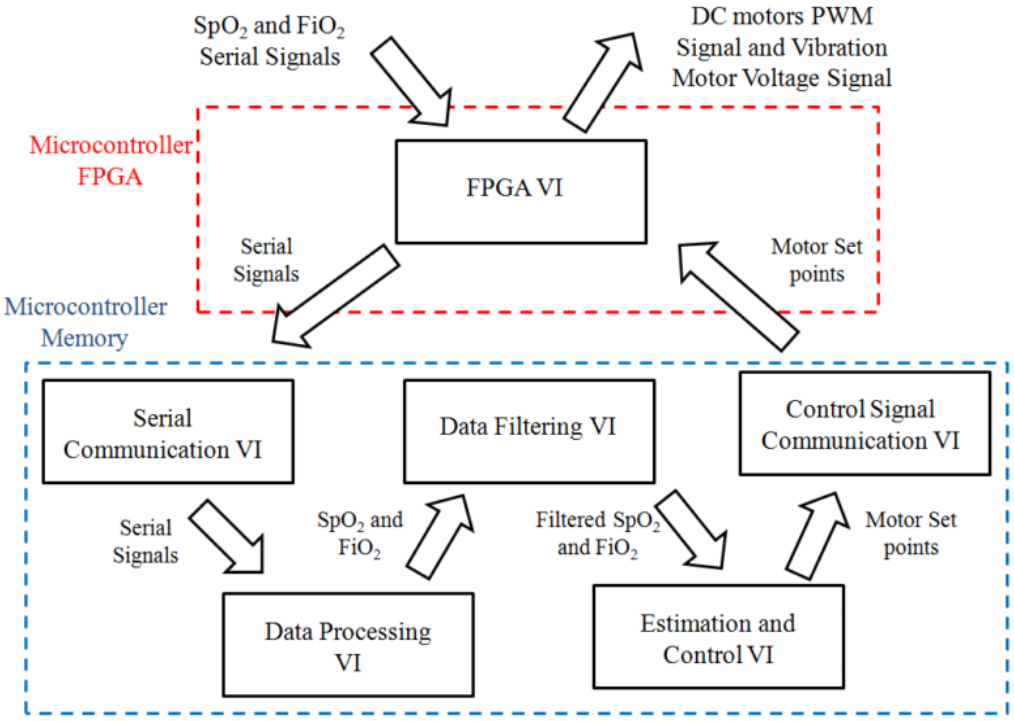

Fig. 2-7: A block diagram of the process where data flow through the porotype software [64]

2.3 Background of the Utilized Statistical Analysis

Descriptive statistics briefly summarizes the collected data. Therefore, the reader can easily understand the nature of the dataset by using the descriptive statistics such measuring the central tendency and variability. However, descriptive statistics are not able to draw a significant conclusion about the collected data. At the point of comparing two or

more data sets, statistical analysis can provide a significant methodical conclusion about the collected data. Background of the statistical analysis methods that are used in this research is provided in the following subsections.

2.3.1 Normal Probability Plot and Shapiro-Wilk Test

Statistical analysis' tests have specific assumptions that need to be met before running them such as normality for parametric tests. Normal or Gaussian distribution is a continuous probability distribution, which is bell-curved and symmetric with a mean (μ) that describes the center of the curve of a set of data and with standard deviation (σ) that describes the dispersion of this data around the center [77]. Before the use of any parametric test, a verification of the normality assumption is essential. A variety of graphical methods and statistical tests are available for testing normality. However, the graphical method has no guarantee that the distribution is normal [78]. Therefore, the normality tests should be supplemented to the graphical methods [79]. Normal probability plot and Shapiro-Wilk test were used to verify the assumption normality for the collected data, which was considered to be analyzed in the current research.

The normal probability plot is a graphical method to assess whether the collected data is approximately normal or not [80]. The normal distributed data should form an approximate straight line when they plotted versus a theoretical normal distribution with no departures. Shapiro-Wilk test has been considered as the most powerful test of normality [78]. Hence, Shapiro-Wilk test was used to test the normality of the data in addition to the normal probability plot. The Shapiro-Wilk test count on the correlation of the data and their corresponding normal scores. The hypotheses of testing the normality of specific data and statistical test as follows:

H_0: The data is normally distributed

H_a: The data is not normally distributed

The Shapiro-Wilk test formula is

$$SW - W = \frac{(\sum_{i=1}^{n} a_i x_i)^2}{\sum_{i=1}^{n}(x_i - \bar{x})^2}, \tag{2.12}$$

where x_i is the data values, $\bar{x}$ is the sample mean, n is number of observations, and a_i is weight values.

Based on the $SW - W$ and corresponding to sample size, the p-value can be found. In this research α of 0.05 is chosen to reject or not the null hypothesis. For the case, the test not rejecting the null hypothesis, p-value> 0.05, the parametric test can be used; otherwise, an alternative nonparametric test is suggested to be employed.

2.3.2 Paired T-Test

At the point that the primary objective is to assess the effect before and after the treatment or the method of treating (Clinical trial), a paired t-test is advantageous for such comparison [77, 81]. The hypotheses as follows:

H_0: $\mu_d = 0$

H_a: $\mu_d \neq 0$

where

$$\mu_d = \mu_1 - \mu_2 . \tag{2.13}$$

The null hypothesis indicating no difference between means and the alternative hypothesis states that there is a difference. The paired t-test was used for comparing the normally distributed variables of frequency episodes where SpO_2 outside the target range

and mean duration of those episodes. The test statistic for the paired t-test of the introduced hypotheses is

$$t = \frac{\bar{x}_d}{SE},$$

$$SE = \frac{s_d}{\sqrt{n}}, \tag{2.14}$$

$$df = n - 1,$$

where n is the number of observations, $\bar{x}_d$ is the mean, SE is the standard error of the mean difference, s_d is the standard deviation, and df is the degrees of freedom. Based on the value of t and df, the p-value is found. The null hypothesis is rejected when p-value $<$ 0.05.

2.3.3 Wilcoxon (Matched Pairs) Signed Rank Test

Wilcoxon signed rank test is an appropriate alternative nonparametric test to the paired t-test when its assumption such as normality is not valid [82, 83]. It is relatively liberal; the assumptions required to be met for using this nonparametric test are that the data be continuous and paired [83]. In the current research, this test was used when normality assumption was not valid, for any comparison that was mentioned in the previous section. The only difference is that the hypotheses are identified if there is a difference based on the medians, for example:

H_0: $M_d = 0$

H_a: $M_d \neq 0$

where

$$M_d = M_1 - M_2 . \tag{2.15}$$

The null hypothesis is stating no difference between the two medians while the alternative hypothesis is indicating that there is a difference. The test statistic for the Wilcoxon signed rank test of the introduced sets of hypotheses is

$$z = \frac{T^{+} - \left[\frac{n(n+1)}{4}\right]}{\sqrt{\frac{n(n+1)(2n+1)}{24}}}, \tag{2.16}$$

where T^{+} is the sum of positive ranks n is the number of positive and negative ranks excluding ties.

The null hypothesis is rejected, p-value < 0.05, where the differences in positive and negative ranks are sufficiently large.

2.3.4 Friedman Test with Post-Hoc Comparison

Friedman test is the nonparametric alternative of the one-way ANOVA. It is like the Wilcoxon signed rank test with an advantage of being able to be used with more than two matched subjects [83]. The post-hoc test was used to locate the differences among the groups. In the non-clinical investigation of this study, Friedman test with post-hoc comparison was used to determine the differences in frequency episodes where SpO_2 outside the target range and mean duration of that episodes when manual routine control, adaptive P-controller, and adaptive PI-controller were used. The hypotheses that were considered at running this test for comparison among the mentioned variables as follows:

H_0: There are no differences among the medians of the used control algorithms for one of the considered variables at nonclinical test

H_a: There is at least one difference among the medians of the used control algorithms for one of the considered variables at nonclinical test

The Friedman evaluate the rank totals of each considered group by

$$F_r = \frac{12}{Nk(k+1)}\left[\sum_{j-1}^{k} R_j^2\right] - [3N(k+1)]\,,$$
$$df = k - 1\,, \tag{2.17}$$

where R_j is the sum of the ranks for group j, N is the number of subjects, and k is the number of groups (three in ours case) [83, 84].

Based on F_r and df, the p-value is found and compare to α, which is 0.05, to decide to reject or not the null hypothesis. The approach that was used to apply post-hoc comparison is using Wilcoxon signed rank test in between the considered groups [83, 85]. Only α value is needed to be adjusted using Bonferroni's inequality; α is divided by k to get α_{adj}. The adjusted critical value, α_{adj}, is 0.017 for $k = 3$. Another approach that was used is examining the following condition if it is true then there is a significant difference between the considered groups as

$$|\bar{R}_1 - \bar{R}_2| \geq Z_{\alpha/[k(k-1)]}\sqrt{\frac{k(k+1)}{(6N)}}\,, \tag{2.17}$$

where $\bar{R}_1$ and $\bar{R}_2$ are the mean ranks for the two considered groups. $Z_{\alpha/[k(k-1)]}$ is the critical z value for $\alpha' = \alpha/[k(k-1)]$ [83, 86, 87].

2.3.5 Statistical Power

The statistical power of a test is the probability of leading to a correct conclusion about the null hypothesis [88]. In other words, statistical power is the probability of avoiding type II error. A type II error occurs when it is concluded that not rejecting the null hypothesis, when in fact it must be rejected. The statistical power is

$$Power = 1 - \beta = 1 - probability\left[z_{power} \leq (t - t^1)\right]\,, \tag{2.19}$$

where z_{power} is a position on the x-axis of the z-distribution, t^1 is the level of t for degrees of freedom, and t is the calculated t from the data. Also, the probability of making type II error is β [89].

For both planning and diagnosis, statistical power analysis is possible to be used [88]. Statistical power was used in this study to identify the sample size at a selected power level and determine whether the study has acceptable power.

An estimation of the number of subjects that are required for a power of $> 85\%$, for a paired t-test, was calculated. For determining the sample size of a test, there are three variables need to be known or assumed: statistical power level, mean difference, and variance of the data as SD [89]. The formula for calculating is

$$n = 2\left(\frac{SD}{mean}\right)^2 \left(z_\alpha + z_\beta\right)^2, \tag{2.20}$$

where $\left(z_\alpha + z_\beta\right)^2$ is the power index, which express the relationship between the standard deviation and the sample size.

Chapter 3 : Non-clinical Investigation of the Performance of an Automatic Arterial Oxygen Controller

In this chapter, the non-clinical investigation is introduced. The experimental design with the procedure and data collection with analysis of the non-clinical study are presented. Finally, the results and discussion of the non-clinical investigation are presented.

3.1 Nonclinical Investigation of the Performance

The non-clinical or preclinical investigation is essential study stage to evaluate the controller, which is considered to be clinically evaluated. The primary goals of this investigation are to assess the controller in (a) maintaining SpO_2 within a prescribed range and showing the stability of the system's response, (b) estimating neonatal respiratory model parameters, and (c) functioning with no mechanical or communication failure.

3.2 Experiment Setup of the Nonclinical Test

The experimental setup of the non-clinical study (hardware-in-the-loop test) is shown in Fig. 3-1. The medical air and oxygen gas cylinders are connected to the air-oxygen blender valve. The mixed air, from the air-oxygen blender, flows through an adjustable flow meter to oxygen sensor that is attached to heater humidifier. The oxygen sensor sends the measured percentage of FiO_2 to the computer that is running the neonatal oxygenation response model simulator implemented using LabVIEW®. The output response, SpO_2, is transmitted to the microcontroller which is running the controller algorithm code that was developed by using both LabVIEW® and MATLAB®. Based on the received data, the control algorithm, a control signal is sent to the amplifier and then to the DC motor which is connected by a shaft to a miter gear. Miter gears control a shaft, which is attached to the control knob and helical shaft coupler, in a way that the air-oxygen

blender supplies the mixed air with the desired level of FiO_2. Manual override is possible by switching to manual control mode. Automated adjustments are enabled only when the switch is used to select automatic mode. The FiO_2 developed by the blend valve is received through an oxygen analyzer and recorded along with other measurements.

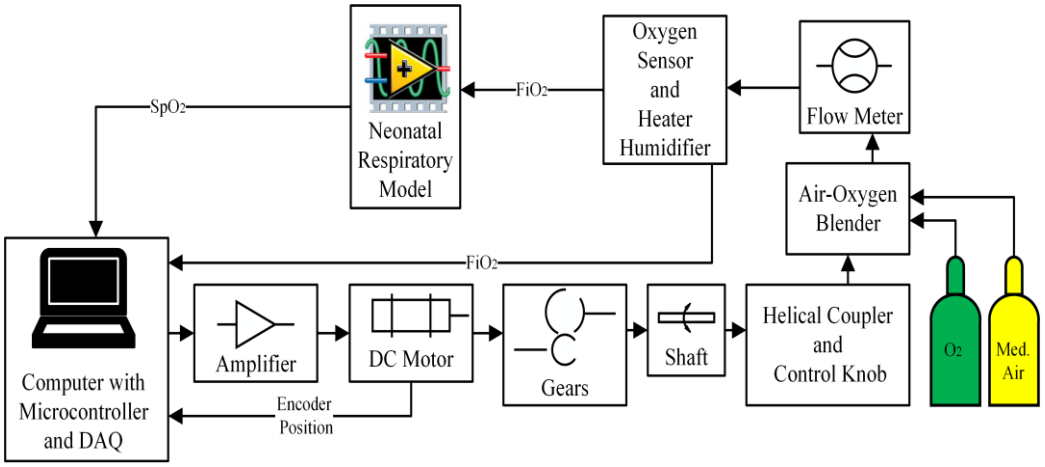

Fig. 3-1: Schematic of the experimental setup of the non-clinical test

3.3 Manual Control Algorithm

The manual control algorithm was developed to be followed for a nonclinical lab test to be compared to the automated control algorithms. This algorithm was developed to demonstrate the capability of using the closed-loop control device in manual mode by the simple transition between automatic and manual modes and generating data from the mathematical model while manual control was used for comparison. To closely treat the neonatal respiratory model as a premature infant being treated in a NICU, the manual algorithm for the non-clinical test has been developed based on the policy stated in [90] and the developed protocol in [91]. In addition, the restriction that has been considered for the automatic control algorithms such as the FiO_2 adjustment limitation of 2% and the allowance of 10 seconds in between adjustments are also considered in the following manual control algorithm:

1. Monitor model's SpO_2 every minute at maximum.
2. Reduce FiO_2 by about 2% as SpO_2 level exceeds the upper limit of SpO_2 target range.
3. Increase FiO_2 by about 2% as SpO_2 level when under the lower limit of SpO_2 target range.
4. Allow about 10 seconds for assessment at each applied adjustment.

Fig. 3-2 shows the flow diagram for the developed manual control algorithm.

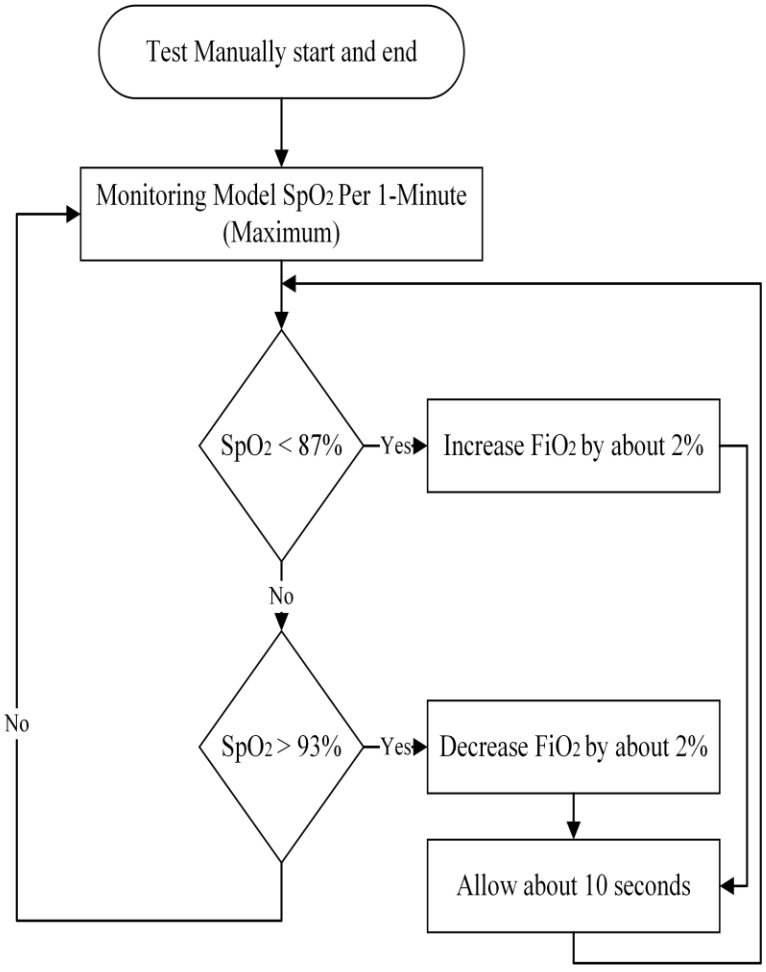

Fig. 3-2: The flow diagram of the developed manual algorithm

3.4 Design of Experiment and Experimental Procedure

To assess the performance of the control algorithm, the design of experiments and experimental procedure need to be comprehensive, efficient, and analyzable. As introduced previously in Sec 2.1, the neonatal respiratory model can have a response as a result of adjusting FiO_2 that is similar to the response of collected clinical data by using an appropriate combination of G_{FiO_2}, τ_{FiO_2}, and a set of disturbances. The different combinations of these parameters found by analyzing clinical data allow for representation of a wide range of response characteristics and different severities of lung disease which affect stability and the relationship between FiO_2 and SpO_2 [64]. Hence, the experimental design of the current test has 3 controllable factors and 3 levels for each factor are considered. The levels of G_{FiO_2} and τ_{FiO_2} are selected by searching the average values of the three-most frequent G_{FiO_2} and τ_{FiO_2} within a numerical category of fitted transfer functions, which was calculated in previous study [68]. Therefore, the selected levels of the G_{FiO_2} are $(2.5, 4.5, 6.5)$ and τ_{FiO_2} are $(45, 65, 75)$; Fig. 3-3 and Fig. 3-4 show the observation frequency of both parameters based on the collected clinical data. The three sets of disturbances (levels: I, II, and III) are purposely designed to generate frequent and diverse fluctuations of the SpO_2, which challenges the control algorithms. Each set of disturbances includes different frequencies of disturbances, which allows the control algorithm to show the ability responding to different types of patients. Fig. 3-5 shows the three different sets of disturbances.

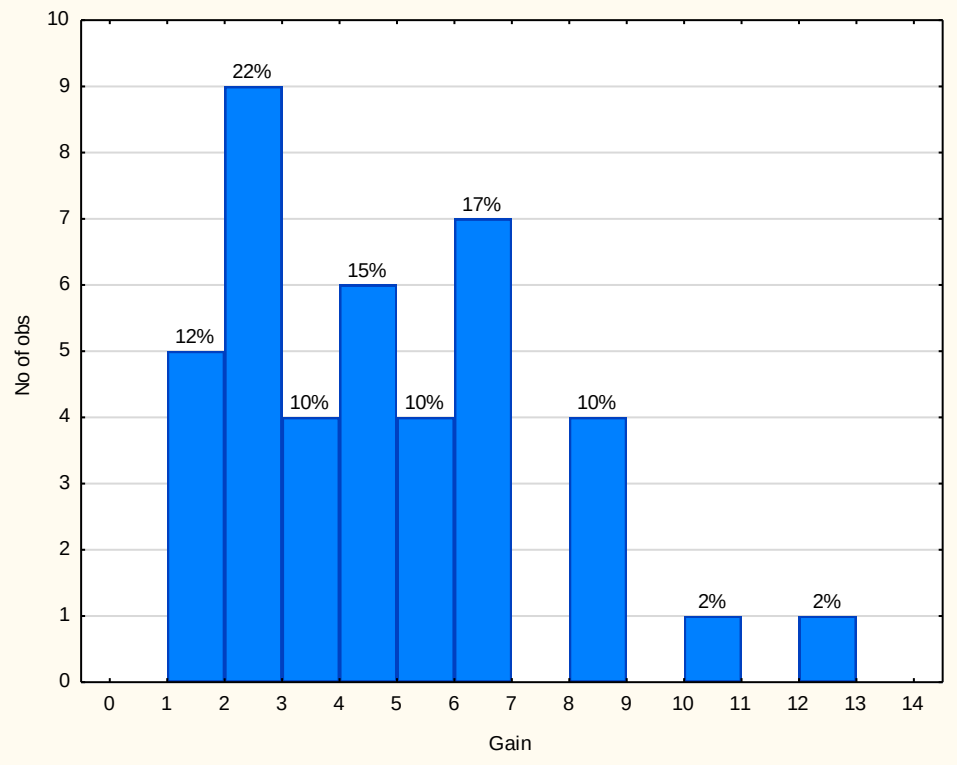

Fig. 3-3: The gains frequency of fitted transfer function

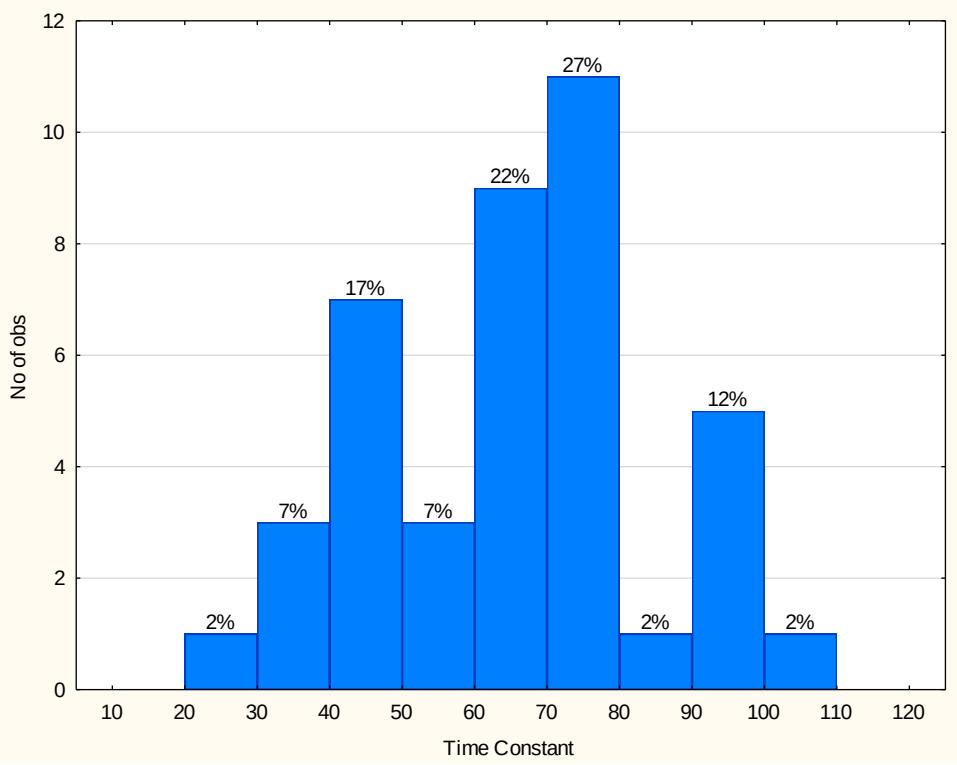

Fig. 3-4: The time constants frequency of fitted transfer function

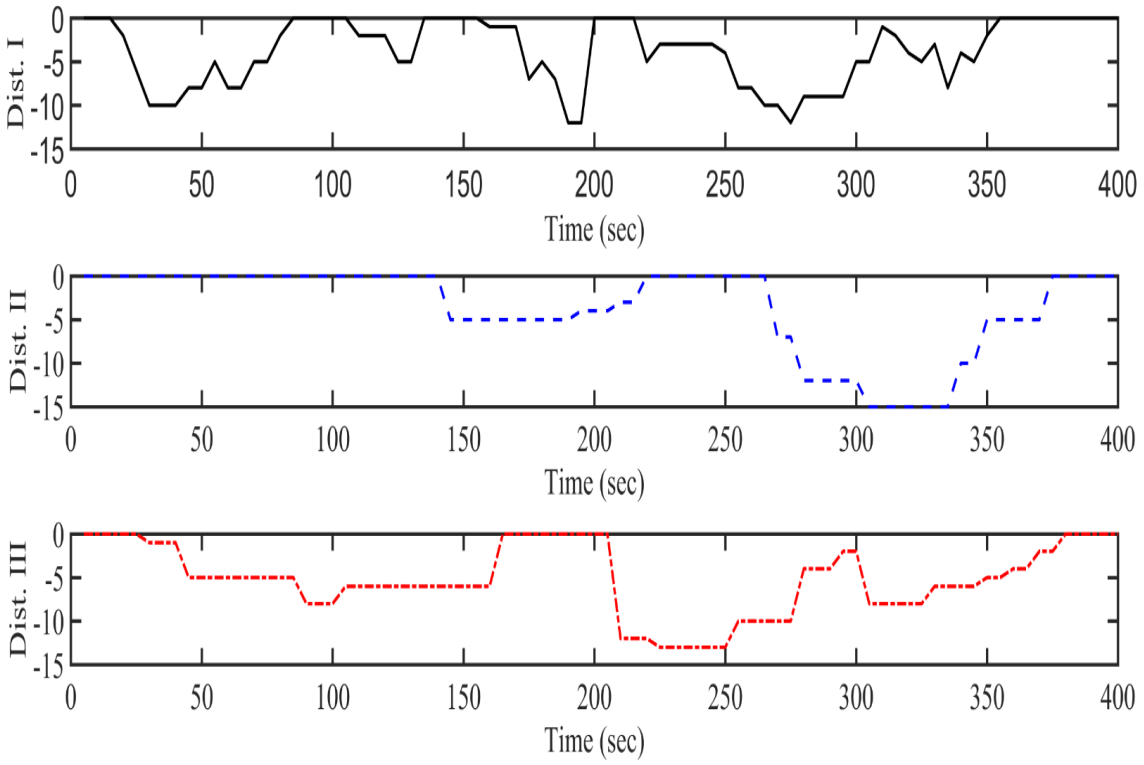

Fig. 3-5: The three different sets of disturbances (I, II, III)

By using a factorial design for the current experiment, we allow all possible combinations of the selected levels of factors, which guarantees the highest diversity of the model's oxygenation response [92, 93]. Therefore, there were 27 different experimental conditions that the controllers address to maintain the SpO_2 within the prescribed range $(87\% - 93\%)$. The target range of SpO_2 varies depending on the particular NICU or clinician's judgment [94, 95]. The selected target range for the current preclinical study is typical for many patients [96].The effect of factors was not the purpose of the current study; however, the factors were employed to generate several behaviors of neonatal respiratory model response while receiving the FiO_2, so the test is more inclusive of all observed dynamics. Therefore, one inclusive experiment that includes the 27 -experimental conditions is appropriate for testing and comparing several control algorithms. This experiment was a 3-hour period, for each control algorithm, where each experimental

condition persists for about 400 seconds. Thus, the experiment of 27 different experimental conditions with their periods is shown in Table 3-1.

The experimental procedure that was used for both manual and automatic control for the nonclinical test is as follows:

1. Ensure the power supply, cables, gas hoses are appropriately connected.
2. Ensure the respiratory model settings correspond to the experimental conditions.
3. The flow meter is fixed at 3 L/min.
4. Turn the control knob of Air-Oxygen blender to 21% and wait until around 21% of FiO_2 shows on the oxygen sensor.
5. Set the microcontroller onto the proper mode (manual or automatic).
6. Run the experiment using the user interface for a 3-hour period.
7. Save the experimental data.
8. Repeat steps 1-7 for each control algorithm.

Table 3-1: Experiment with 27 experimental conditions

Run	Gain	Time Constant	Disturbance	Time (s)
1	2.5	45	I	400
2	2.5	45	II	400
3	2.5	45	III	400
4	2.5	65	I	400
5	2.5	65	II	400
6	2.5	65	III	400
7	2.5	75	I	400
8	2.5	75	II	400
9	2.5	75	III	400
10	4.5	45	I	400
11	4.5	45	II	400
12	4.5	45	III	400
13	4.5	65	I	400
14	4.5	65	II	400
15	4.5	65	III	400
16	4.5	75	I	400
17	4.5	75	II	400
18	4.5	75	III	400
19	6.5	45	I	400
20	6.5	45	II	400
21	6.5	45	III	400
22	6.5	65	I	400
23	6.5	65	II	400
24	6.5	65	III	400
25	6.5	75	I	400
26	6.5	75	II	400
27	6.5	75	III	400
			Total	10800

3.5 Data Collection and Analysis

The SpO_2 model response and FiO_2 input are recorded every 5 seconds during the running of test for both manual algorithm and automated algorithms. For the automated algorithms, the estimated parameters such as gain, time constant, and disturbance are also recorded. The observed and desired encoder position are recorded every one second. The analysis of these measuring allowed for the evaluation of the closed-loop oxygen control

device to maintain SpO_2 of the neonatal model within a target range, estimating neonatal respiratory model parameters, and functioning with no mechanical or communication failure.

Graphical and numerical analysis are used to describe and compare the collected data of SpO_2 for each control algorithm during the hardware-in-the-loop test. [77]. The percentages of time in the following oxygenation states are calculated and displayed in the histogram for the implemented control algorithms: SpO_2 within the target range ($87\% \leq SpO_2 \leq 93\%$), below the target range ($SpO_2 < 87\%$), and above target range ($SpO_2 > 93\%$). Moreover, the variability and ability to maintain the response within the target range of SpO_2 are evaluated by calculating the following: (a) coefficient of variation (CV) over the 3-hour period, (b) frequency of episodes where SpO_2 is outside the target range per 10-minute (the number of episodes of any duration over a 10-minute window), (c) mean duration of those episodes in seconds, and (d) frequency of episodes of hypoxemia (SpO_2 < 80%), prolonged hypoxemia (SpO_2 < 80% for ≥ 60 seconds), hyperoxemia (SpO_2 > 95%), prolonged hyperoxemia (SpO_2 > 95% for ≥ 60 seconds), and SpO_2 overshoot (SpO_2 > 95% lasting for at least 60 seconds and occurring within 120 seconds following a hypoxemic event) per 30-minute were calculated for each used control algorithm [51, 55, 57, 95, 97]. Small values of these parameters for the control algorithm indicate better effectiveness at targeting the SpO_2 range with lower fluctuation. Since the calculated data (b, c, and d) do not meet the assumption of normality for at least one of the used algorithms, the performance of the three algorithms is assessed by using Friedman non-parametric repeated measures analysis of variance ($\alpha = 0.05$) with the post-hoc test ($\alpha_{adj} = 0.017$) or with the other approach that was introduced in Sec. 2.3.4. The compared data are

reported as median and interquartile (IQR). The normal probability plots combined with Shapiro-Wilk test results of the calculated data (b, c, and d) are located in Appendix A.

For the two automated control algorithms, evaluation of the estimation system is required. The differences between estimated SpO_2 values and the desired value of SpO_2 (90%) are graphically compared to the differences between the observed SpO_2 of the model and the desired value during the experiment. Similarly, the estimated and observed disturbances are graphically displayed to evaluate the performance of the disturbance estimator. To measure the performance of the DP-EEKF, the percentage of time that the observed SpO_2 was within the target range is calculated and graphically displayed. Moreover, the percentage of time the estimated gain and time constant are within limits of a difference of 0.5 and 5, respectively, were compared to the selected TF parameters. For the identification of any functional failure between desired and observed encoder position, their measuring were recorded and plotted in figures.

3.6 Results

The experiment setup was successfully applied as described in Sec. 3.2. The developed manual control was used for the non-clinical hardware-in-the-loop test as introduced in Sec. 3.3. This non-clinical hardware-in-the-loop test was applied to evaluate the performance of the automatic controller, which was developed to automate the adjustment of FiO_2 in the NICU. The parameters' levels were selected based on their frequencies of observation as discussed in Sec. 3.4. For a comprehensive assessment of the performance of the controller, the neonatal respiratory model's adjustable parameters were set by using full factorial design along the 3-hour period. The SpO_2 data of the neonatal respiratory model during the hardware-in-the-loop test were collected for three different

control algorithms. A typical experimental test was completed in a 3-hour period for each control algorithm. Fig. 3-6, Fig. 3-7, and Fig. 3-8 show the recording of SpO_2 and FiO_2 for the 3-hour period while using the three control algorithms.

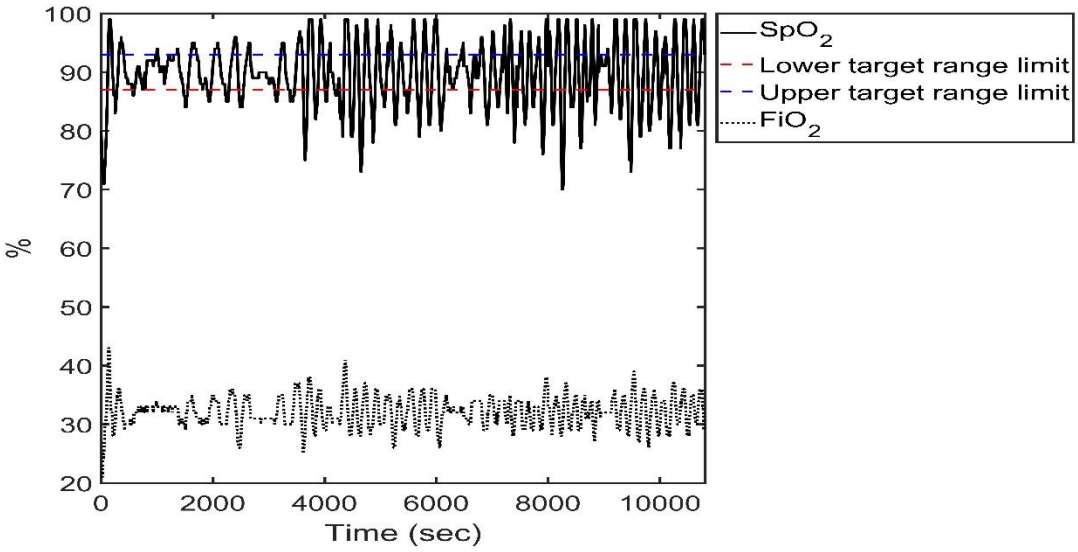

Fig. 3-6:The recording of SpO_2 and FiO_2 for the 3-hour period while using Manual Control

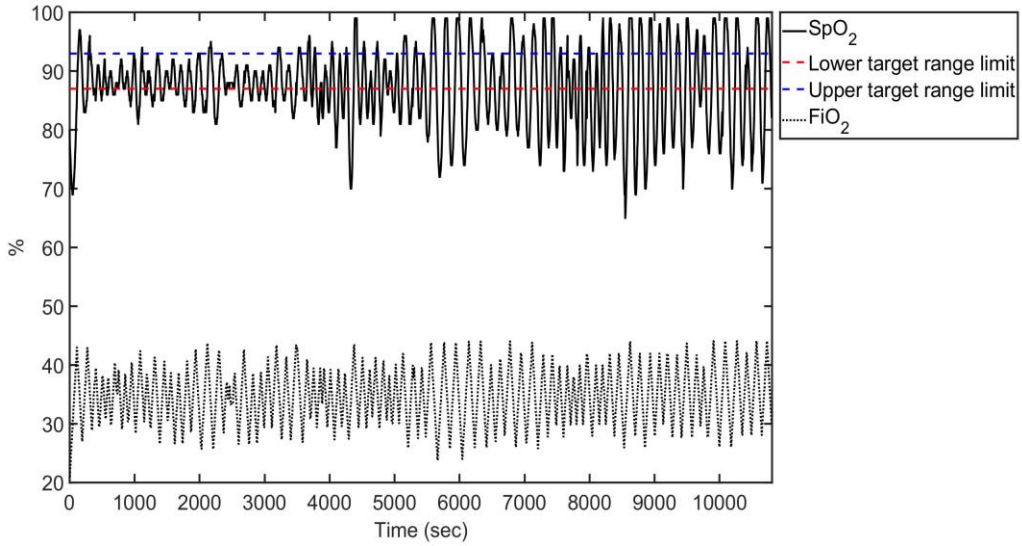

Fig. 3-7: The recording of SpO_2 and FiO_2 for the 3-hour period while using P-Controller with Estimation System

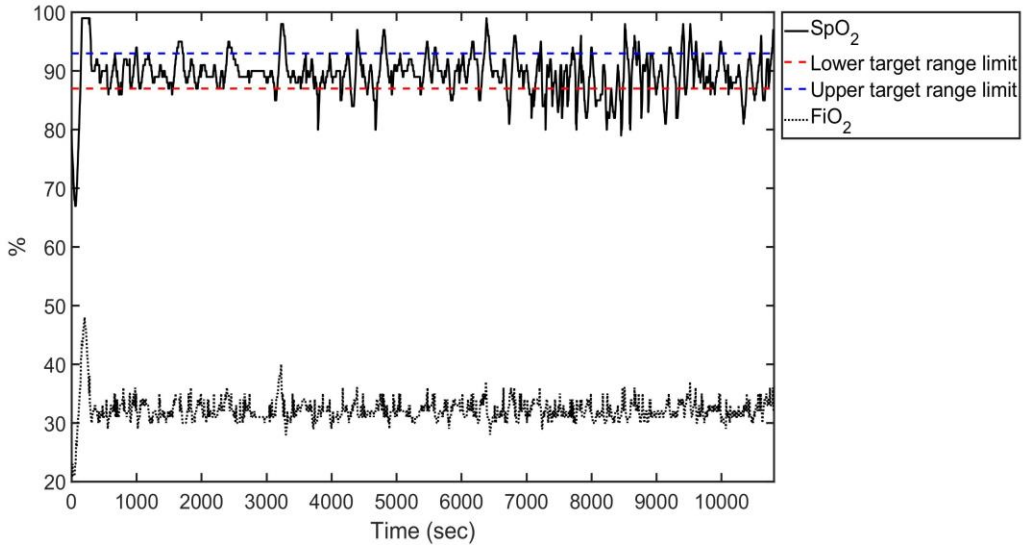

Fig. 3-8: The recording of SpO_2 and FiO_2 for the 3-hour period while using PI-Controller with Estimation System

The adaptive PI-controller shows the highest performance at maintaining the SpO_2 of the neonatal respiratory model within the target range; 75% of the proportion of time was spent within the prescribed range. On the other hand, both the manual control and adaptive P-control failed to achieve performance up to 50% of the proportion time where SpO_2 was within the target range. For the manual control, 48% of the proportion of time was spent within the target range. For the adaptive P-Controller, 39% of the proportion of time was spent within the target range.

The proportions of the time while the values of SpO_2 were below the lower target range or above the target range were varied between the applied algorithms. For the PI-control, SpO_2 values were below than the lower target range limit for 15% and above the upper target range limit for only 10% of the proportion of time. For the P-control, SpO_2 values were below than the lower target range limit for 43% and above the upper target range limit for 18% of the proportion of time. For the manual control, SpO_2 values were

below the lower target range limit for 27% and above the upper target range limit for 25% of the percentage of the time. Fig. 3-9 graphically summarizes the performance of the control algorithms for targeting SpO_2.

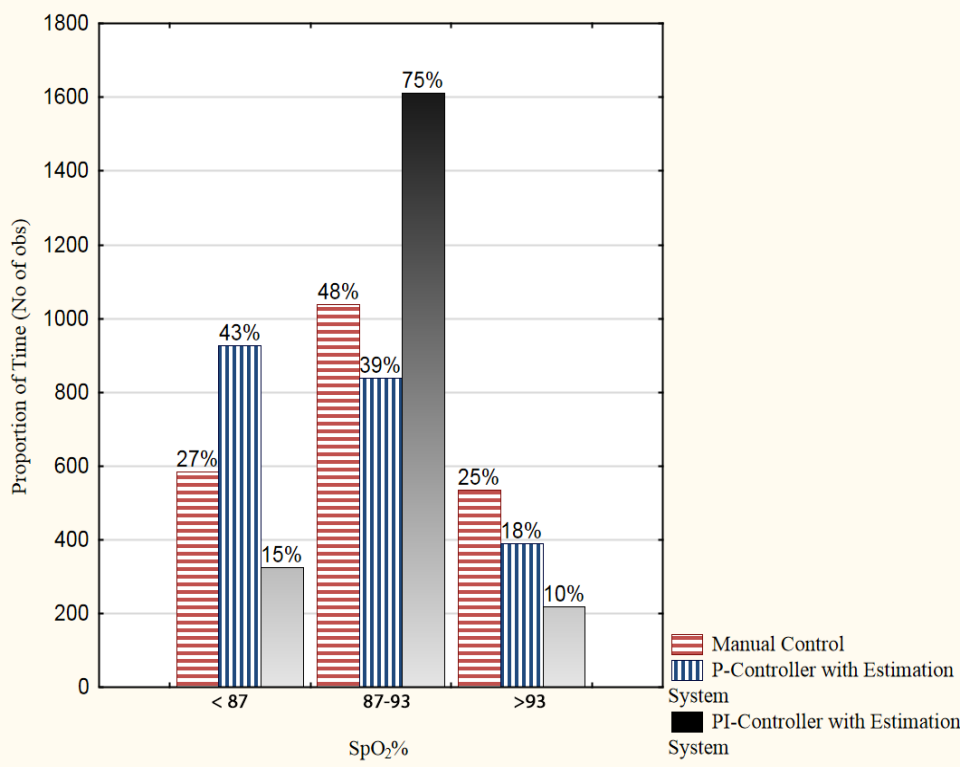

Fig. 3-9: Histogram of the proportion of time of SpO_2 within, below, and above the target range (87-93) during 3-hour period

Table 3-2 demonstrates the significant differences in the variability of SpO_2 values of the three used control algorithms. CVs of SpO_2 were 6.19 for manual control, 7.77 for P-controller, and 4.17 for PI-controller. There were significant differences among the control modes' desaturation episodes with $SpO_2 < 87$. The least frequency of episodes with the minimum mean duration of time with $SpO_2 < 87$ was detected while using the PI-control. The episodes above the target range where $SpO_2 > 93$ occurred similarly during the utilization of both manual control and the P-controller; however, the PI-control

significantly differed with the least frequent episodes. No significant differences were found in the mean duration of episodes where $SpO_2 > 93$.

Table 3-2: SpO_2 variability of the three control algorithms

	Manual Control	Adaptive P-Controller	Adaptive PI-Controller	*P* – Value
SpO_2 CV (%)	6.19	7.77	4.17	*NA*
$SpO_2 < 87\%$ (episodes/10-min)	$3(2-4)^a$	$5(4-6)^b$	$1(1-3)^c$	< 0.05
$SpO_2 < 87\%$ (episode duration, s)	$53.75(46.2-57.75)^d$	$48.71(38.5-54.4)^e$	$30.085(5-40)^f$	< 0.05
$SpO_2 > 93\%$ (episodes/10-min)	$3(2-4)^g$	$3(2-4)^h$	$1(1-2)^i$	< 0.05
$SpO_2 > 93\%$ (episode duration, s)	$46.04(32.7-55.25)$	$30.25(23.33-46.25)$	$25.165(10-52.25)$	*NS*

Post-Hoc Comparison: a and c differ from b; e differs from f; g and h differ from i.
Median (IQR)

Table 3-3 demonstrates the significant differences in the frequency of hypoxemic events while using the three control algorithms. The reported results show the potential of the PI-controller with estimation system at reducing the number of hypoxemic events. However, the P-controller shows poor performance comparing to both manual and PI-controller. No significant differences were indicated for the prolonged hypoxemic, hyperoxaemic, prolonged hyperoxaemic, and overshoot.

Table 3-3: Hypoxemia, hyperoxemia, and overshoot episodes

	Manual Control	Adaptive P-Controller	Adaptive PI-Controller	*P* – Value
$SpO_2 \leq 80\%$ (episodes < 60 s duration/30-min)	$2(0-4)^a$	$3.5(1-11)^b$	$0(0-0)^c$	< 0.05
$SpO_2 \leq 80\%$ (episodes ≥ 60 s duration/30-min)	$0(0-0)$	$0.5(0-2)$	$0(0-0)$	NS
$SpO_2 \geq 95\%$ (episodes < 60 s duration/30-min)	$5(3-7)$	$4.5(2-9)$	$1.5(1-3)$	NS
$SpO_2 \geq 95\%$ (episodes ≥ 60 s duration/30-min)	$1.5(1-2)$	$0(0-2)$	$0.5(0-1)$	NS
Overshoot (episodes/30-min)	$1(0-1)$	$0(0-2)$	$0(0-0)$	NS
Post-Hoc Comparison: a, b, and c differ from each other. Median (IQR)				

The histogram of FiO_2 (Fig. 3-10) illustrate that the model was supplied with varied levels of FiO_2 for each control algorithm. The model was supplied with the range of FiO_2 $(31\% - 35\%)$ for the proportion of time equal 64% for manual control, 42% for P-controller, and 87% for PI-controller. The range of FiO_2 $(26\% - 30\%)$ was supplied for the proportion of time equal 27% for manual control, 41% for P-controller, and 9% for PI-controller. The range of FiO_2 equal $(36\% - 40\%)$ was supplied for the proportion of time equal 9% for manual control, 16% for P-controller, and 2% for PI-controller. Finally, range of FiO_2 $(21\% - 25\%)$ and for any values larger than 40% were supplied similarly for the proportion of time of all controllers.

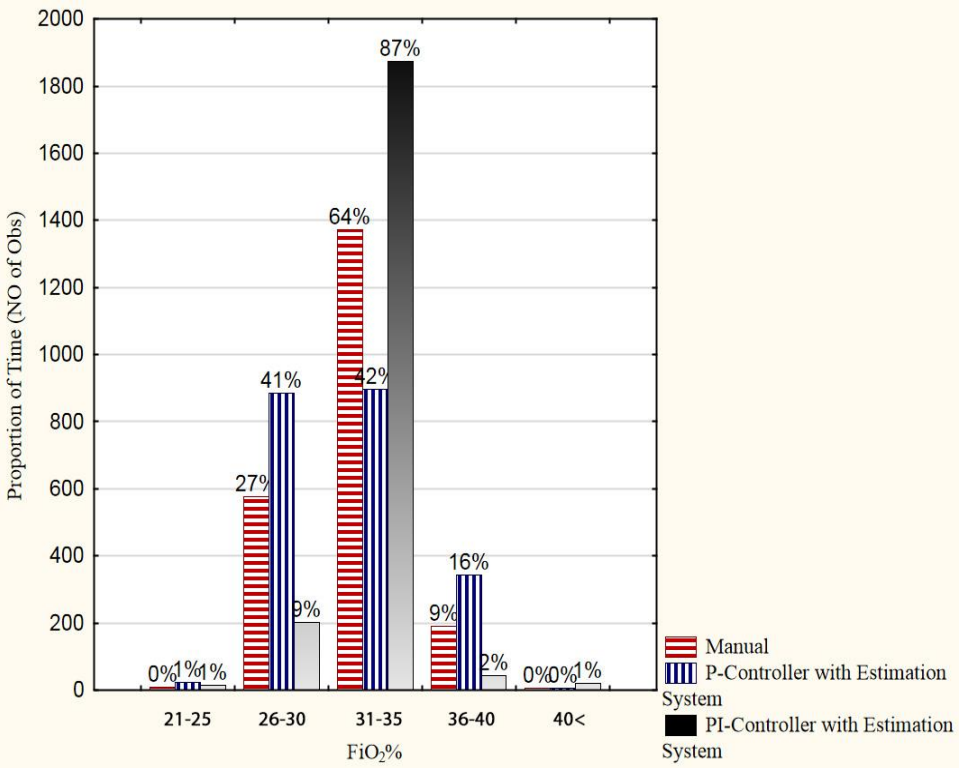

Fig. 3-10: Histogram of FiO_2 during 3-hour period for each control algorithm

For the two automated control algorithms, the difference between the estimated SpO_2 values and the desired value of SpO_2 (90%) are graphically compared to the difference between the observed SpO_2 of the TF and the desired value. It is evident, from Fig. 3-11 and Fig. 3-12, that the estimation of the SpO_2 difference during the use of both automated control algorithms shows good estimation performance. On the other hand, the disturbance estimator performances were different during the test of each automatic controller. The estimated disturbances were closer to the applied disturbances while using the PI-control. Fig. 3-13 and Fig. 3-14 show the applied disturbance versus estimated disturbance for the P-controller and PI-controller with the estimation system, respectively.

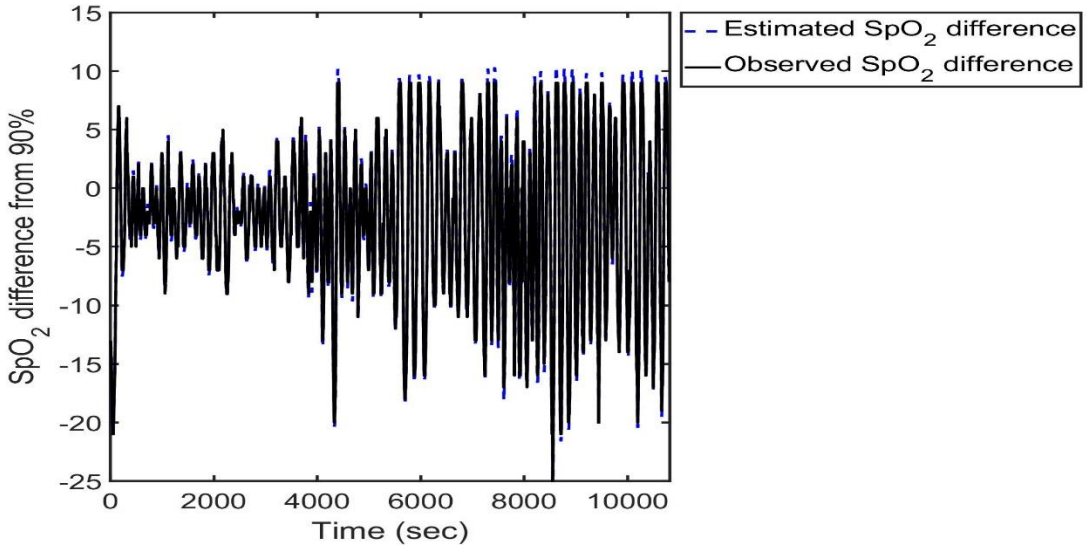

Fig. 3-11: Estimated versus Observed SpO_2 for P-Controller with Estimation System

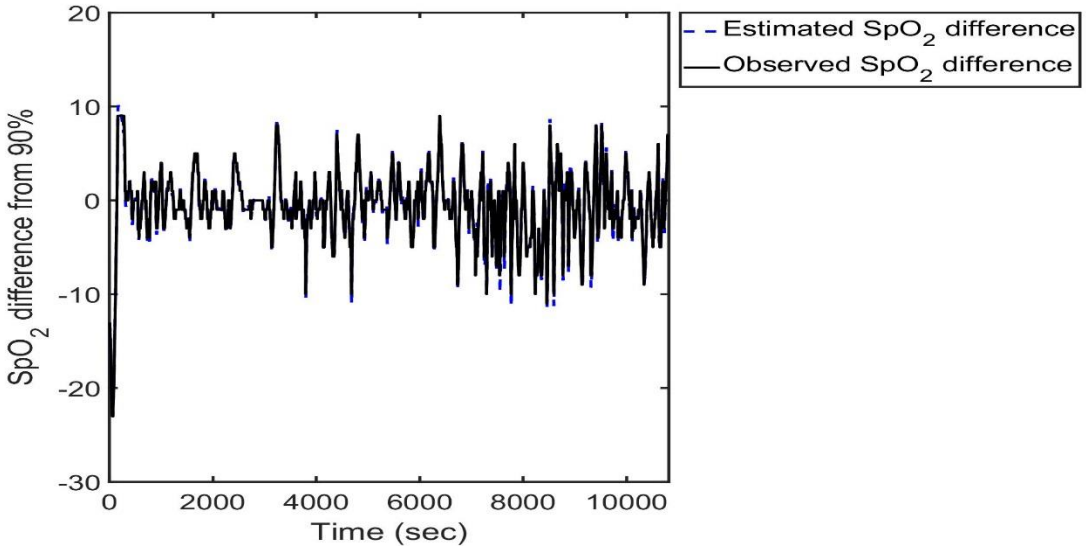

Fig. 3-12: Estimated versus Observed SpO_2 for PI-Controller with Estimation System

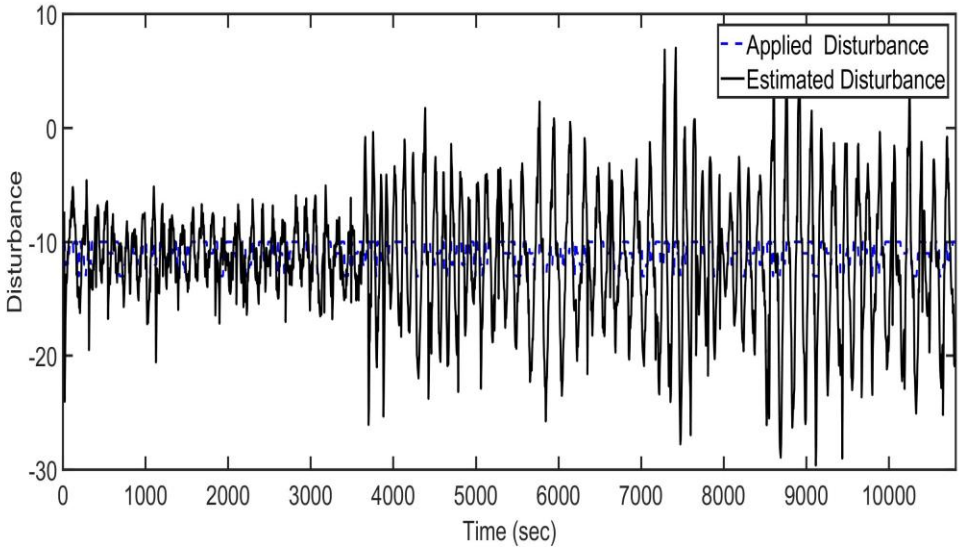

Fig. 3-13: Estimated disturbance versus applied disturbance while using P-Controller with Estimation System

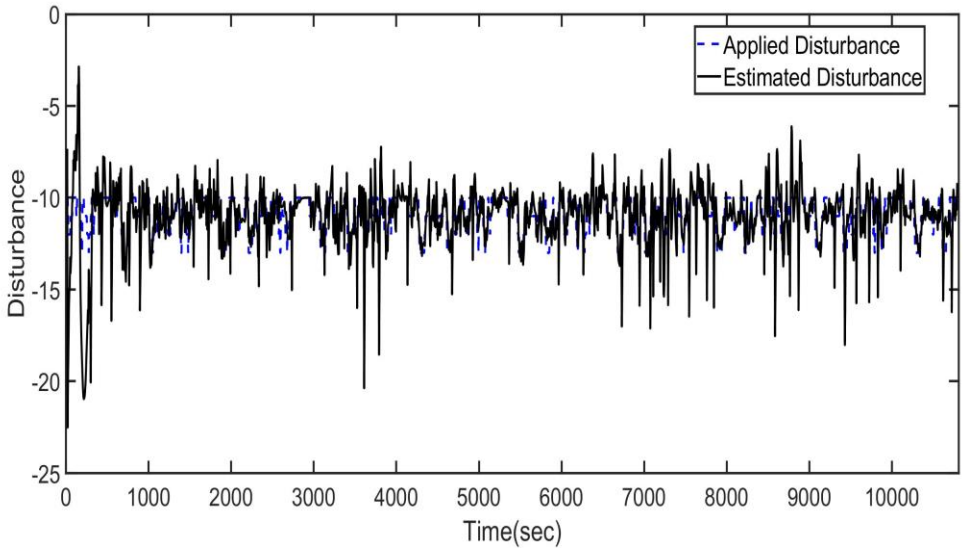

Fig. 3-14: : Estimated disturbance versus applied disturbance while using PI-Controller with Estimation System

The percentages of time, where the estimated gain was within 0.5 error limit, were calculated for both automated algorithms. The DP-EEKF estimated 55% of the time where the gain was within 0.5 error limit during the use of PI-controller. In contrast, it estimated

within the limit of 33% of the time during the use of the P-Controller. The performances of DP-EEKF at estimating the gain while using both automated algorithms are shown in Fig. 3-15 and Fig. 3-16. The DP-EEKF was slightly better at estimating the time constant while using the P-control. Fig. 3-17 and Fig. 3-18 show the performances of DP-EEKF at estimating the time constant for both used automated algorithms. Finally, the graphical comparison of the desired encoder position to the observed encoder position shows no functional failure since they were almost the same in Fig. 3-19 and Fig. 3-20.

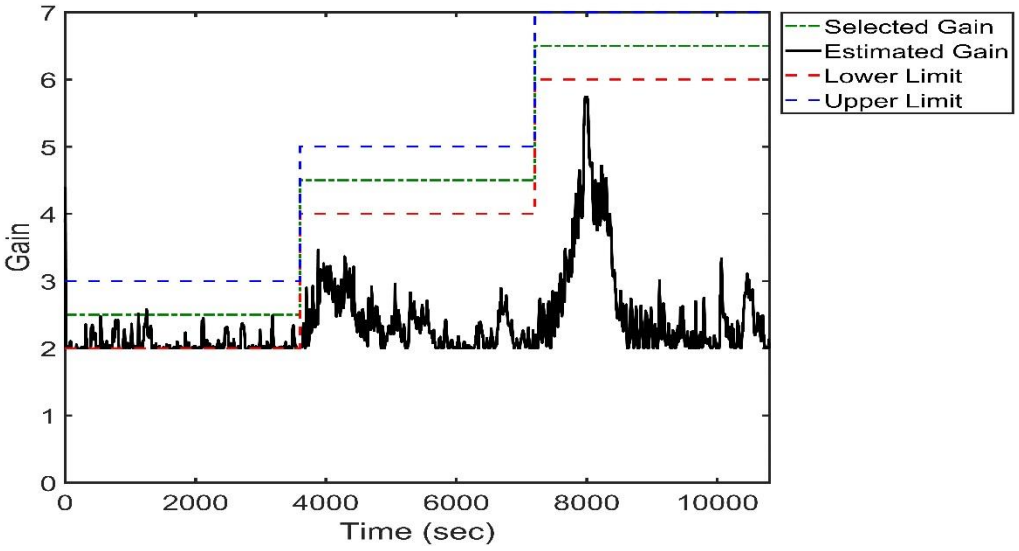

Fig. 3-15: The estimated gain during the use of P-Controller with Estimation System

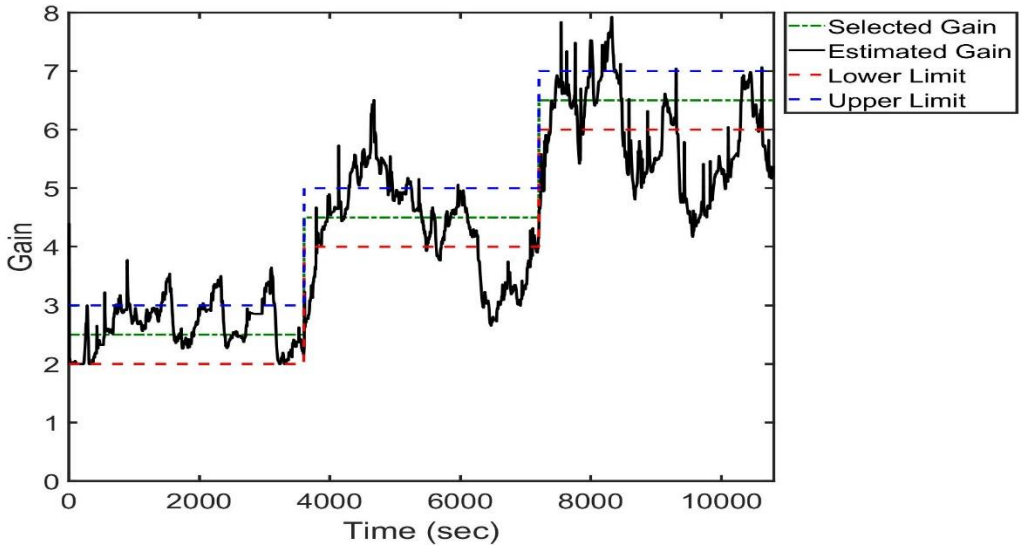

Fig. 3-16: The estimated gain during the use of PI-Controller with Estimation System

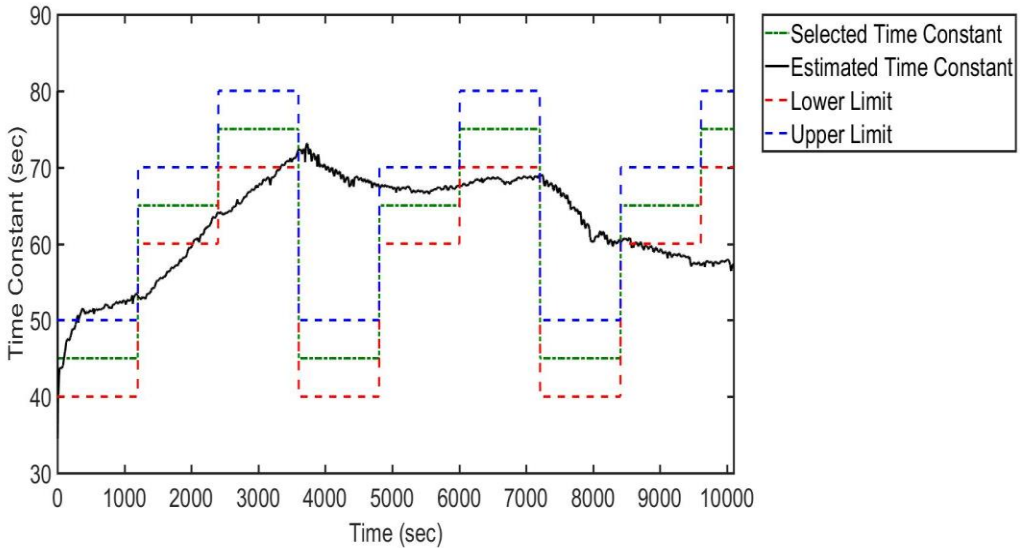

Fig. 3-17: The estimated time constant during the use of P-Controller with Estimation System

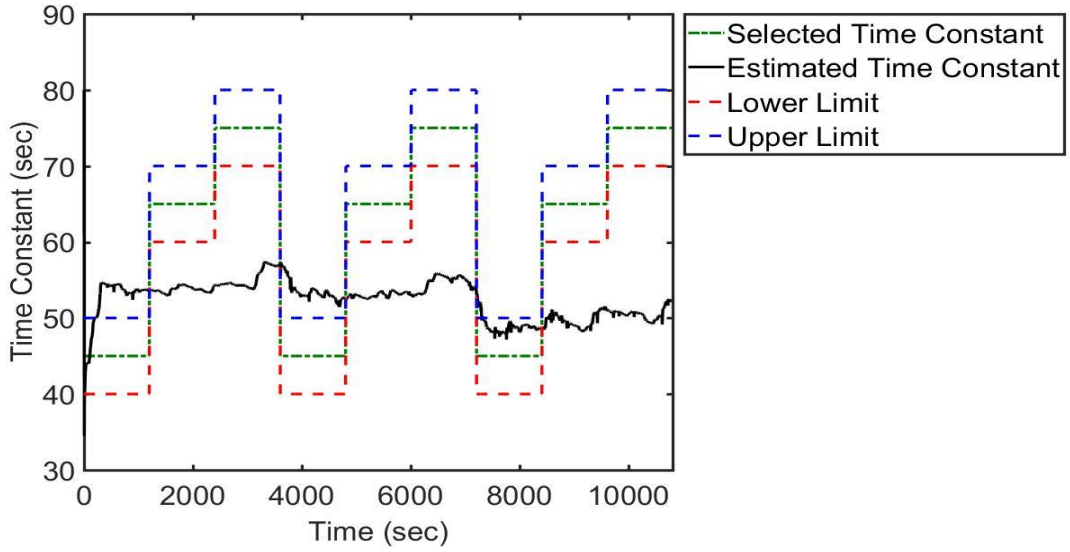

Fig. 3-18: The estimated time constant during the use of PI-Controller with Estimation System

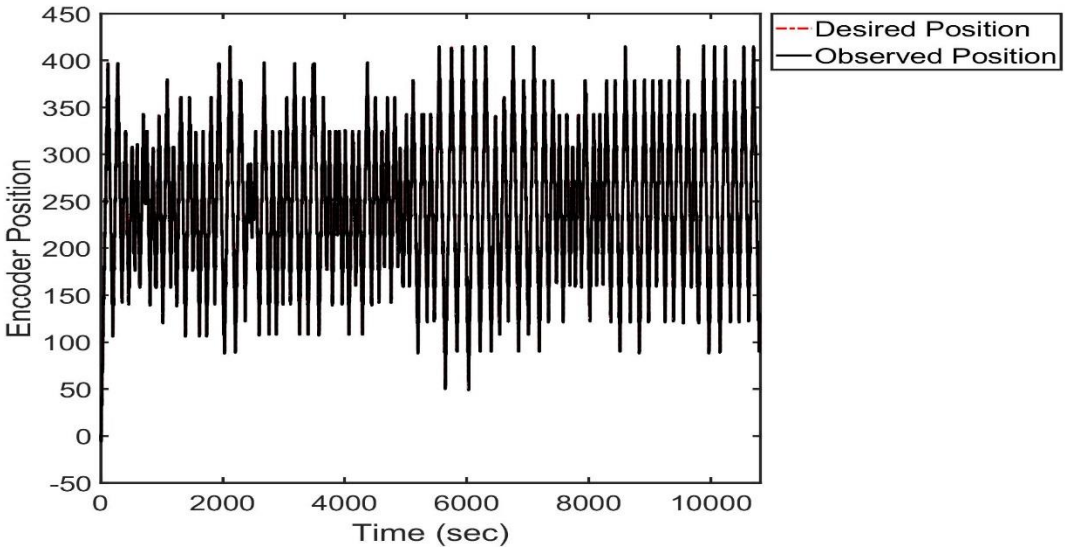

Fig. 3-19: Desired versus Observed encoder position during the use P-Controller with Estimation System

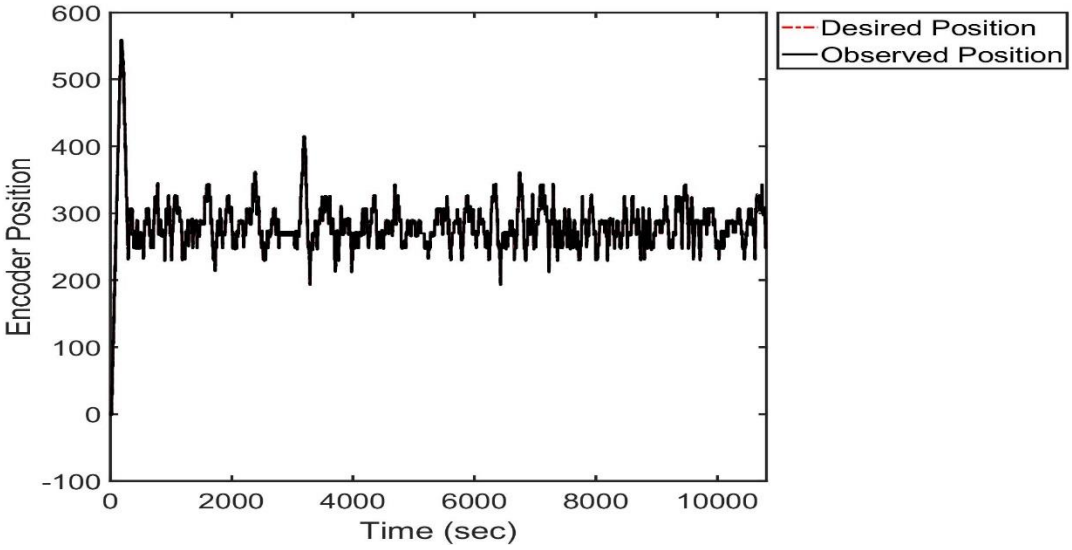

Fig. 3-20: Desired versus Observed encoder position during the use of PI-Controller with Estimation System

3.7 Discussion

The functional automatic arterial oxygen controller requires an algorithm that is capable of responding promptly to the variations of SpO_2 with minimal fluctuation. Also, the software and the hardware of the controller must function with no mechanical or communication failure. By the implementation of the non-clinical hard-ware-in-the-loop evaluation, we found that the adaptive PI-controller could make timely responses to SpO_2 variations and could improve the proportion of time while SpO_2 of the neonatal respiratory model within the desired target range.

Comparing the adaptive PI-controller and P-controller in addition to the manual control, the minimum CV of SpO_2 (4.17) was found while using the PI-controller. This finding distinctly shows the ability to reduce the fluctuation level of the SpO_2 while PI-controller in use. The CV of SpO_2 was (7.77) for P-controller and (6.19) for developed manual control. As a result of this, the PI-controller was more successful at minimizing the

frequency and duration of episodes of SpO_2 outside of the target range comparing to the other two control algorithms. Also, we found that the PI-controller significantly reduced the episodes of hypoxemia. However, the P-controller significantly increased these episodes compared to the other two control algorithms. Further, the other episodes of prolonged hypoxemia, hyperoxemia, prolonged hyperoxemia, and overshoot were not significantly reduced. However, the reported descriptive statistics (median and IQR) show the lowest values while using the PI-controller.

It is noticeable from the results section that PI-controller and manual control were supplying the model with more appropriate FiO_2 range ($31\% - 35\%$) for the larger period. Therefore, their overall performance at targeting the desired range was better than the P-controller. Also, the low supplying level of FiO_2 ($21\% - 30\%$) was found while using P-controller and manual control which resulted in the greater proportion of time where SpO_2 was below the lower target range limit ($SpO_2 < 87$) with higher frequent episodes and longer period. Similarly, the supplying higher level of FiO_2 range ($36\% - 40\%$) was responsible for generating more episodes and a longer period where SpO_2 was above the upper target range limit ($SpO_2 > 93$) which is directly related to the increasing of the proportion of time where SpO_2 was above the upper limit.

In this non-clinical hardware-in-the-loop test, the PI-controller shows better performance, compared to the P-controller and manual control, in mitigation of the episodes where SpO_2 values were not within the target range. The possible reason is that the PI-controller can reduce the steady-state error by using K_i, which is the proportional gain on the integral of the history of the error. On the other hand, increasing K_P while using P-controller is the possible way to decrease steady-state error, which might stimulate

system instability especially in the presense of a time delay due to the sample rate of the sensors and other factors. The difficulty of promptly response to the variations of SpO_2 is the most likely reason for manual control.

Further, the utilized estimation system was more compatible with PI-controller. The disturbance estimator was much more accurate in estimating the applied disturbances while using the PI-controller than during use of the P-controller. Therefore, the DP-EEKF shows a clear trend and better performance at estimating the designed gains. While during the use of P-controller, DP-EEKF was insufficient to develop a short trend of gain estimation. In the current automatic control algorithms, both disturbance and gain estimator were actively used to develop the control signal of the controller. As a result of this compatibility between the PI-controller and the estimation system, the overall performance of PI-controller was superior in this evaluation.

The poor estimation of the time constant did not affect the performance of either of the used automatic control algorithms since the estimated time constant is not used in the current automated control algorithms. However, it is considered for further research purposes and future improvements to this work in the area of control design. It is worth mentioning that the extended Kalman filter estimation is based on a linearization about the current estimate [98]. Thus, the indicated poor performance while using the P-controller with its fast-varying dynamic response might be related to the principle that a poor prior or later estimation leads to movement of the filter off the linear region, which generates the inaccurate estimations.

The developed manual control was used for comparison purposes and for examining the capability of the device to switch safely to manual control and efficiently

operate. There was no functional failure while operating under automatic modes or manual mode. During the automatic controller operation, the desired position of the encoder (which is based on the control signal) was compared to the observed encoder position (which is measured through an encoder on the DC motor). This comparison highlighted the ability of the device to function with no mechanical or communication failure.

At least in this hardware-in-the-loop test, the PI-controller with the estimation system was effective in maximizing the proportion of time where SpO_2 of the neonatal respiratory model is within the prescribed target range. The significant difference in minimizing the number of episodes where SpO_2 is out of the target range and their durations were indicated. The neonatal respiratory model used to evaluate the performance of the closed-loop respiratory device provides the advantage of comparing different control algorithms by using typical, challenging, and comprehensive model behavior. To the best of our knowledge, no other automatic controller based on a discrete disturbance estimator and DP-EEKF has ever been experimentally non-clinically or clinically evaluated. Based on the performance investigation in this study, the adaptive PI-controller deserved to be evaluated clinically.

Chapter 4 : Clinical Investigation of the Performance of an Automatic Arterial Oxygen Controller

In this chapter, the clinical investigation of the performance of the automatic controller is introduced. The study settings, protocol, and data collection and analysis of the clinical study are presented. Finally, the results and discussion of the clinical investigation are presented.

4.1 Clinical Investigation of the Performance

The clinical investigation is crucial study stage for such an automatic controller to be evaluated in NICU. The primary objective was demonstrating the clinical feasibility of the controller in NICU in a study with two human subjects at two different target range of SpO_2. The analyses were applied to the data that was collected in NICU to show (a) the ability of the automatic device to performs better or at least similar to the manual care at targeting the SpO_2 prescribed range, (b) the stability of the system's response and avoiding both hypoxemic and hyperoxaemic episodes, and (c) the ability to transition smoothly from automatic to manual mode and vice versa.

4.2 Experiment Setup of the Clinical Trial

The experimental setup of the clinical trial is shown in Fig. 4-1. The medical air and oxygen gas cylinders are connected to the Air-Oxygen blender. The mixed air, from Air-Oxygen blender, flow through both adjustable flow meter to the oxygen sensor that attached to heater humidifier. Through high flow nasal cannula, the preterm infant received FiO_2. The computer with microcontroller and data acquisition system, which is running the algorithm code that was developed by using LabVIEW®. and MATLAB®, can collect

SpO_2 from the baby through a pulse oximeter. Based on the received data and control algorithm, a control signal is sent to the amplifier, and then to the DC motor that deriving the shaft by mean of the miter gears. The shaft is attached to the control knob and helical shaft coupler, in a way that the Air-Oxygen blender supply the mixed air with adjusted percentage of FiO_2 to maintain SpO_2 within the prescribed range. The manual override is possible to be switched to manual control. The FiO_2 developed by the blend valve is received through an oxygen analyzer and recorded along with other measurements.

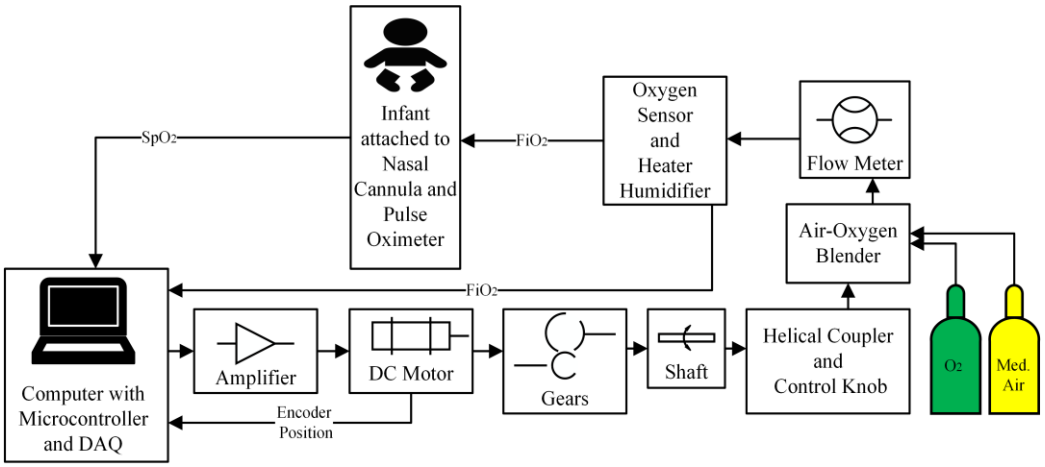

Fig. 4-1: Schematic of the experimental setup of the clinical trial

4.3 Study Settings and Subjects

The study was conducted at the NICU of the MU Women's and Children's Hospital. The study was approved by the local institutional review board (IRB), and the control device was inspected by the clinical engineering department of the hospital.

Preterm infants with RDS and requiring supplemental oxygen through high flow nasal cannula and gestational age $<$ 31 weeks or less than 1500 g at birth with no heart defects were eligible for the study. A written informed parental consent was obtained for enrollment in the study. Two human subjects, who met the inclusion criteria, were enrolled in the study. However, the enrolled subjects were requiring supplemental oxygen through

high flow nasal cannula at two different target ranges and two different flow rates. The human subject I was set at a lower target range $(87\% - 94\%)$ with a flow rate of 4 L/min. The human subject II was set at a higher target range $(91\% - 99\%)$ with a flow rate of 2 L/min.

4.4 Study Protocol

This study was designed as crossover clinical trial in NICU at Women's and Children's' Hospital. The two major advantages of the crossover design are that it eliminates the interpatient variability and allows within-subject comparison between treatments [81, 89]. The timeline of this study consisted of 4 consecutive periods. A 3-hour period of routine manual oxygen control followed by a 3-hour period of automated control, and then the cycle was repeated totaling a 12-hour period. The carryover effects were not considered in this crossover clinical trial because of the low possibility of the result to be contaminated with the previous control algorithm [22].

Before starting the clinical trial, NICU team members at MU Women's and Children's Hospital was informed of the study objectives and procedures including but not limited to the intended SpO_2 ranges of both manual and automated control and the procedure of transitions from automatic to manual control and vice versa before starting the trial. The manual care providers (nurses) were instructed to use their everyday routine approach during the manual mode. While the study was taking place at NICU, the nurse/infant ratio was about $1:3$ in the NICU at MU Women's and Children's Hospital. During the clinical trial, two or three members of the research team were available for ensuring the functionality of the automatic controller and for consultation about the device if needed.

4.5 Data Collection and Analysis

Monitor variables including SpO_2, FiO_2, and heart rate (HR) was recorded every 5 seconds during both manual and automatic control. The offline analysis allowed for comparison of clinical feasibility of the automatic controller, to manual care, at maintaining SpO_2 of the enrolled subject within a target range and minimizing its variability.

The proportion of recorded time in the following oxygenation states was calculated and displayed in the histogram for both manual and automated control for subject I: SpO_2 within the target range ($87\% \leq SpO_2 \leq 94\%$), below the lower limit of the target range ($SpO_2 < 87\%$), above the lower limit of the target range ($SpO_2 > 94\%$), in hypoxia ($SpO_2 < 75\%$), and in hyperoxia ($SpO_2 > 98\%$) [56]. For subject II, SpO_2 within the target range ($91\% \leq SpO_2 \leq 99\%$), below the lower limit of the target range ($SpO_2 < 91\%$), above the lower limit of the target range ($SpO_2 > 99\%$).

Further, the variability of SpO_2 was evaluated by calculating the following for both manual and automated control of the enrolled subjects: (a) coefficient of variation (CV) over the 6-hour period of each control mode, (b) frequency episodes where SpO_2 outside the target range per 1-hour, (c) mean duration of that episodes in seconds, and (d) frequency of episodes of hypoxemia ($SpO_2 < 80\%$), prolonged hypoxemia ($SpO_2 < 80\%$ for ≥ 60 seconds), hyperoxemia ($SpO_2 > 95\%$), prolonged hyperoxemia ($SpO_2 > 95\%$ for ≥ 60 seconds), and SpO_2 overshoot ($SpO_2 > 95\%$ lasting for at least 60 seconds and occurring within 120 seconds following a hypoxemic event) per 30-minute were calculated for each used control algorithm [51, 55, 57, 95, 97]. Small values of these calculated variables for the control algorithm indicate better performance at targeting the SpO_2 range with lower variability. Calculated data (b and c), of both subjects, meet the assumption of normality

except for the frequency episodes where $SpO_2 > 94\%$ and $SpO_2 \leq 80\%$ for the duration longer than 60 seconds for subject I. Also, episodes duration where $SpO_2 > 99\%$, $SpO_2 \leq 80\%$, and $SpO_2 = 100\%$ for the duration longer than 60 seconds for subject II did not meet the assumption of normality. Therefore, the performance of the two control modes was assessed by using paired t-test (normally distributed data) and Wilcoxon signed ranked test (not normally distributed data). These normally distributed compared data are reported as $\text{mean} \pm \text{SD}$. For not normal compared data, the results are reported as median and interquartile (IQR).

The power of avoiding type II error was calculated with considering normality for the considered variables. The episodes of bradycardia ($\text{HR} < 100$ beats/min, period ≥ 10 seconds) were detected for each control mode period [56]. Based on a collected data, an estimation of the number of subjects that are required for a power of $> 85\%$ is calculated. The histogram of FiO_2 levels in the 6-hour periods of both manual and automated mode were calculated. The normal probability plots combined with Shapiro-Wilk test results of SpO_2 frequency and mean duration where SpO_2 outside the target range are located in Appendix B.

4.6 Results

The subjects were enrolled for the study in the NICU at MU Women's and Children's Hospital. The experiment setup was successfully applied as described in Sec. 4.2. The study settings, subject, and protocol, as introduced in Sec. 4.3 and 4.4, were thoroughly followed. For minimizing interpatient variability and allowing within-subject comparison, the study was designed as crossover clinical trial. The 12-hour period of the clinical trial was completed with a total of 6-hour period of automatic and manual mode.

Fig. 4-2 and Fig. 4-3 show the recording of SpO_2 and FiO_2 for the 12-hour period while using both manual and automatic control for subject I and II. As shown, the clinical trial started with a 3-hour period while applying manual control then switched to automatic control for a 3-hour period and then the cycle was repeated for a 12-hour period in total.

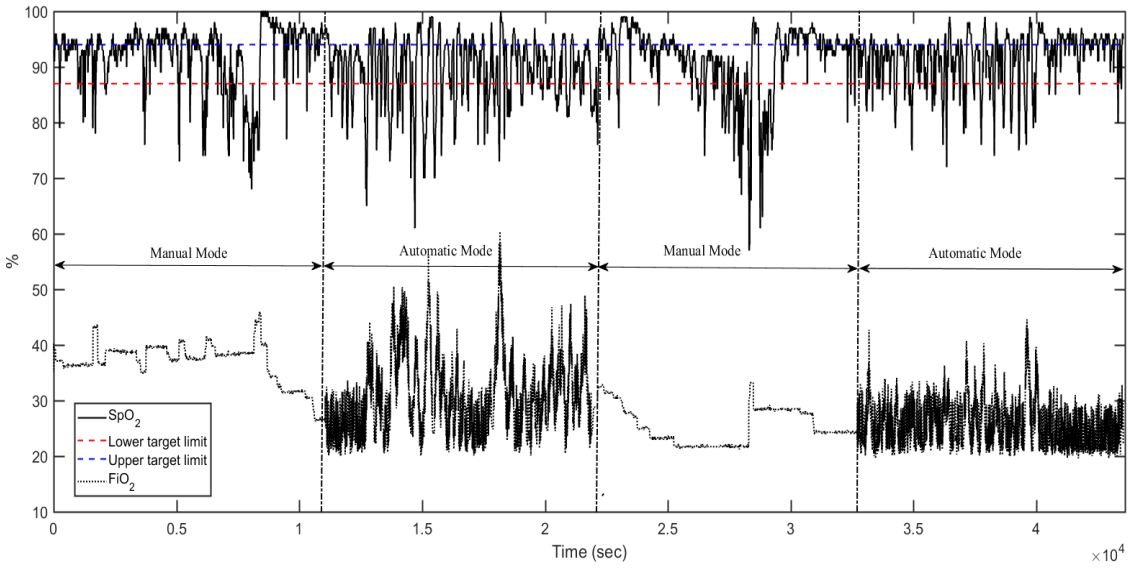

Fig. 4-2: The recording of SpO_2 and FiO_2 for the 12-hour period while using both manual and automatic control (Subject I)

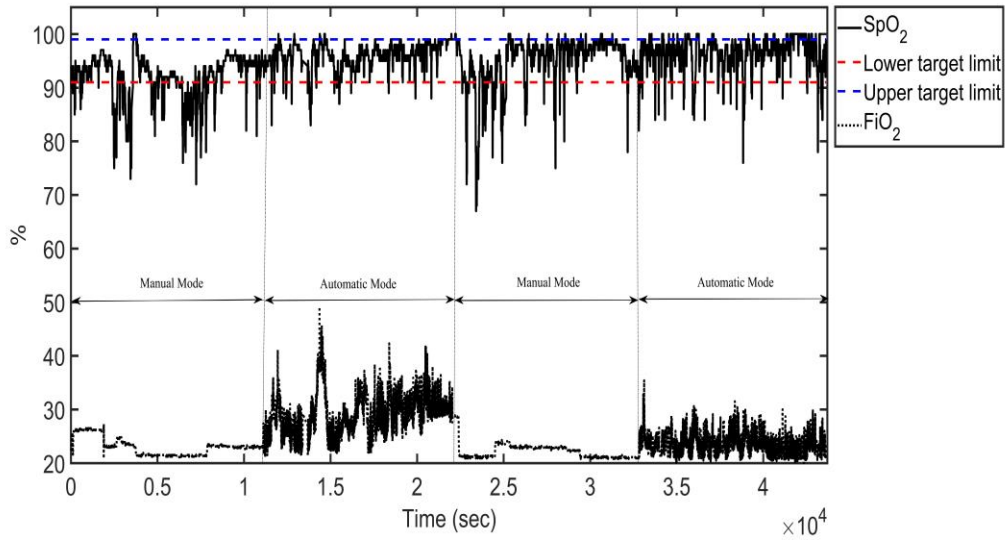

Fig. 4-3: The recording of SpO_2 and FiO_2 for the 12-hour period while using both manual and automatic control (Subject II)

The histogram of SpO_2 data of subject I (Fig. 4-4) shows an increase in the proportion of time within the target range while using automated control; 53% of the proportion of time was spent within the desired range. For the everyday manual routine care, 45% of the proportion of time was spent within the target range. Also, the automatic controller minimizes the proportion of time where the SpO_2 was above the upper limit of the target range (23%), in hyperoxia (1%), and hypoxia (2%). For the manual control, SpO_2 values were above the upper limit of the target range for 34%, and in hyperoxia and hypoxia for 3% of the proportion of time. However, manual control shows a smaller proportion of time when SpO_2 was below the lower limit of the target range (15%). For the automatic controller, SpO_2 values were below the lower limit of the target range for 21%.

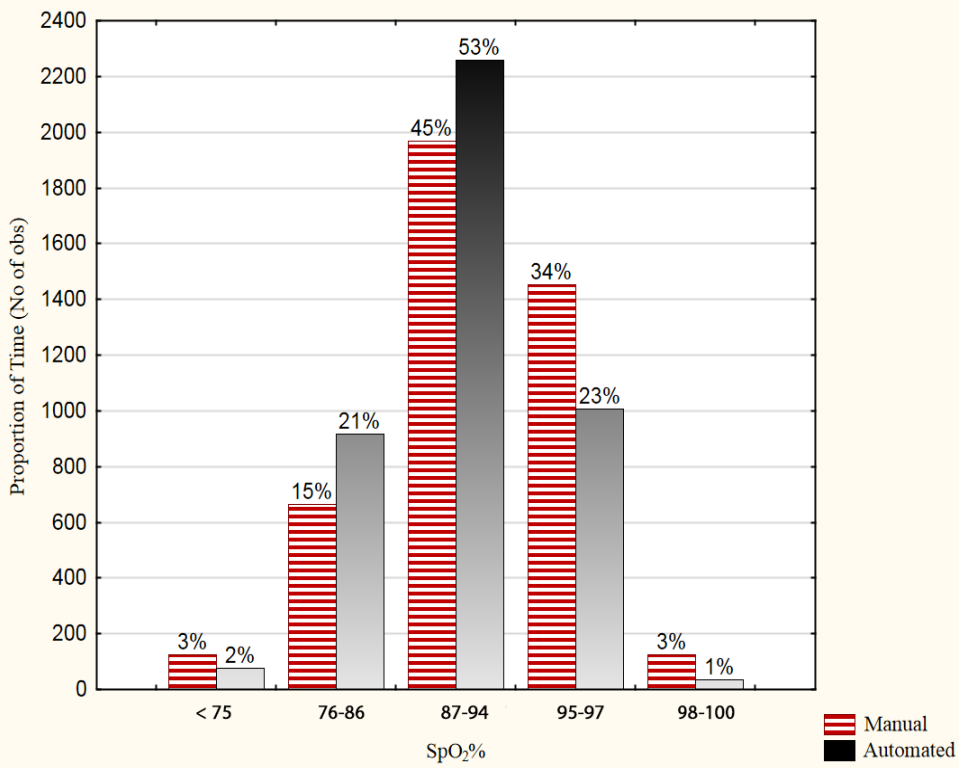

Fig. 4-4: Histogram of the proportion of time of SpO_2 within, below, and above the target range (87%-94%) for manual and automated control (Subject I)

The histogram of SpO_2 data of subject II (Fig. 4-5) shows an increase in the proportion of time within the target range while using automated control; 88% of the proportion of time was spent within the desired range. For the everyday manual routine care, 78% of the proportion of time was spent within the target range. However, the automatic controller failed to decrease the proportion of time where the SpO_2 was above the upper limit of the target range (7%). For the manual control, SpO_2 values were above the upper limit of the target range for only 2% of the proportion of time. The manual control shows a larger proportion of time when SpO_2 was below the lower limit of the target range (20%). For the automatic controller, SpO_2 values were below the lower limit of the target range for 5%.

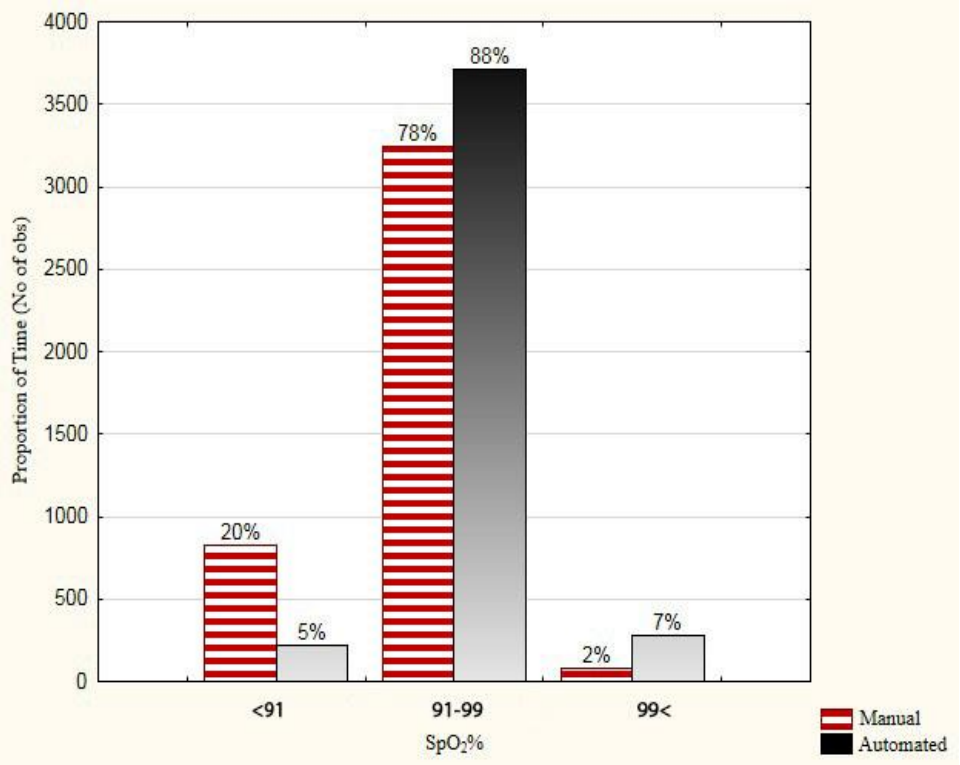

Fig. 4-5: Histogram of the proportion of time of SpO_2 within, below, and above the target range (91%-99%) for manual and automated control (Subject II)

Table 4-1 demonstrates the SpO_2 variability and heart rate of subject I. For the comparable calculated variables, no significant difference has been detected. However, the calculated power was less than 35% for all compared variables. For the frequency of the episodes $(SpO_2 < 87\%)$ and $(SpO_2 > 94\%)$, the calculated powers were 34.1% and 8.4%. For the mean duration of the episodes $(SpO_2 < 87\%)$ and $(SpO_2 > 94\%)$, the calculated powers were about 15% and 30%. The calculated CV for the automatic controller (6.24) slightly smaller than for manual control (6.72). The bradycardia events were detected twice while manual and one time during automatic control.

Table 4-1: SpO_2 variability and Heart Rate (Subject I)

	Manual Control	Automated Control	P-Value	Power
SpO_2 CV (%)	6.72	6.24	NA	NA
$SpO_2 < 87\%$ (episodes/1-hour)	9.67 ± 5.35	14.83 ± 4.49	0.13	34.1%
$SpO_2 < 87\%$ (episode duration, s)	69.45 ± 37.4	50.53 ± 20.09	0.39	15.44%
$SpO_2 > 94\%$ (episodes/1-hour)	$18(12 - 26)$	$11.5(11 - 14)$	0.46	8.4%[1]
$SpO_2 > 94\%$ (episode duration, s)	111.43 ± 84.01	53.48 ± 18.49	0.13	27.9%
Bradycardia (episodes/6-hour)	2	1	NA	NA
Normal Data: Mean±SD Non-Normal: Median(IQR)				

Table 4-2 demonstrates the SpO_2 variability and heart rate of subject II. For the comparable calculated variables, no significant difference has been detected. However, the calculated power was less than 66% for all compared variables. For the frequency of the episodes $(SpO_2 < 91\%)$ and $(SpO_2 > 99\%)$, the calculated powers were 24.65% and 21.07%. For the mean duration of the episodes $(SpO_2 < 91\%)$ and $(SpO_2 > 99\%)$, the calculated powers were about 66% and 9%. The calculated CV for the automatic controller (3.13) smaller than for manual control (5.34). The bradycardia events were detected twice while manual in use and none while automatic control in use.

[1] Calculated with normality assumption where Mean±SD was 17.17 ± 9.87 (Manual mode) and 14.17 ± 6.43 (Automatic mode).

Table 4-3 demonstrates that there are no significant differences in the frequency of hypoxemic, prolonged hypoxemic, hyperoxaemic, prolonged hyperoxaemic, and overshoot events while using the manual and automatic control for subject I. Table 4-4 shows that there is only significant difference in the frequency of hypoxemic events between the two control modes for subject II.

Table 4-2: SpO2 variability and Heart Rate (Subject II)

	Manual Control	Automated Control	P-Value	Power
SpO_2 CV (%)	5.34	3.13	NA	NA
$SpO_2 < 91\%$ (episodes/1-hour)	9.83 ± 5.04	6.17 ± 3.31	0.089	24.65%
$SpO_2 < 91\%$ (episode duration, s)	58.74 ± 26.33	24.84 ± 12.94	0.063	65.79%
$SpO_2 > 99\%$ (episodes/1-hour)	2.17 ± 1.72	7.17 ± 8.68	0.16	21.07%
$SpO_2 > 99\%$ (episode duration, s)	$18.09(10 - 31.5)$	$17.38(8.67 - 34.82)$	0.89	8.72%[2]
Bradycardia (episodes/6-hour)	2	0	NA	NA
Normal Data: Mean±SD Non-Normal: Median(IQR)				

[2] Calculated with normality assumption where Mean±SD was 31.45 ± 40.43 (Manual mode) and 19.71 ± 15.9 (Automatic mode).

Table 4-3: Hypoxemia, hyperoxemia, and overshoot episodes (Subject I)

	Manual Control	Automated Control	P-Value	Power
$SpO_2 \leq 80\%$ (episodes < 60 s duration/1-hr)	6 ± 4.43	5 ± 3.79	NS	6%
$SpO_2 \leq 80\%$ (episodes ≥ 60 s duration/1-hr)	$1(1-1)$	$0(0-2)$	NS	8.86%[3]
$SpO_2 \geq 95\%$ (episodes < 60 s duration/1-hr)	11.33 ± 8.52	9.17 ± 3.76	NS	7.75%
$SpO_2 \geq 95\%$ (episodes ≥ 60 s duration/1-hr)	5.33 ± 2.88	5.5 ± 3.67	NS	5%
Overshoot (episode duration, s)	1 ± 0.89	2.16 ± 2.64	NS	13.87%
Normal Data: Mean±SD Non-Normal: Median(IQR)				

Table 4-4: Hypoxemia, hyperoxemia, and overshoot episodes (Subject II)

	Manual Control	Automated Control	P-Value	Power
$SpO_2 \leq 80\%$ (episodes < 60 s duration/1-hr)	$2.5(2-4)$	$0(0-1)$	< 0.05	NA
$SpO_2 \leq 80\%$ (episodes ≥ 60 s duration/1-hr)	NA	NA	NA	NA
$SpO_2 \geq 95\%$ (episodes < 60 s duration/1-hr)	1.83 ± 1.72	5.33 ± 5.99	NS	21.13%
$SpO_2 \geq 95\%$ (episodes ≥ 60 s duration/1-hr)	$0(0-1)$	$0(0-2)$	0.16	21.07%[4]
Overshoot (episode duration, s)	NA	NA	NA	NA
Normal Data: Mean±SD Non-Normal: Median(IQR)				

[3] Calculated with normality assumption where Mean±SD was 1 ± 0.63 (Manual mode) and 0.67 ± 1.03 (Automatic mode).
[4] Calculated with normality assumption where Mean±SD was 0.33 ± 0.52 (Manual mode) and 1.67 ± 2.04 (Automatic mode).

Table 4-5 shows the required sample size and the estimated number of human subjects for power goal higher than 85% based on the analysis of the clinical data for subject I. For the frequency of the episodes ($SpO_2 < 87\%$), enrolling three preterm infants were estimated to evaluate the significant difference. While the frequency of the episodes ($SpO_2 > 94\%$), a number of twenty-two preterm infants was estimated. For the mean duration of the episodes ($SpO_2 < 87\%$), eight preterm infants were estimated for assessing the significant difference. While the mean duration of the episodes ($SpO_2 > 94\%$), four preterm infants were estimated. Charts of the required sample size versus the power goal for the compared variables of subject I are in Appendix C.

Table 4-5: Calculated Sample Size at 85% of power and Estimated Number of Required Subjects for Power >85% (Subject I)

	Sample Size at 85% of Power	Estimation Number of required Subjects for Power > 85%
$SpO_2 < 87\%$ (episodes/1-hour)	17	3
$SpO_2 < 87\%$ (episode duration, s)	44	8
$SpO_2 > 94\%$ (episodes/1-hour)	128	22
$SpO_2 > 94\%$ (episode duration, s)	21	4

Table 4-6 shows the required sample size and the estimated number of human subjects for power goal higher than 85% based on the analysis of the clinical data for subject II. For the frequency of the episodes ($SpO_2 < 91\%$), enrolling five preterm infants were estimated to evaluate the significant difference. While the frequency of the episodes ($SpO_2 > 99\%$), a number of six preterm infants was estimated. For the mean duration of the episodes ($SpO_2 < 91\%$), two preterm infants were estimated for assessing the

significant difference. While the mean duration of the episodes ($SpO_2 > 99\%$), eighteen preterm infants were estimated. Charts of the required sample size versus the power goal for the compared variables of subject II are in Appendix D.

Table 4-6: Calculated Sample Size at 85% of power and Estimated Number of Required Subjects for Power >85% (Subject II)

	Sample Size at 85% of Power	Estimation Number of required Subjects for Power > 85%
$SpO_2 < 91\%$ (episodes/1-hour)	25	5
$SpO_2 < 91\%$ (episode duration, s)	9	2
$SpO_2 > 99\%$ (episodes/1-hour)	31	6
$SpO_2 > 99\%$ (episode duration, s)	107	18

The histogram of FiO_2 for subject I (Fig. 4-6) illustrate the infant was supplied with the range of FiO_2 $(21\% - 25\%)$ for the proportion of time equal 39% for automatic control and 27% for manual control. The range of FiO_2 $(26\% - 30\%)$ was supplied for the proportion of time equal 30% for automatic control and 19% for manual control. The range $(31\% - 35\%)$ was supplied for the proportion of time equal 18% for the automatic controller and 14% for the manual control. The range of FiO_2 $(36\% - 40\%)$ was supplied for the proportion of time equal 8% for automatic control and 35% for manual control. For any value of FiO_2 larger than 40% was supplied for the proportion of time was 5% for both control modes.

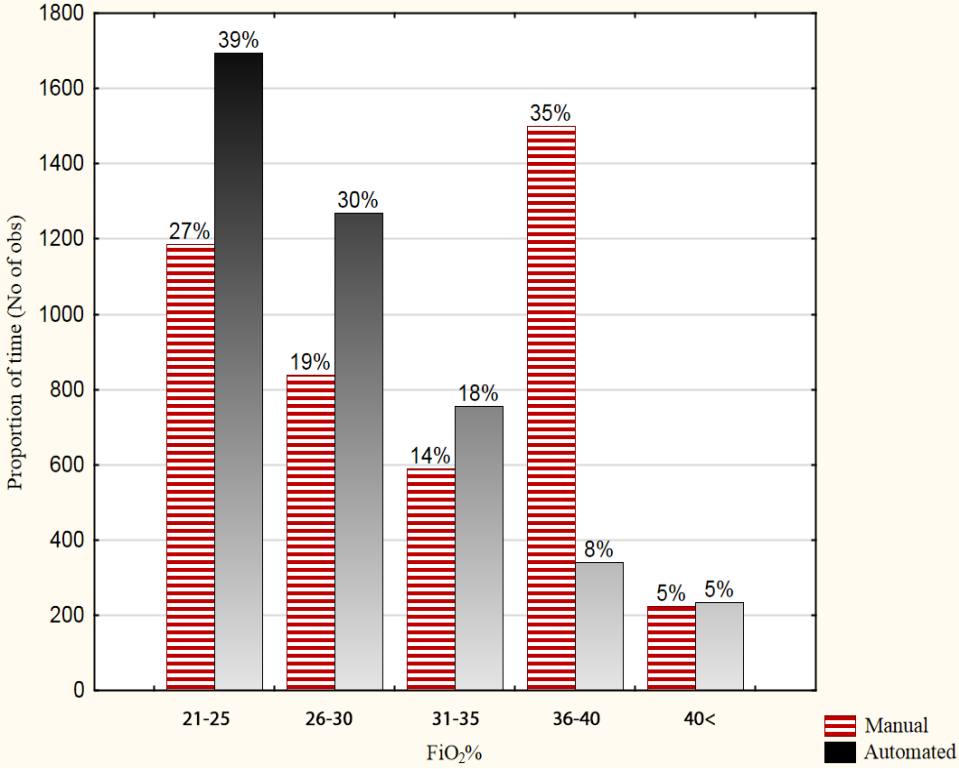

Fig. 4-6: Histogram of FiO_2 during the 6-hour manual and automated control (Subject I)

The histogram of FiO_2 for subject II (Fig. 4-7) illustrate that the infant was supplied with the range of FiO_2 $(21\% - 25\%)$ for the proportion of time equal 52% for automatic control and 89% for manual control. The range of FiO_2 $(26\% - 30\%)$ was supplied for the proportion of time equal to 32% for automatic control and 10% for manual control. The range $(31\% - 35\%)$ was supplied for the proportion of time equal to 13% for the automatic controller and 0% for the manual control. For any value of FiO_2 larger than 35% was supplied for the proportion of time was 4% for the automatic control while no such a value detected while manual control.

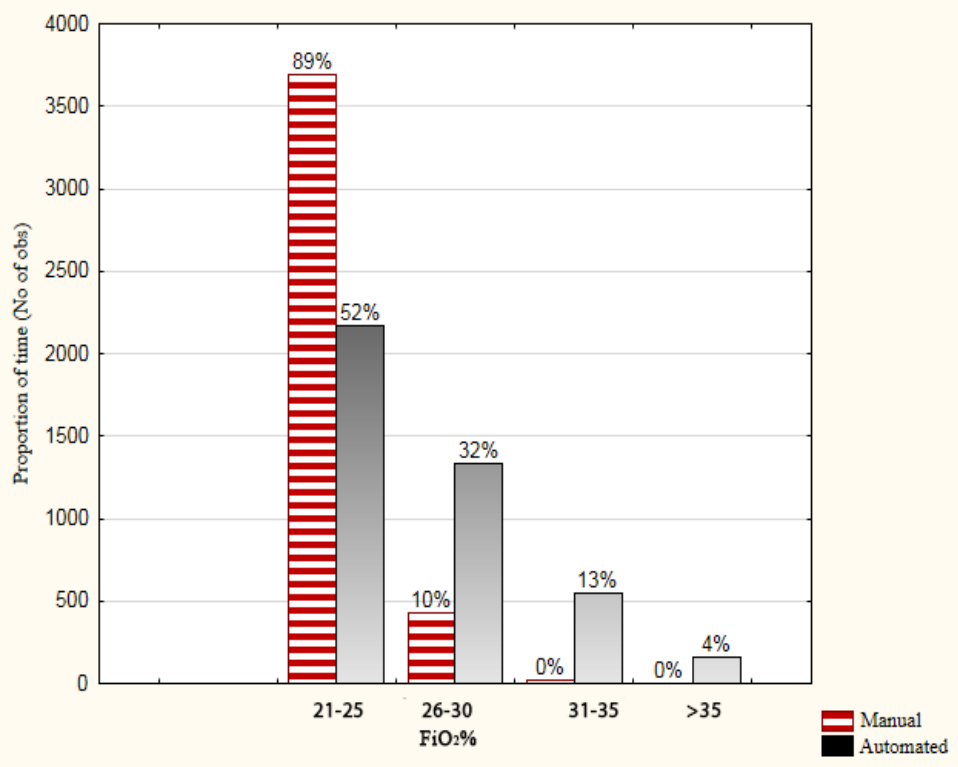

Fig. 4-7: Histogram of FiO_2 during the 6-hour manual and automated control (Subject II)

4.7 Discussion

The two human subjects were considered for a crossover clinical trial at the NICU of the Women's and Children's Hospital. The design and algorithm of the controller were successfully shown to have the ability to transition from automatic to manual control, and vice versa. The transition feature allows the controller to be utilized for assisting clinicians in NICUs since fully substituting manual care with any automatic control is not likely to be accepted for all cases [14, 15, 17, 21]. The data in Fig. 4-2 and Fig. 4-3 show that there is no pronounced "bump" or step variation in the control signal and stability and performance are not adversely affected during the transitions between manual mode and automatic mode at hours 3, 6, and 9.

The automatic arterial oxygen controller shows the possibility of more effectively targeting the prescribed range of SpO_2 with lower exposure to FiO_2 for the saturation target

of 87% to 94% (subject I). For the saturation target of 91% to 99% (subject II), the automatic controller shows the possibility of improving the process of targeting the desired range but with higher exposure to FiO_2. The higher exposure to FiO_2 resulted in an insignificant higher number of ($SpO_2 > 99$) episodes for subject II. The automatic controller showed prompt responses to the variations in the SpO_2. Conversely, the manual care showed slow responses to these variations. An apparent high step adjustment was indicated during the second period of manual mode (Fig. 4-2), for subject I, as a response to very low level of SpO_2. The reason for that severe very low level of the infant SpO_2 was the manual late response when the reduction was initiated. The slow response of the manual care might be because of the lower nurse to patient ratio which was highlighted previously [11].

The automatic controller increased the proportion of time spent within the prescribed range by 8% for subject I and by 10% for subject II compared to manual care. As a result, it decreased the proportion of time spent outside the desired range. Regardless of the calculated P-value and by purely considering the $\text{mean} \pm \text{SD}$ for normally distributed data and median (IQR) for not normally distributed data, we can notice the performance for both control algorithms at minimizing the unfavorable episodes. For subject I where the target range was $87\% - 94\%$, the SpO_2 values were lower than the target range more frequent in automatic mode but with shorter durations. The shorter duration of the episodes, while in automatic mode, indicates that the recovery of these episodes was faster in automatic mode than in the manual mode. This finding is similar to the results discussed in another study that had a larger number of human subjects and had applied different automatic control algorithms [15, 57]. For subject II where the target

range was $91\% - 99\%$, the controller successfully decreased the number and duration of the episodes where the SpO_2 was below the lower limit of the target range.

Further, the automatic controller was able to reduce the frequency and period of episodes where SpO_2 values were above the target range for subject I. These reductions during the automatic mode were because of the lower exposure to FiO_2, which is demonstrated in Fig. 4-6, such reductions help avoid serious lung, brain, and retinal damage [4, 5]. Conversely, the SpO_2 values were higher than the target range more frequently in automatic mode for the higher target range (subject II). The duration of these episodes was sort of similar while using both manual and automatic control modes. The insignificant increase for these episodes because of the higher exposure to FiO_2 while using the automatic controller. However, the manual control was supplying a lower range of FiO_2 which decreased the proportion of time for the SpO_2 to be above the target range but seemingly increased the proportion of time for the SpO_2 to be below the lower limit of the target range which is reported as a reason for mortality [4, 15]. Also, the reduction of the hypoxemia was noticed for both subjects, and it was significant for subject II. However, the mean and the standard deviation of the overshoot for subject I suggest consideration of enhancing the current control algorithm to more quickly reduce FiO_2 after desaturation event recovery.

It is noticeable that the human subject with the lower target range was experiencing more severe RDS and was in need of more frequent adjustments of FiO_2. The higher variability of SpO_2 and the higher risk of mortality for preterm infants who are set at a lower target range of SpO_2 has been reported previously[22, 58, 99]. The episodes of bradycardia were more frequent while manual control was in use, for both enrolled human

subjects, compared to the automatic control. The slow response to the variation where SpO_2 was below the target range may be a factor in the detected number of bradycardia events during manual control because it was noticed, for both target ranges, that the bradycardia events existed while SpO_2 was much lower than the target range for a considerable amount of time [97].

The applied statistical tests show no significant difference between manual and automated control within one-subject comparison, which indicated that both control algorithms had a similar performance at minimizing undesirable episodes. However, the calculated power shows that there is a high possibility of type II as a result of a small number of sample size. Type II is failing to reject the null hypothesis when in fact it must be rejected [88]. In this study, the null hypothesis indicates similar performance between the manual and the automatic control. At least with these calculated power levels, the controller shows similar performance to the manual control.

To increase the power level up to 85% and to detect any significant difference in targeting SpO_2 range and reducing its variability, the required sample size was calculated. Based on the calculated sample size of subject I and subject II, an estimation of the number of human subjects was provided. The inclusion of 22 human subjects would be able to detect any significance or insignificance at a power level higher than 85% for the lower target range. The inclusion of 18 human subjects would be able to detect any significance or insignificance at a power level higher than 85% for the higher target range. However, the calculated sample size in this study was based only on the variability's variables that shown in Table 4-1 and Table 4-2. The inclusion of more human subjects allows further

power analysis with a consideration of the proportion time within the target range, the CV, and bradycardia.

At least in these clinical trials where the automatic arterial oxygen controller was applied to two human subjects, the clinical feasibility of the device was demonstrated. The crossover clinical trial provided the advantage of comparing within one-subject and of observing the transition from manual to automatic and vice versa. Based on the results, it is possible to conclude that the current automatic controller can improve the maintenance of targeting SpO_2 with lower exposure to FiO_2 for the low target range (subject I). Also, it can improve the maintenance of targeting SpO_2 with higher exposure to FiO_2 for the high target range. However, the 12-hour period of the clinical trials may not be representative of the number of days and weeks that most preterm infants require respiratory support in NICUs. To the best of our knowledge, no other automatic controller with same control algorithm or using parameter estimation has ever been clinically evaluated.

Chapter 5 : Conclusion and Future Work

5.1 Conclusion of the Non-Clinical Investigation

The results obtained from the current non-clinical study are restricted to the used neonatal respiratory model and the developed experimental design and procedure which are introduced in Sec. 3.4. The main conclusions drawn from the non-clinical study are as follows:

- The closed-loop respiratory support device based on the adaptive PI-controller was very efficient at targeting the desired SpO_2 range by applying automated adjustments of FiO_2, and deserves clinical evaluation.
- The PI-controller with the estimation system shows capability to make timely responses to the variations in SpO_2 with minimal instability as was shown in the variability table.
- The PI-controller with the estimation system was able to significantly reduce the number of hypoxemic events of the neonatal model.
- The estimation system based on the discrete disturbance estimator and the DP-EEKF was more compatible with the PI-controller compared to the P-controller and shows acceptable performance at estimating model gain and disturbance.
- The study demonstrates the functionality of the developed closed-loop device while applying the three used control algorithms.
- The results demonstrated the abilities to transition from automatic to manual and vice versa and to operate in a manual mode with no conflict to the other integrated electrical, mechanical, and medical components.

5.2 Conclusion of the Clinical Investigation

The results obtained from the current clinical trial are limited to the study setting, subject, and protocol which are introduced in Sec 4.3 and 4.4. The main conclusions drawn from the clinical study are as follows:

- The developed adaptive PI-controller shows clinical feasibility to improve the maintenance of SpO_2 within the intended target range with lower exposure to FiO_2 for the low target range and higher exposure to FiO_2 for the high target range and deserves more clinical evaluation.
- The statistical analysis shows the performance of the automatic controller was similar to the manual care.
- The descriptive statistic shows the potential of the oxygen controller to improve the maintenance of SpO_2 within the intended target range and to minimize the number of undesirable episodes and their periods.
- The results show the ability to transition smoothly from automatic to manual mode and vice versa which allows the device to assist the clinicians not fully substituting them.
- The power analysis recommends larger sample size to identify the significance at the higher power level.

5.3 Future Work

The present study provides further recommended research in investigating the performance of the closed-loop control device:

- The results and findings of the clinical trial part of this study with the inclusion of four human subjects allow developing a pilot clinical study that demonstrates the

clinical feasibility of the device at a higher power level and with consideration of more variables such as the proportion of time where SpO_2 is below, above, and within the target range.

- The calculated sample size provides researchers with a required number of human subjects to identify the significance of the performance at a power level higher than 85%.
- The experimental crossover design might be considered for a longer period for each control mode to be more representative of the actual case in the NICUs.
- The study shows the potential of the automatic controller to be considered for reliability analysis.
- A consideration of enhancing the control algorithm is recommended to improve the controller performance for the overshoot episodes.

REFERENCES

[1] Kenner, C., Lott, J. W., and Flandermeyer, A. A., 1998, Comprehensive neonatal nursing: A physiologic perspective, WB Saunders Co, Philadelphia, PA.
[2] Kenner, C., and Lott, J. W., 2007, Comprehensive neonatal care: An interdisciplinary approach, Saunders Elsevier Inc., St. Louis, MO.
[3] Gardner, S. L., Carter, B. S., Enzman-Hines, M., and Hernandez, J. A., 2011, Merenstein & gardner's handbook of neonatal intensive care, Mosby Elsevier Inc., St. Louis, MO.
[4] Silverman, W. A., 2004, "A cautionary tale about supplemental oxygen: The albatross of neonatal medicine," Pediatrics, 113(2), pp. 394-396.
[5] Tin, W., Milligan, D., Pennefather, P., and Hey, E., 2001, "Pulse oximetry, severe retinopathy, and outcome at one year in babies of less than 28 weeks gestation," Archives of Disease in Childhood-Fetal and Neonatal Edition, 84(2), pp. F106-F110.
[6] Hagadorn, J. I., Furey, A. M., Nghiem, T.-H., Schmid, C. H., Phelps, D. L., Pillers, D.-A. M., and Cole, C. H., 2006, "Achieved versus intended pulse oximeter saturation in infants born less than 28 weeks' gestation: The AVIOx study," Pediatrics, 118(4), pp. 1574-1582.
[7] Laptook, A., Salhab, W., Allen, J., Saha, S., and Walsh, M., 2006, "Pulse oximetry in very low birth weight infants: Can oxygen saturation be maintained in the desired range?," Journal of perinatology, 26(6), pp. 337-341.
[8] Ford, S. P., Leick-Rude, M. K., Meinert, K. A., Anderson, B., Sheehan, M. B., Haney, B. M., Leeks, S. R., Simon, S. D., and Jackson, J. K., 2006, "Overcoming barriers to oxygen saturation targeting," Pediatrics, 118(Supplement 2), pp. S177-S186.
[9] Lim, K., Wheeler, K. I., Gale, T. J., Jackson, H. D., Kihlstrand, J. F., Sand, C., Dawson, J. A., and Dargaville, P. A., 2014, "Oxygen saturation targeting in preterm infants receiving continuous positive airway pressure," The Journal of pediatrics, 164(4), pp. 730-736.
[10] Clarke, A., Yeomans, E., Elsayed, K., Medhurst, A., Berger, P., Skuza, E., and Tan, K., 2014, "A randomised crossover trial of clinical algorithm for oxygen saturation targeting in preterm infants with frequent desaturation episodes," Neonatology, 107(2), pp. 130-136.
[11] Sink, D. W., Hope, S. A. E., and Hagadorn, J. I., 2011, "Nurse: patient ratio and achievement of oxygen saturation goals in premature infants," Archives of Disease in Childhood-Fetal and Neonatal Edition, 96(2), pp. F93-F98.
[12] Collins, P., Levy, N., Beddis, I., Godfrey, S., and Silverman, M., 1979, "Apparatus for the servocontrol of arterial oxygen tension in preterm infants," Medical and Biological Engineering and Computing, 17(4), pp. 449-452.
[13] Beddis, I., Collins, P., Levy, N., Godfrey, S., and Silverman, M., 1979, "New technique for servo-control of arterial oxygen tension in preterm infants," Archives of disease in childhood, 54(4), pp. 278-280.
[14] Claure, N., 2007, "Automated regulation of inspired oxygen in preterm infants: oxygenation stability and clinician workload," Anesthesia & Analgesia, 105(6), pp. S37-S41.
[15] Bancalari, E., and Claure, N., 2012, "Control of oxygenation during mechanical ventilation in the premature infant," Clinics in perinatology, 39(3), pp. 563-572.

[16] Claure, N., and Bancalari, E., 2013, "Role of automation in neonatal respiratory support," Journal of perinatal medicine, 41(1), pp. 115-118.
[17] Claure, N., and Bancalari, E., 2013, "Automated closed loop control of inspired oxygen concentration," Respiratory care, 58(1), pp. 151-161.
[18] Hummler, H., Fuchs, H., and Schmid, M., 2014, "Automated Adjustments of Inspired Fraction of Oxygen to Avoid Hypoxemia and Hyperoxemia in Neonates–A Systematic Review on Clinical Studies," Klinische Pädiatrie, 226(04), pp. 204-210.
[19] Claure, N., and Bancalari, E., "Closed-loop control of inspired oxygen in premature infants," Proc. Seminars in Fetal and Neonatal Medicine, Elsevier, pp. 198-204.
[20] Claure, N., and Bancalari, E., 2015, "Oxygen saturation targeting by automatic control of inspired oxygen in premature infants," NeoReviews, 16(7), pp. e406-e412.
[21] Fathabadi, O. S., Gale, T. J., Olivier, J., and Dargaville, P. A., 2016, "Automated control of inspired oxygen for preterm infants: What we have and what we need," Biomedical Signal Processing and Control, 28, pp. 9-18.
[22] Mitra, S., Singh, B., El-Naggar, W., and McMillan, D. D., 2018, "Automated versus manual control of inspired oxygen to target oxygen saturation in preterm infants: a systematic review and meta-analysis," Journal of Perinatology.
[23] Solimano, A. J., Smyth, J. A., Mann, T. K., Albersheim, S. G., and Lockitch, G., 1986, "Pulse oximetry advantages in infants with bronchopulmonary dysplasia," Pediatrics, 78(5), pp. 844-849.
[24] Coté, C. J., Goldstein, E. A., Coté, M. A., Hoaglin, D. C., and Ryan, J. F., 1988, "A single-blind study of pulse oximetry in children," Anesthesiology, 68(2), pp. 184-188.
[25] Morozoff, P. E., Evans, R. W., and Smyth, J. A., "Automatic control of blood oxygen saturation in premature infants," Proc. Control Applications, 1993., Second IEEE Conference on, IEEE, pp. 415-419.
[26] Miksch, S., Seyfang, A., Horn, W., and Popow, C., "Abstracting steady qualitative descriptions over time from noisy, high-frequency data," Proc. Joint European Conference on Artificial Intelligence in Medicine and Medical Decision Making, Springer, pp. 281-290.
[27] Seyfang, A., Miksch, S., Horn, W., Urschitz, M. S., Popow, C., and Poets, C. F., "Using time-oriented data abstraction methods to optimize oxygen supply for neonates," Proc. Conference on Artificial Intelligence in Medicine in Europe, Springer, pp. 217-226.
[28] Urschitz, M. S., Horn, W., Seyfang, A., Hallenberger, A., Herberts, T., Miksch, S., Popow, C., Müller-Hansen, I., and Poets, C. F., 2004, "Automatic control of the inspired oxygen fraction in preterm infants: a randomized crossover trial," American journal of respiratory and critical care medicine, 170(10), pp. 1095-1100.
[29] Hallenberger, A., Poets, C. F., Horn, W., Seyfang, A., and Urschitz, M. S., 2014, "Closed-loop automatic oxygen control (CLAC) in preterm infants: a randomized controlled trial," Pediatrics, 133(2), pp. e379-e385.
[30] Sun, Y., Kohane, I., and Stark, A., "Fuzzy logic assisted control of inspired oxygen in ventilated newborn infants," Proc. Proceedings of the Annual Symposium on Computer Application in Medical Care, American Medical Informatics Association, p. 757.
[31] Morozoff, E. P. P., 1996, "Modelling and fuzzy logic control of neonatal oxygen therapy," Theses (School of Engineering Science)/Simon Fraser University.

[32] Mamdani, E., Østergaard, J., and Lembessis, E., 1983, "Use of fuzzy logic for implementing rule-based control of industrial processes," Advances in Fuzzy Sets, Possibility Theory, and Applications, Springer, pp. 307-323.
[33] Mamdani, E. H., "Twenty years of fuzzy control: experiences gained and lessons learnt," Proc. Fuzzy Systems, 1993., Second IEEE International Conference on, IEEE, pp. 339-344.
[34] Sun, Y., Kohane, I. S., and Stark, A. R., 1997, "Computer-assisted adjustment of inspired oxygen concentration improves control of oxygen saturation in newborn infants requiring mechanical ventilation," The Journal of pediatrics, 131(5), pp. 754-756.
[35] López, J. A., Araque Campo, R., and Matiz Rubio, A., 2014, "Automixer: equipment for the reduction of risks associated with inadequate oxygen supply," Ingeniería e Investigación, 34(1), pp. 60-65.
[36] Franklin, G. F., Powell, J. D., and Emami-Naeini, A., 2011, Feedback control of dynamic systems, Pearson.
[37] Tehrani, F. T., and Bazar, A. R., "An Automatic Control System for Oxygen Therapy of Newborn Infants," Proc. Engineering in Medicine and Biology Society, 1991. Vol. 13: 1991., Proceedings of the Annual International Conference of the IEEE, IEEE, pp. 2180-2182.
[38] Tehrani, F., and Bazar, A., 1994, "A feedback controller for supplemental oxygen treatment of newborn infants: a simulation study," Medical engineering & physics, 16(4), pp. 329-333.
[39] Tehrani, F., "A control system for oxygen therapy of premature infants," Proc. Engineering in Medicine and Biology Society, 2001. Proceedings of the 23rd Annual International Conference of the IEEE, IEEE, pp. 2059-2062.
[40] Tehrani, F. T., "Computer simulation of the respiratory control system in the newborn infant," Proc. Engineering in Medicine and Biology Society, 1990., Proceedings of the Twelfth Annual International Conference of the IEEE, IEEE, pp. 1848-1850.
[41] Tehrani, F. T., 1993, "Mathematical analysis and computer simulation of the respiratory system in the newborn infant," IEEE Transactions on Biomedical Engineering, 40(5), pp. 475-481.
[42] Morozoff, E. P., and Smyth, J. A., "Evaluation of three automatic oxygen therapy control algorithms on ventilated low birth weight neonates," Proc. 2009 Annual International Conference of the IEEE Engineering in Medicine and Biology Society, IEEE, pp. 3079-3082.
[43] Landau, I., Lozano, R., M'Saad, M., and Karimi, A., 1998, Communications and control engineering, Springer, New York.
[44] Sano, A., and Kikucki, M., "Adaptive control of arterial oxygen pressure of newborn infants under incubator oxygen treatments," Proc. IEE Proceedings D (Control Theory and Applications), IET, pp. 205-211.
[45] Grodins, F. S., Buell, J., and Bart, A. J., 1967, "Mathematical analysis and digital simulation of the respiratory control system," DTIC Document.
[46] He, W., Kaufman, H., and Roy, R., 1986, "Multiple model adaptive control procedure for blood pressure control," IEEE transactions on biomedical engineering(1), pp. 10-19.
[47] Yu, C., He, W., So, J. M., Roy, R., Kaufman, H., and Newell, J. C., 1987, "Improvement in arteral oxygen control using multiple-model adaptive control procedures," IEEE transactions on biomedical engineering(8), pp. 567-574.

[48] Taube, J. C., Pillutla, R., and Mills, J., "Criteria for an adaptive fractional inspired oxygen controller," Proc. Engineering of Computer-Based Medical Systems, 1988., Proceedings of the Symposium on the, IEEE, pp. 129-132.
[49] Bhutani, V. K., Taube, J. C., Antunes, M. J., and Delivoria‐Papadopoulos, M., 1992, "Adaptive control of inspired oxygen delivery to the neonate," Pediatric pulmonology, 14(2), pp. 110-117.
[50] Taube, J., and Bhutani, V., "Automatic control of neonatal fractional inspired oxygen," Proc. Engineering in Medicine and Biology Society, 1991. Vol. 13: 1991., Proceedings of the Annual International Conference of the IEEE, IEEE, pp. 2176-2177.
[51] Dargaville, P., Sadeghi Fathabadi, O., Plottier, G., Lim, K., Wheeler, K., Jayakar, R., and Gale, T., 2016, "Development and preclinical testing of an adaptive algorithm for automated control of inspired oxygen in the preterm infant," Archives of Disease in Childhood. Fetal and Neonatal Edition, pp. F1-F6.
[52] Sadeghi Fathabadi, O., Gale, T. J., Lim, K., Salmon, B. P., Dawson, J. A., Wheeler, K. I., Olivier, J. C., and Dargaville, P. A., 2015, "Characterisation of the oxygenation response to inspired oxygen adjustments in preterm infants," Neonatology, 109(1), pp. 37-43.
[53] Jones, J., Lockwood, G., Fung, N., Lasenby, J., Ross-Russell, R., Quine, D., and Stenson, B., 2015, "Influence of pulmonary factors on pulse oximeter saturation in preterm infants," Archives of Disease in Childhood-Fetal and Neonatal Edition, pp. fetalneonatal-2015-308675.
[54] Plottier, G. K., Wheeler, K. I., Ali, S. K., Fathabadi, O. S., Jayakar, R., Gale, T. J., and Dargaville, P. A., 2016, "Clinical evaluation of a novel adaptive algorithm for automated control of oxygen therapy in preterm infants on non-invasive respiratory support," Archives of Disease in Childhood-Fetal and Neonatal Edition.
[55] Claure, N., Gerhardt, T., Everett, R., Musante, G., Herrera, C., and Bancalari, E., 2001, "Closed-loop controlled inspired oxygen concentration for mechanically ventilated very low birth weight infants with frequent episodes of hypoxemia," Pediatrics, 107(5), pp. 1120-1124.
[56] Claure, N., D'ugard, C., and Bancalari, E., 2009, "Automated adjustment of inspired oxygen in preterm infants with frequent fluctuations in oxygenation: a pilot clinical trial," The Journal of pediatrics, 155(5), pp. 640-645. e642.
[57] Claure, N., Bancalari, E., D'Ugard, C., Nelin, L., Stein, M., Ramanathan, R., Hernandez, R., Donn, S. M., Becker, M., and Bachman, T., 2011, "Multicenter crossover study of automated control of inspired oxygen in ventilated preterm infants," Pediatrics, 127(1), pp. e76-e83.
[58] Van Kaam, A. H., Hummler, H. D., Wilinska, M., Swietlinski, J., Lal, M. K., Te Pas, A. B., Lista, G., Gupta, S., Fajardo, C. A., and Onland, W., 2015, "Automated versus manual oxygen control with different saturation targets and modes of respiratory support in preterm infants," The Journal of pediatrics, 167(3), pp. 545-550.
[59] Waitz, M., Schmid, M. B., Fuchs, H., Mendler, M. R., Dreyhaupt, J., and Hummler, H. D., 2015, "Effects of automated adjustment of the inspired oxygen on fluctuations of arterial and regional cerebral tissue oxygenation in preterm infants with frequent desaturations," The Journal of pediatrics, 166(2), pp. 240-244. e241.

[60] Lal, M., Tin, W., and Sinha, S., 2015, "Automated control of inspired oxygen in ventilated preterm infants: crossover physiological study," Acta Paediatrica, 104(11), pp. 1084-1089.
[61] Dorf, R. C., and Bishop, R. H., 2010, Modern control systems, Pearson.
[62] Dugdale, R., Cameron, R., and Tealman, G., 1988, "Closed-loop control of the partial pressure of arterial oxygen in neonates," Clinical Physics and Physiological Measurement, 9(4), pp. 291-305.
[63] Åström, K. J., 1980, "A robust sampled regulator for stable systems with monotone step responses," Automatica, 16(3), pp. 313-315.
[64] Keim, T., Amjad, R., and Fales, R., "Modeling and Feedback Control of Inspired Oxygen for Premature Infants," Proc. ASME 2011 Dynamic Systems and Control Conference and Bath/ASME Symposium on Fluid Power and Motion Control, American Society of Mechanical Engineers, pp. 501-508.
[65] Keim, T., Amjad, R., and Fales, R., "Modeling and control of the oxygen saturation in neonatal infants," Proc. ASME 2009 Dynamic Systems and Control Conference, American Society of Mechanical Engineers, pp. 105-112.
[66] Krone, B., Fales, R., and Amjad, R., "Model of Neonatal Infant Blood Oxygen Saturation," Proc. ASME 2011 Dynamic Systems and Control Conference and Bath/ASME Symposium on Fluid Power and Motion Control, American Society of Mechanical Engineers, pp. 509-516.
[67] Keim, T., 2011, "Control of arterial oxygen saturation in premature infants," Doctor of philosophy, University of Missouri-Columbia, Columbia, MO.
[68] Krone, B., 2011, "Modeling and control of arterial oxygen saturation in premature infants," University of Missouri--Columbia.
[69] Quigley, D., 2013, "Control of arterial hemoglobin saturation in premature infants using H-infinity synthesis and performance specifications from best clinical practice," University of Missouri--Columbia.
[70] Yu, C., 1986, "An arterial oxygen saturation controller," Rensselaer Polytechnic Institute.
[71] Nitzan, M., and Taitelbaum, H., 2008, "The measurement of oxygen saturation in arterial and venous blood," IEEE Instrumentation & Measurement Magazine, 11(3).
[72] Severinghaus, J. W., 1979, "Simple, accurate equations for human blood O2 dissociation computations," Journal of Applied Physiology, 46(3), pp. 599-602.
[73] Amjad, R., Fales, R., and Keim, T., 2014, "Closed loop respiratory support device with dynamic adaptability," Google Patents.
[74] Fathabadi, O. S., Gale, T., Lim, K., Salmon, B., Wheeler, K., Olivier, J., and Dargaville, P., 2014, "Assessment of validity and predictability of the FiO2–SpO2 transfer-function in preterm infants," Physiological measurement, 35(7), p. 1425.
[75] Radke, A., 2006, "On disturbance estimation and its applications in health monitoring."
[76] Miklosovic, R., Radke, A., and Gao, Z., "Discrete implementation and generalization of the extended state observer," Proc. American Control Conference, 2006, IEEE, p. 6 pp.
[77] Peck, R., and Devore, J. L., 2011, Statistics: The exploration & analysis of data, Cengage Learning.

[78] Öztuna, D., Elhan, A. H., and Tüccar, E., 2006, "Investigation of four different normality tests in terms of type 1 error rate and power under different distributions," Turkish Journal of Medical Sciences, 36(3), pp. 171-176.
[79] Elliott, A. C., and Woodward, W. A., 2007, Statistical analysis quick reference guidebook: With SPSS examples, Sage.
[80] Chambers, J. M., 1983, Graphical methods for data analysis.
[81] Chow, S.-C., and Liu, J.-p., 2008, Design and analysis of clinical trials: concepts and methodologies, John Wiley & Sons.
[82] Campbell, M. J., Machin, D., and Walters, S. J., 2010, Medical statistics: a textbook for the health sciences, John Wiley & Sons.
[83] Pett, M. A., 2015, Nonparametric statistics for health care research: Statistics for small samples and unusual distributions, Sage Publications.
[84] Siegel, S., and Castellan, N. J., 1981, "J.(1988). Nonparametric Statistics for the Behavioral Sciences," McGraw-HiU Book Company, New York.
[85] Munro, H., Visintainer, M., and Page, E., 1993, "Differences among group means: one-way analysis of variance," Statistical Methods for Health Care Research, pp. 99-128.
[86] Hettmansperger, T. P., 1984, "Two-sample inference based on one-sample sign statistics," Applied statistics, pp. 45-51.
[87] Siegel, S., and Castellan, N., 1988, "Nonparametric systems for the behavioural sciences," McGraw Hill International Editions.
[88] Murphy, K. R., Myors, B., and Wolach, A., 2014, Statistical power analysis: A simple and general model for traditional and modern hypothesis tests, Routledge.
[89] Cleophas, T. J., and Zwinderman, A. H., 2012, Statistics applied to clinical studies, Springer Science & Business Media.
[90] Chow, L. C., Wright, K. W., and Sola, A., 2003, "Can changes in clinical practice decrease the incidence of severe retinopathy of prematurity in very low birth weight infants?," Pediatrics, 111(2), pp. 339-345.
[91] Lau, Y. Y., Tay, Y. Y., Shah, V. A., Chang, P., and Loh, K. T., 2011, "Maintaining optimal oxygen saturation in premature infants," The Permanente Journal, 15(1).
[92] Montgomery, D. C., 1991, Design and analysis of experiments, John Wiley & Sons.
[93] Hicks, C. R., and Turner, K. V., 1999, Fundamental concepts in the design of experiments, Oxford University Press.
[94] Chang, M., 2011, "Optimal oxygen saturation in premature infants," Korean journal of pediatrics, 54(9), pp. 359-362.
[95] Van Kaam, A. H., Hummler, H. D., Wilinska, M., Swietlinski, J., Lal, M. K., Te Pas, A. B., Lista, G., Gupta, S., Fajardo, C. A., and Onland, W., 2015, "Automated versus manual oxygen control with different saturation targets and modes of respiratory support in preterm infants," The Journal of pediatrics, 167(3), pp. 545-550. e542.
[96] Wilinska, M., Bachman, T., Swietlinski, J., Kostro, M., and Twardoch-Drozd, M., 2014, "Automated FiO 2-SpO 2 control system in Neonates requiring respiratory support: a comparison of a standard to a narrow SpO 2 control range," BMC pediatrics, 14(1), p. 130.
[97] Van Zanten, H., Tan, R., Thio, M., De Man-Van Ginkel, J., Van Zwet, E., Lopriore, E., and Te Pas, A., 2014, "The risk for hyperoxaemia after apnoea, bradycardia and hypoxaemia in preterm infants," Archives of Disease in Childhood-Fetal and Neonatal Edition, 99(4), pp. F269-F273.

[98] Nelson, L., and Stear, E., 1976, "The simultaneous on-line estimation of parameters and states in linear systems," IEEE Transactions on automatic Control, 21(1), pp. 94-98.
[99] Di Fiore, J. M., Walsh, M., Wrage, L., Rich, W., Finer, N., Carlo, W. A., and Martin, R. J., 2012, "Low oxygen saturation target range is associated with increased incidence of intermittent hypoxemia," The Journal of pediatrics, 161(6), pp. 1047-1052. e1041.
[100] Faqeeh, A. A. A., 2014, "Investigation of the effect of tool materials and process parameters on dry drilling of Ti-6Al-4V Alloy," University of Missouri--Columbia.
[101] Faqeeh, A., and El-Gizawy, A. S., 2015, "Optimization of Multiple Quality Characteristics for Dry Drilling Ti-6Al-4V Using TiAlN-Coated Carbide Tool," SAE Int. J. Mater. Manf., 8(1), pp. 172-179.

Appendices

Appendix A: Normal Probability Plots with Shapiro-Wilk Test Results of Non-Clinical Investigation

Appendix A1: normal probability plots with Shapiro-Wilk Test Results of the frequency where $SpO_2 < 87\%$ per 10 minutes

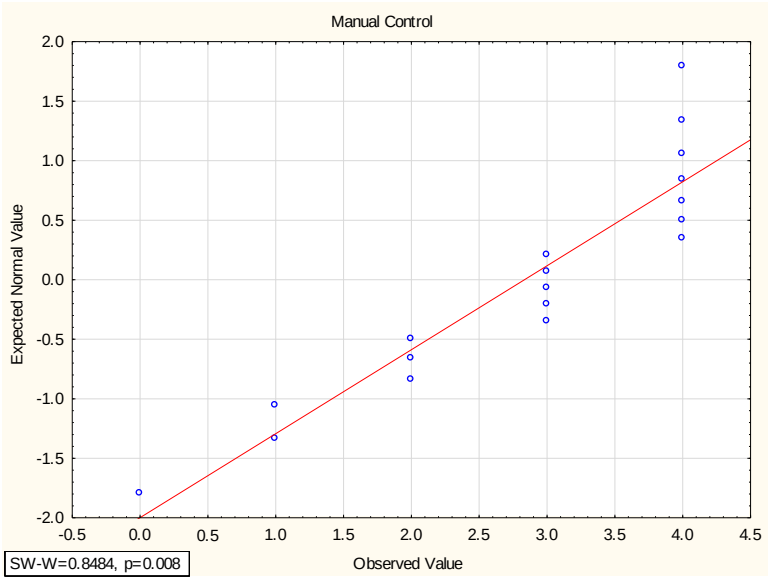

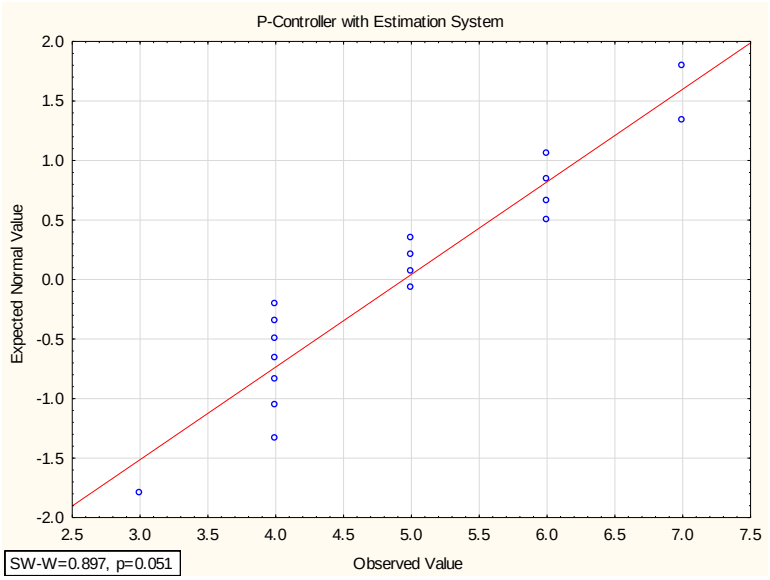

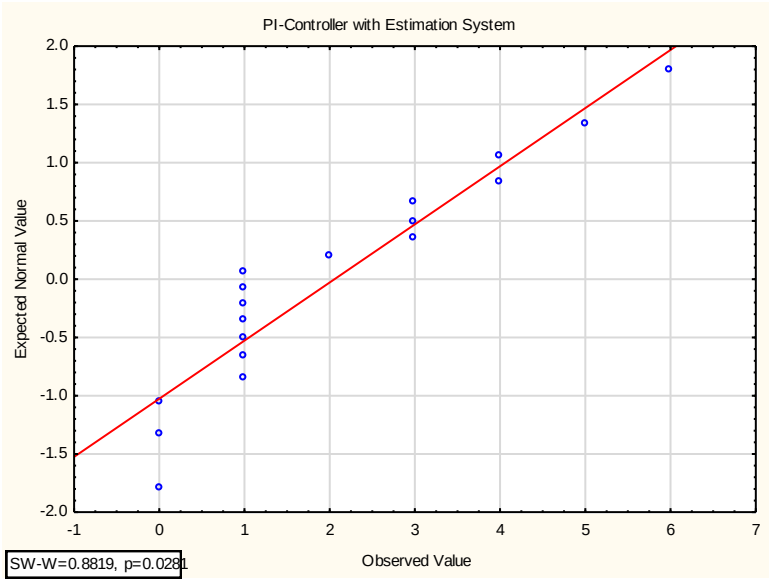
PI-Controller with Estimation System
Expected Normal Value
Observed Value
2.0
1.5
1.0
0.5
0.0
-0.5
-1.0
-1.5
-2.0
-1
0
1
2
3
4
5
6
7
SW-W=0.8819, p=0.0281

Appendix A2: normal probability plots with Shapiro-Wilk Test Results of the mean duration of the episodes where $SpO_2 < 87\%$ per 10 minutes

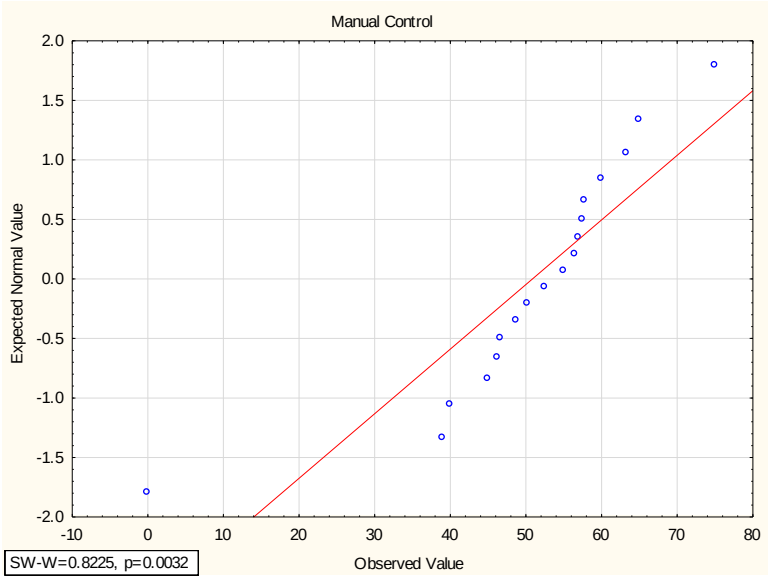

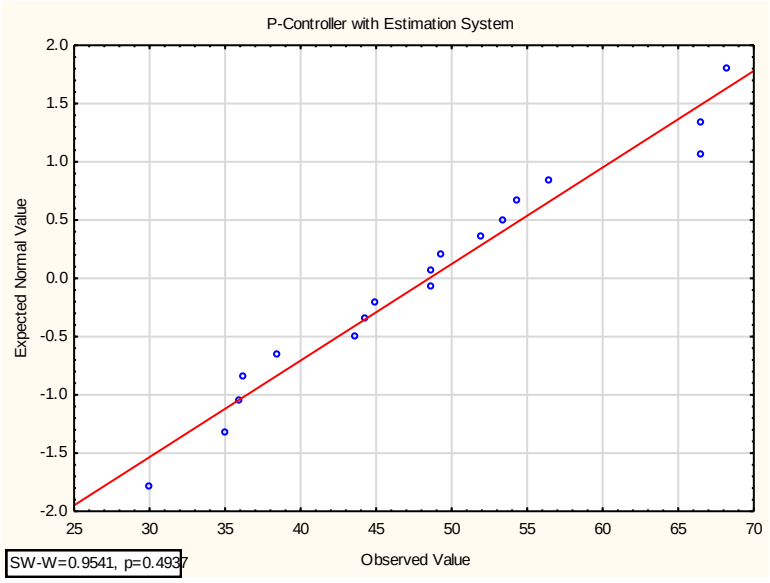

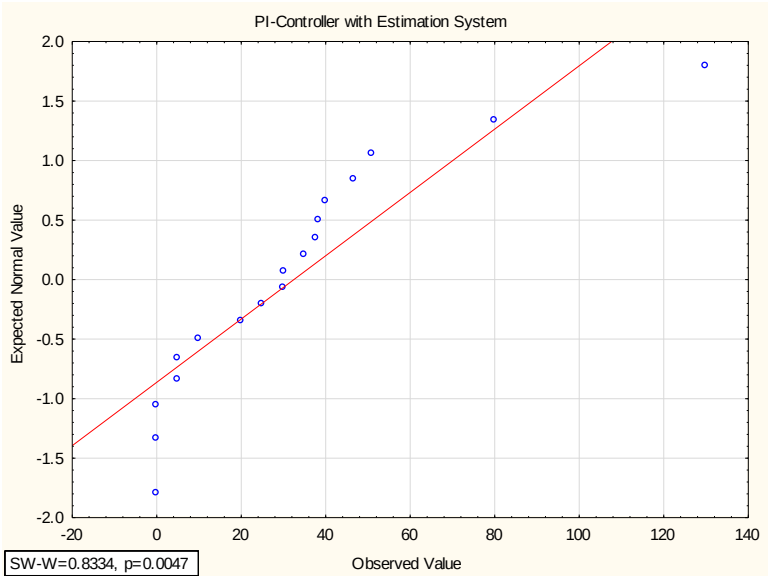
PI-Controller with Estimation System
Expected Normal Value
Observed Value
2.0
1.5
1.0
0.5
0.0
-0.5
-1.0
-1.5
-2.0
-20
0
20
40
60
80
100
120
140
SW-W=0.8334, p=0.0047

Appendix A3: normal probability plots with Shapiro-Wilk Test Results of the frequency where SpO2 > 93% per 10 minutes

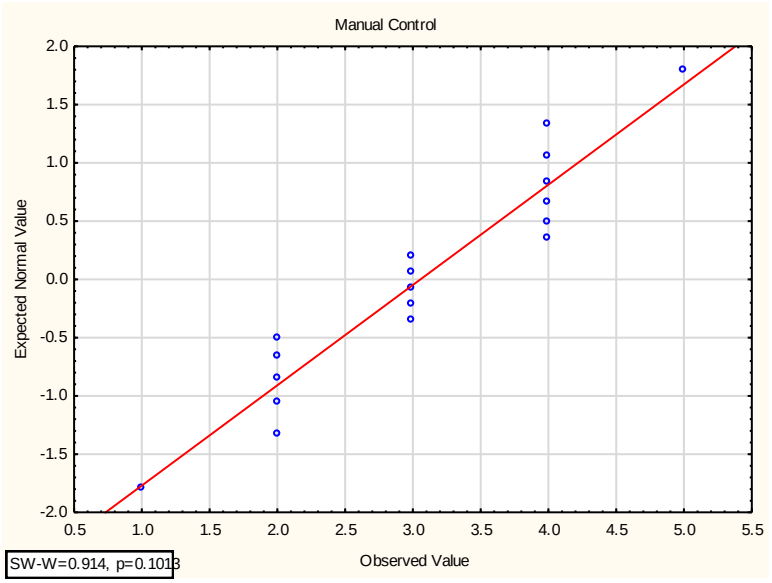

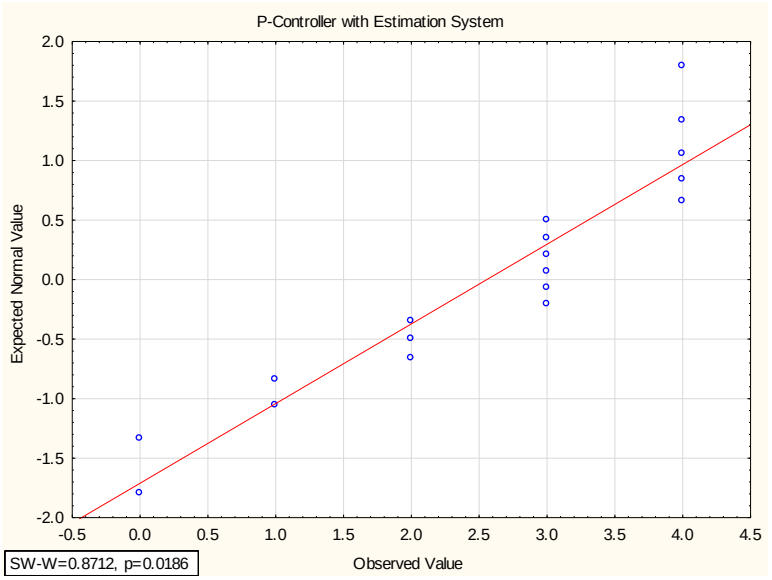

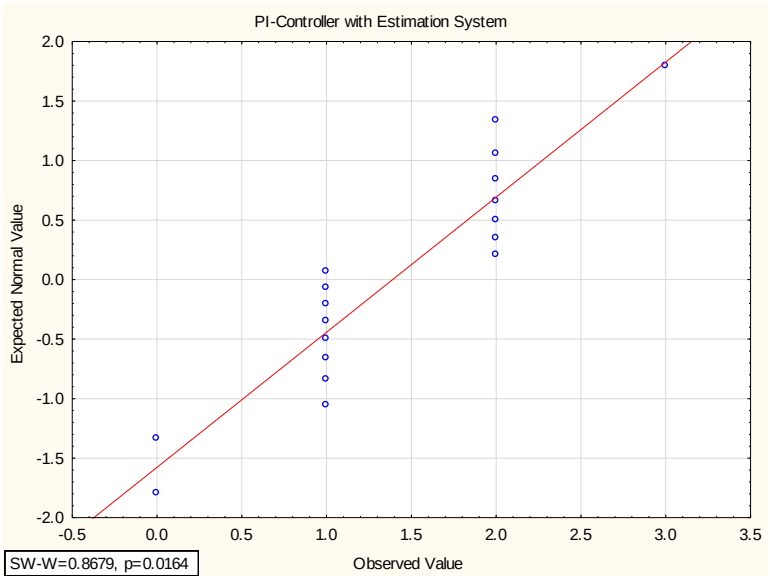
PI-Controller with Estimation System
Expected Normal Value
Observed Value
2.0
1.5
1.0
0.5
0.0
-0.5
-1.0
-1.5
-2.0
-0.5
0.0
0.5
1.0
1.5
2.0
2.5
3.0
3.5
SW-W=0.8679, p=0.0164

Appendix A4: normal probability plots with Shapiro-Wilk Test Results of the mean duration of the episodes where $SpO_2 > 93\%$ per 10 minutes

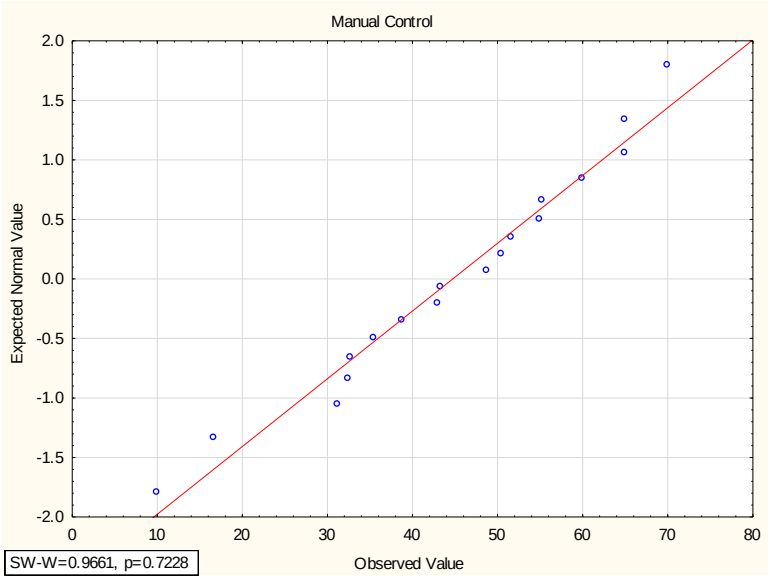

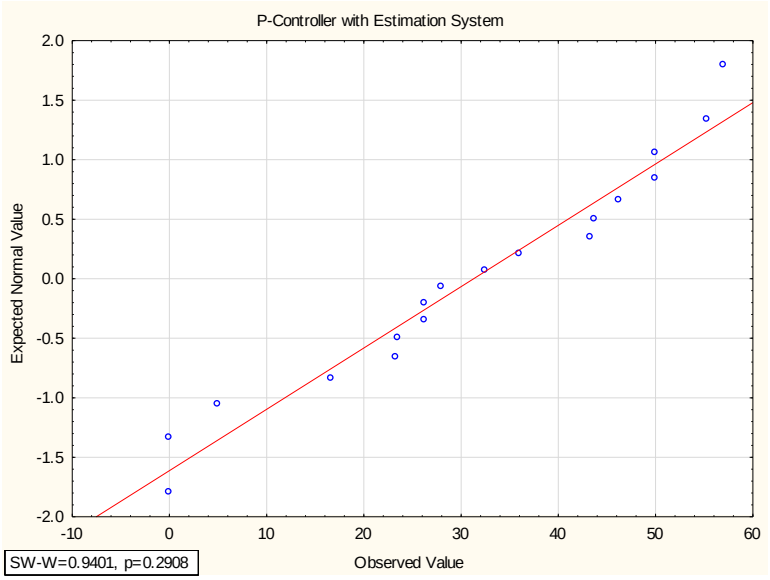

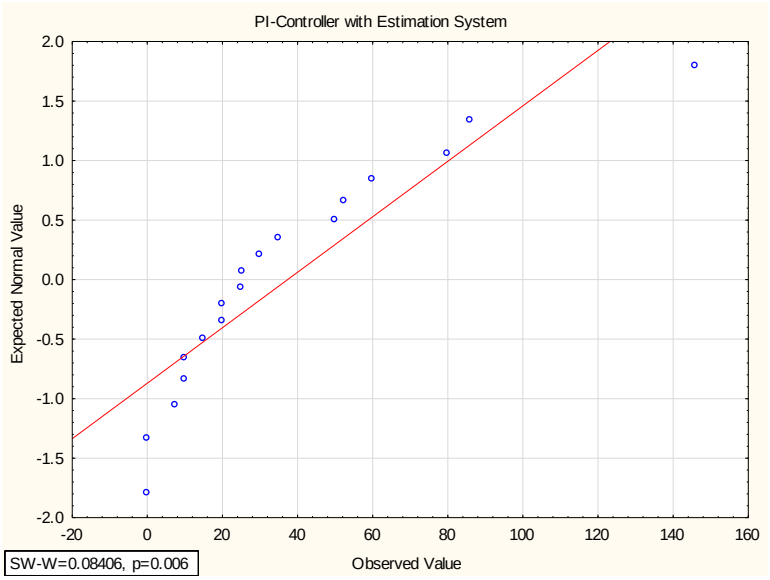
PI-Controller with Estimation System
Expected Normal Value
Observed Value
2.0
1.5
1.0
0.5
0.0
-0.5
-1.0
-1.5
-2.0
-20
0
20
40
60
80
100
120
140
160
SW-W=0.08406, p=0.006

Appendix A5: normal probability plots with Shapiro-Wilk Test Results of the hypoxemic episodes (duration < 60 s) per 30-minute

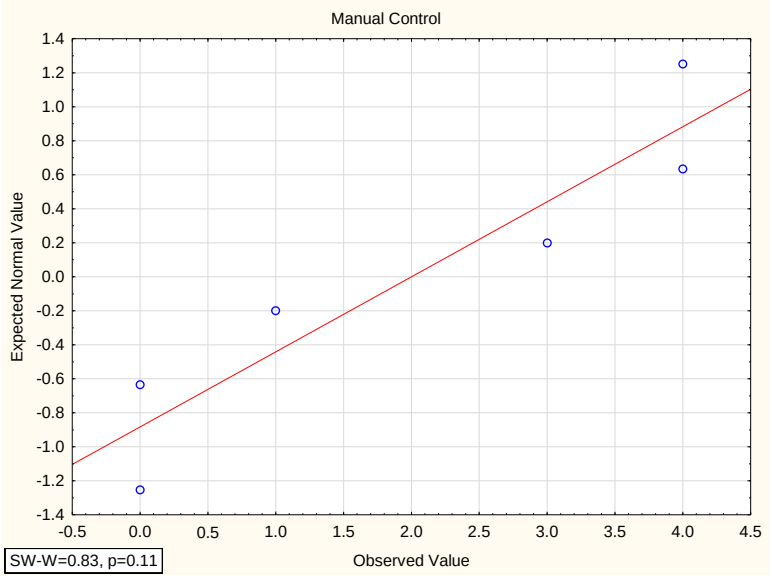

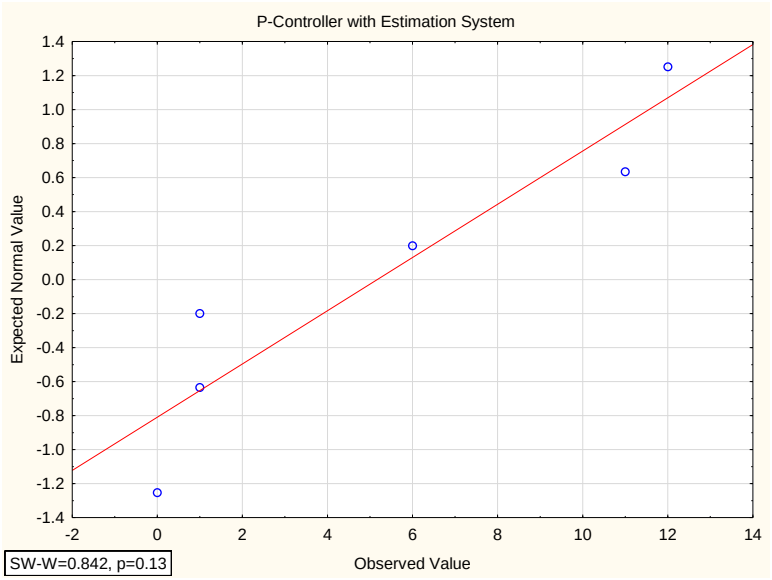

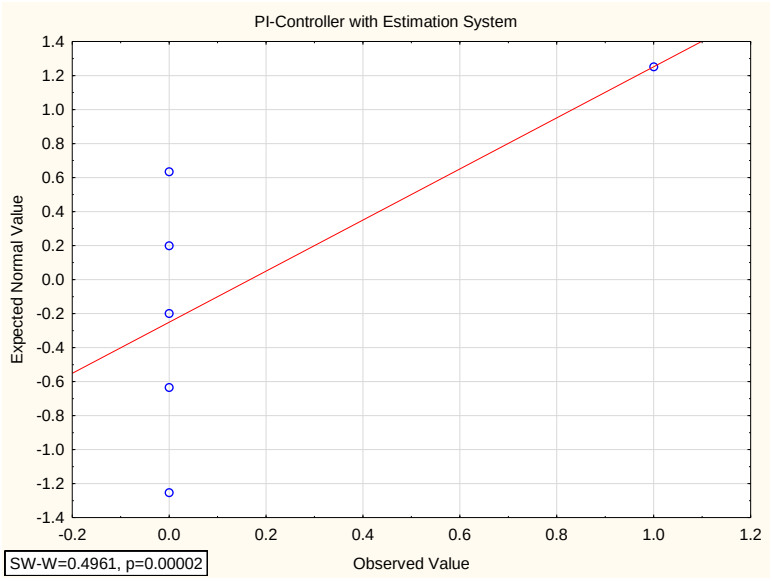
PI-Controller with Estimation System
Expected Normal Value
Observed Value
1.4
1.2
1.0
0.8
0.6
0.4
0.2
0.0
-0.2
-0.4
-0.6
-0.8
-1.0
-1.2
-1.4
-0.2
0.0
0.2
0.4
0.6
0.8
1.0
1.2
SW-W=0.4961, p=0.00002

Appendix A6: normal probability plots with Shapiro-Wilk Test Results of the hypoxemic episodes (duration ≥ 60 s) per 30-minute

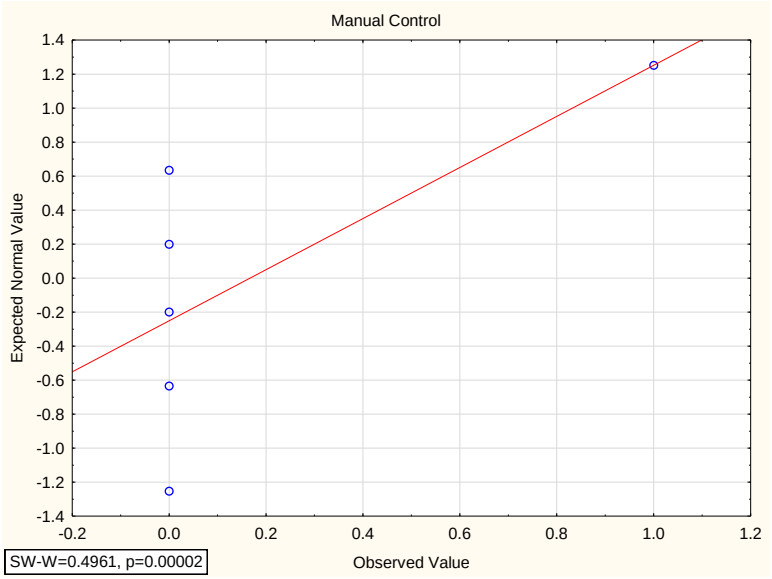

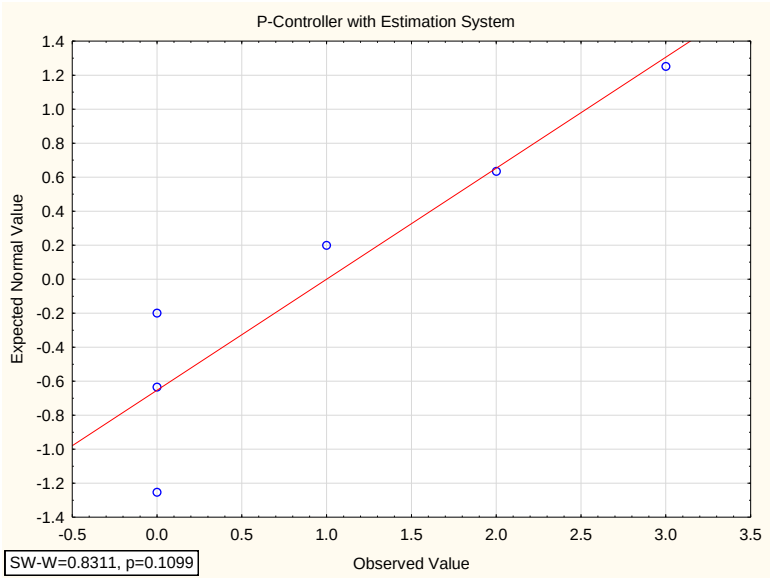

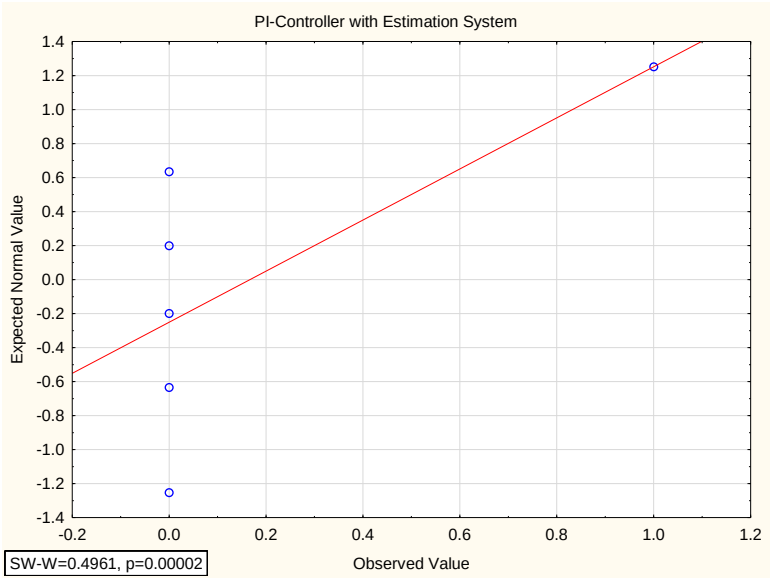
PI-Controller with Estimation System
Expected Normal Value
Observed Value
1.4
1.2
1.0
0.8
0.6
0.4
0.2
0.0
-0.2
-0.4
-0.6
-0.8
-1.0
-1.2
-1.4
-0.2
0.0
0.2
0.4
0.6
0.8
1.0
1.2
SW-W=0.4961, p=0.00002

Appendix A7: normal probability plots with Shapiro-Wilk Test Results of the hyperoxaemic episodes (duration < 60 s) per 30-minute

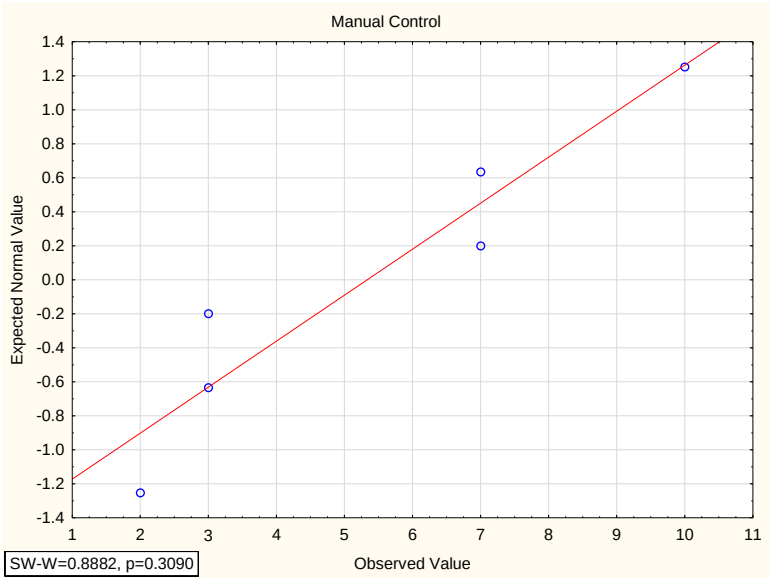

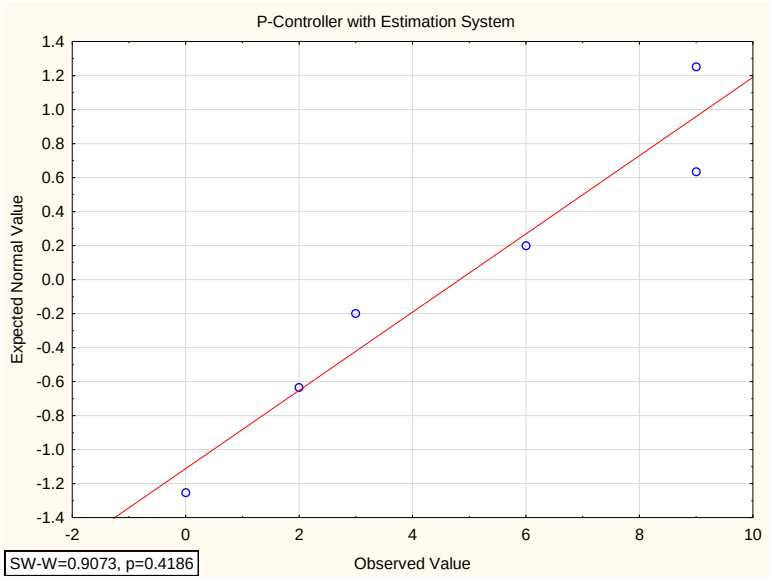

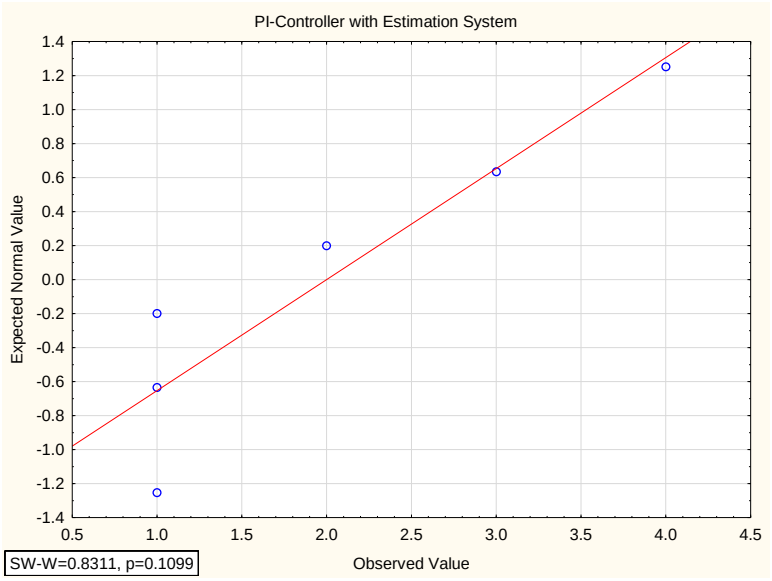
PI-Controller with Estimation System
Expected Normal Value
1.4
1.2
1.0
0.8
0.6
0.4
0.2
0.0
-0.2
-0.4
-0.6
-0.8
-1.0
-1.2
-1.4
0.5
1.0
1.5
2.0
2.5
3.0
3.5
4.0
4.5
Observed Value
SW-W=0.8311, p=0.1099

Appendix A8: normal probability plots with Shapiro-Wilk Test Results of the hyperoxaemic episodes (duration ≥ 60 s) per 30-minute

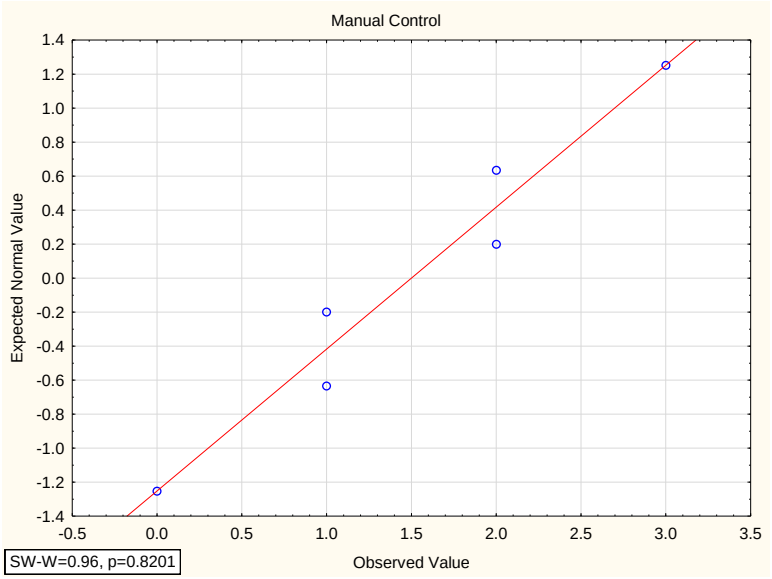

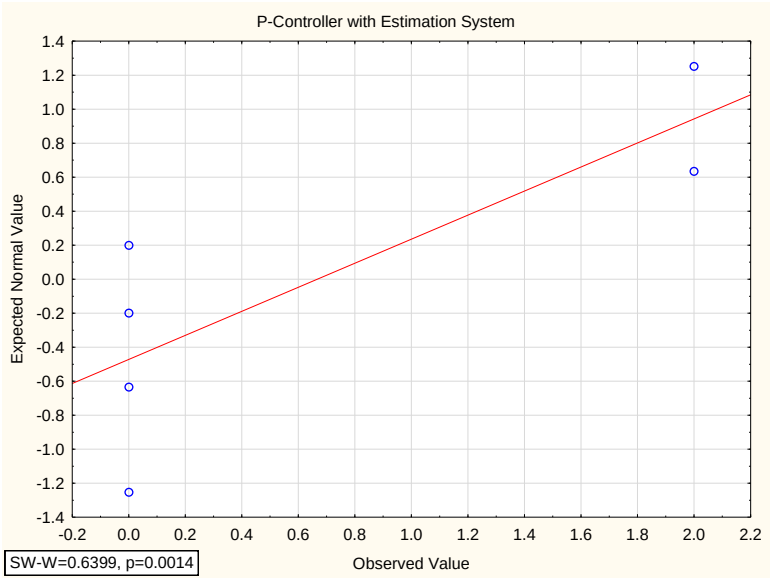

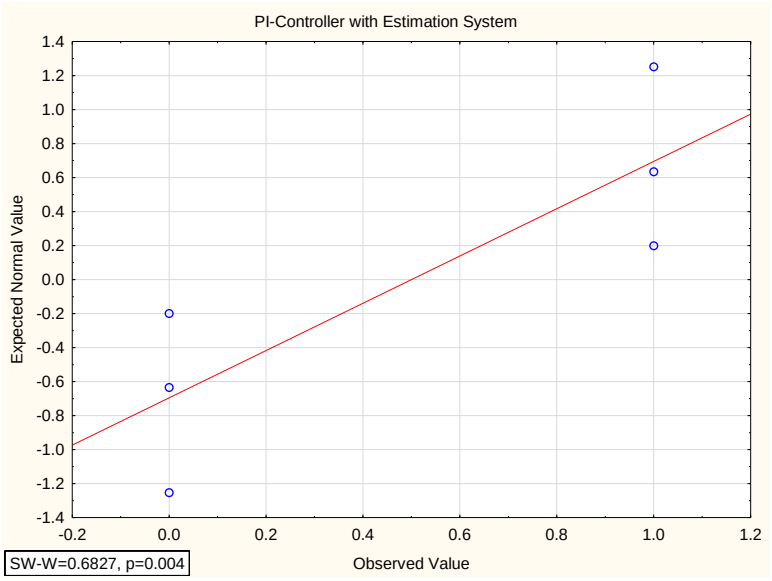
PI-Controller with Estimation System
Expected Normal Value
Observed Value
1.4
1.2
1.0
0.8
0.6
0.4
0.2
0.0
-0.2
-0.4
-0.6
-0.8
-1.0
-1.2
-1.4
-0.2
0.0
0.2
0.4
0.6
0.8
1.0
1.2
SW-W=0.6827, p=0.004

Appendix A9: normal probability plots with Shapiro-Wilk Test Results of the overshoot episodes per 30-minute

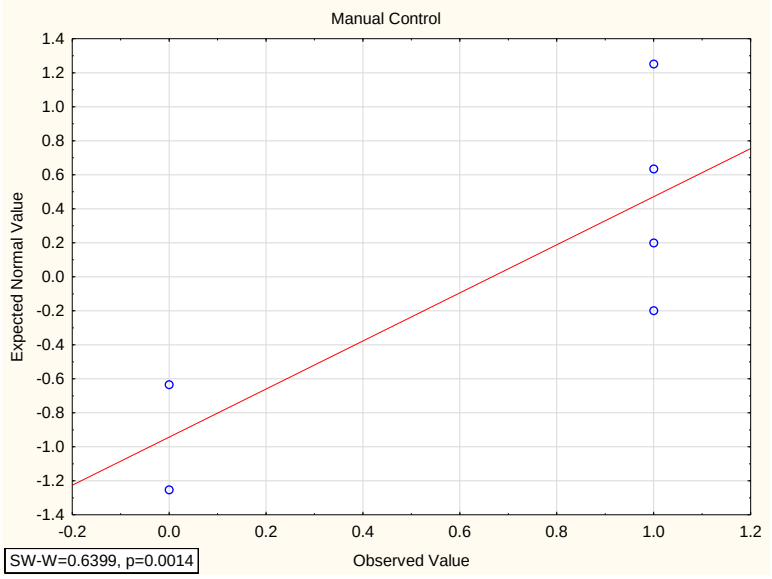

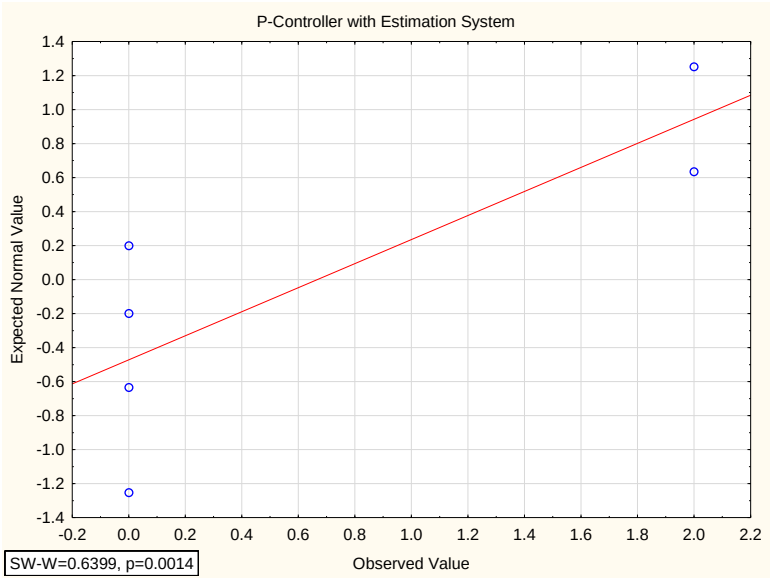

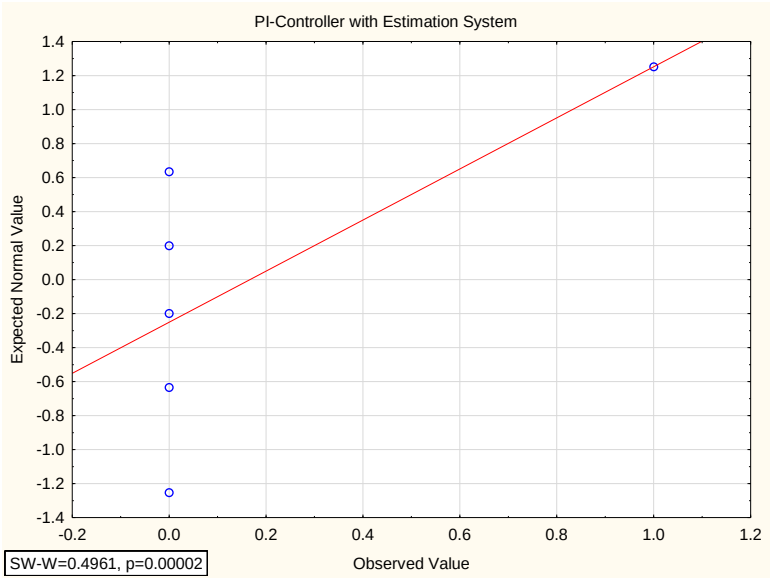
PI-Controller with Estimation System
Expected Normal Value
Observed Value
1.4
1.2
1.0
0.8
0.6
0.4
0.2
0.0
-0.2
-0.4
-0.6
-0.8
-1.0
-1.2
-1.4
-0.2
0.0
0.2
0.4
0.6
0.8
1.0
1.2
SW-W=0.4961, p=0.00002

Appendix B: Normal Probability Plots with Shapiro-Wilk Test Results of Clinical Investigation

Appendix B1: normal probability plots with Shapiro-Wilk Test Results of the frequency where SpO2 < 87% per 1-hour (Subject I)

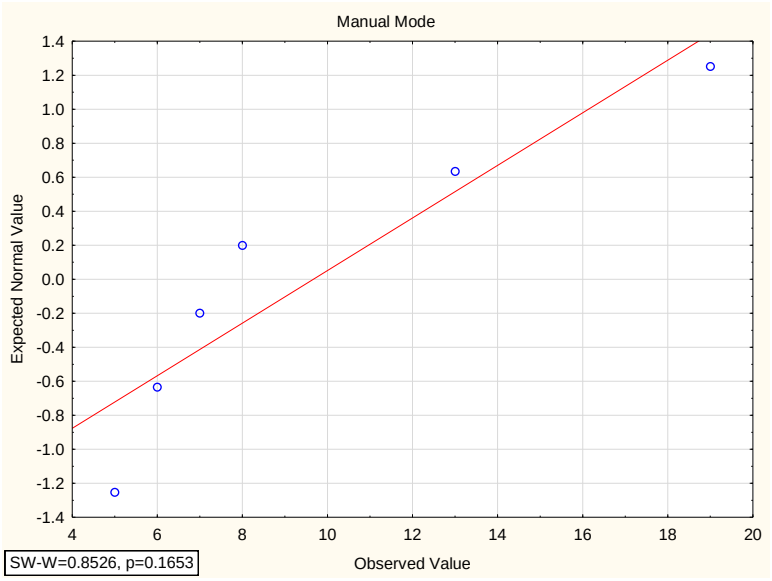

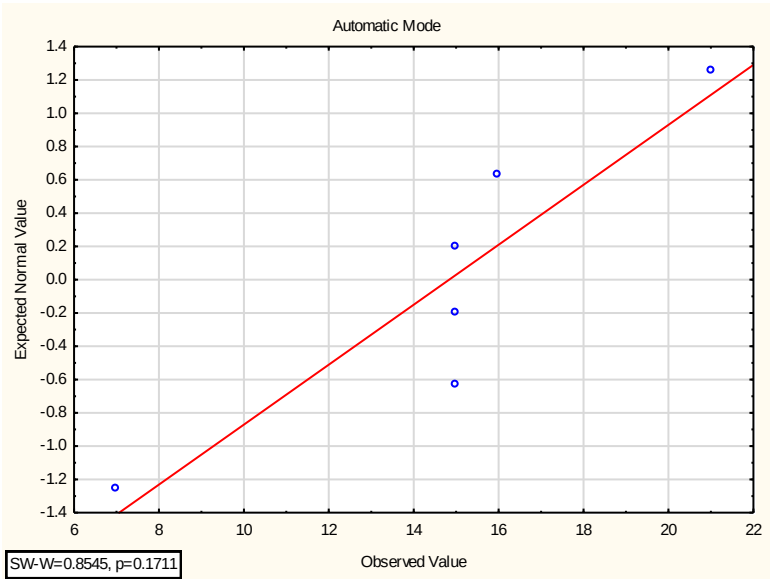

Appendix B2: normal probability plots with Shapiro-Wilk Test Results of the mean duration of episodes where SpO_2 < 87% per 1-hour (Subject I)

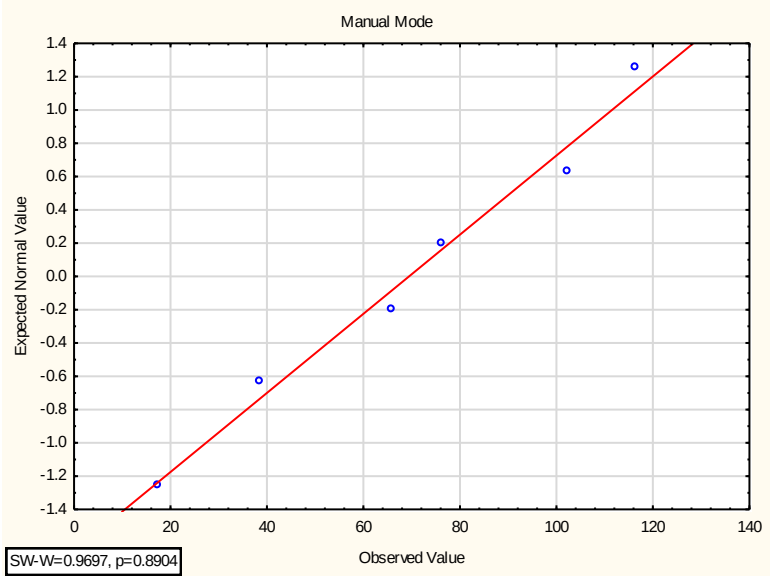

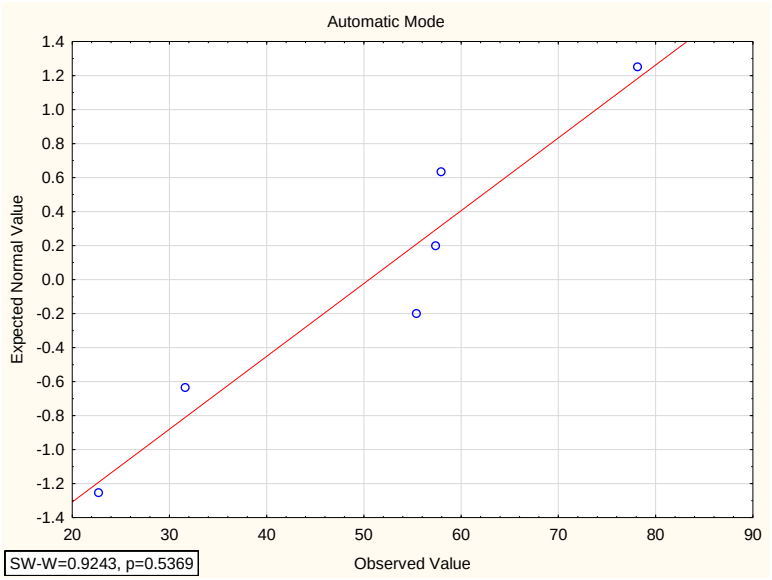

Appendix B3: normal probability plots with Shapiro-Wilk Test Results of the frequency of episodes where SpO_2 > 94% per 1-hour (Subject I)

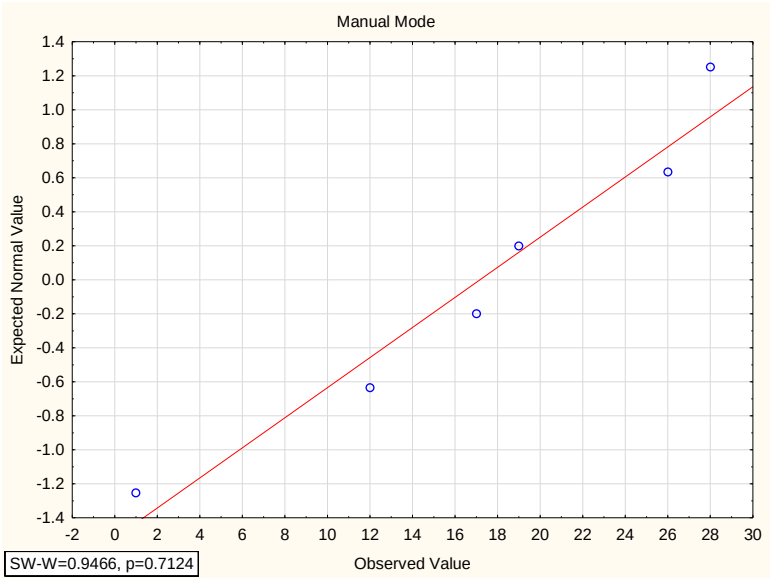

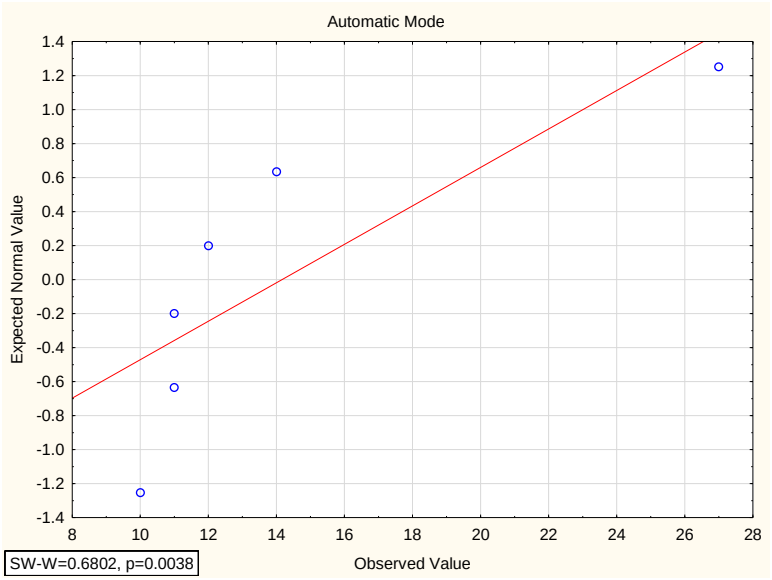

Appendix B4: normal probability plots with Shapiro-Wilk Test Results of the mean duration of episodes where SpO_2 > 94% per 1-hour (Subject I)

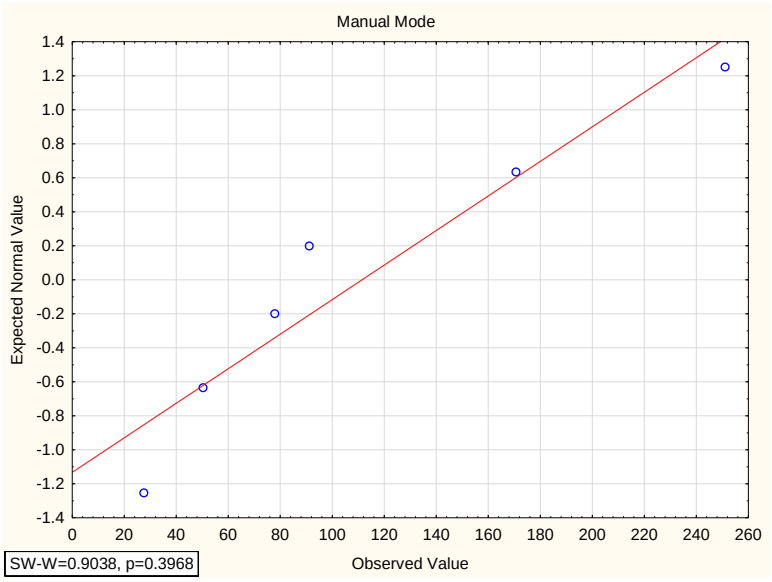

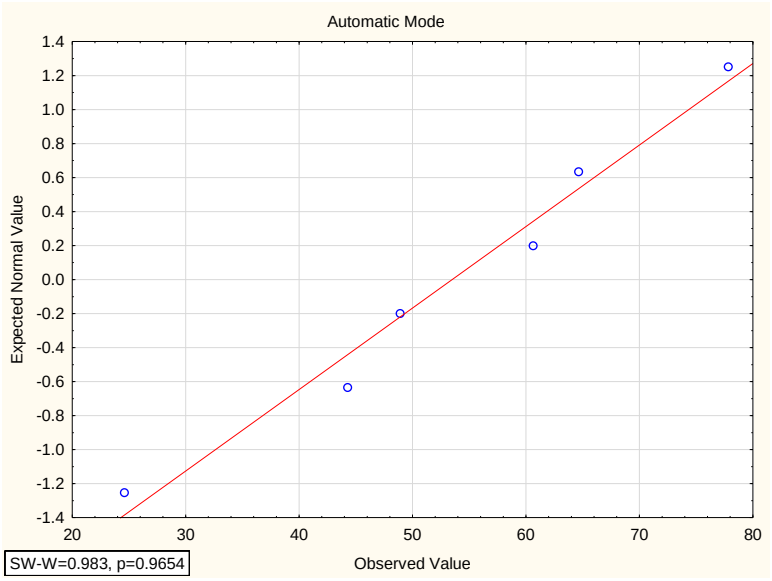

Appendix B5: normal probability plots with Shapiro-Wilk Test Results of the frequency where SpO_2 < 91% per 1-hour (Subject II)

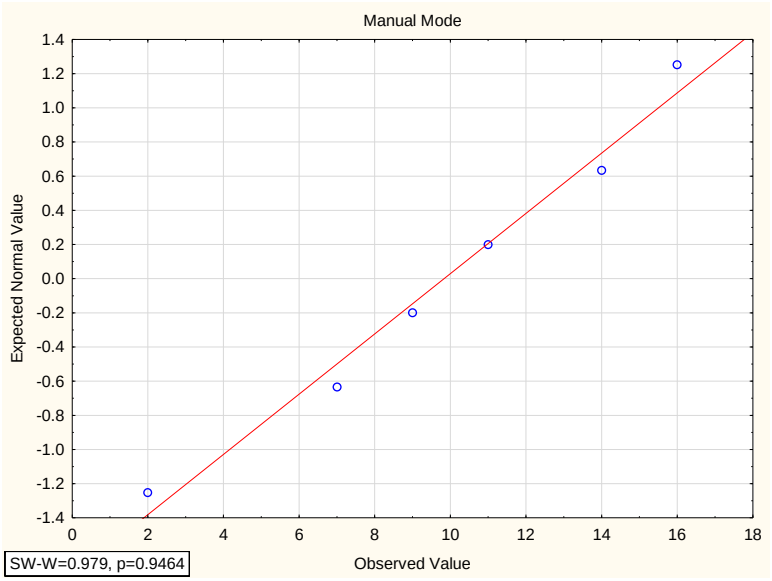

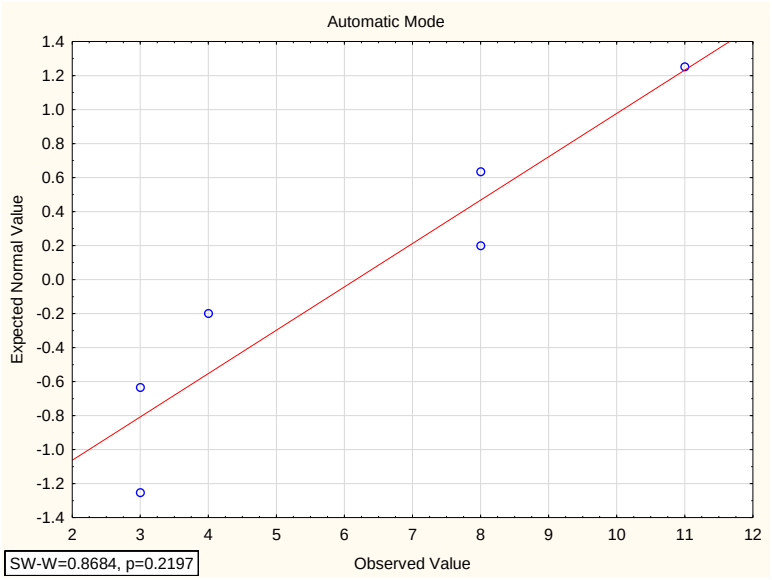

Appendix B6: normal probability plots with Shapiro-Wilk Test Results of the mean duration of episodes where SpO_2 < 91% per 1-hour (Subject II)

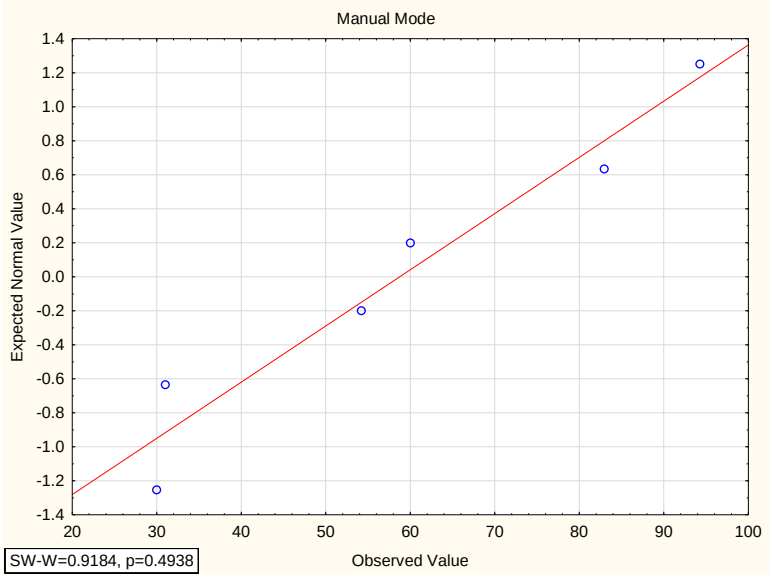

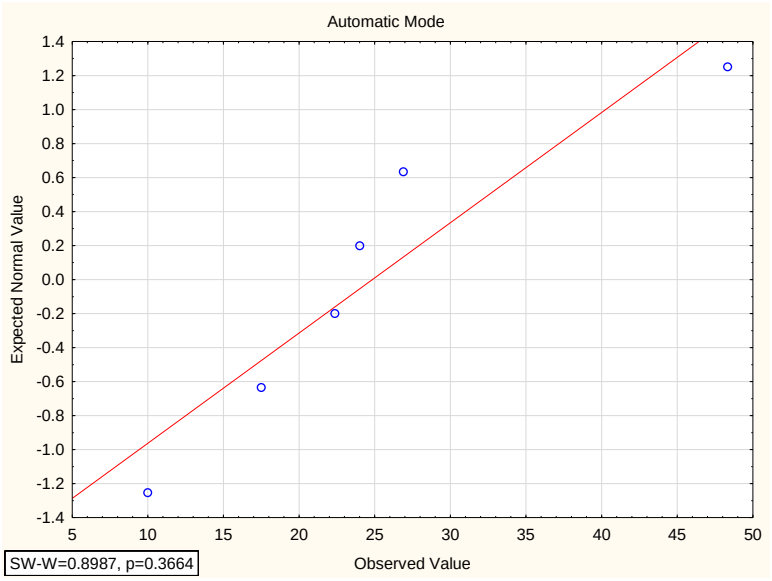

Appendix B7: normal probability plots with Shapiro-Wilk Test Results of the frequency of episodes where SpO_2 > 99% per 1-hour (Subject II)

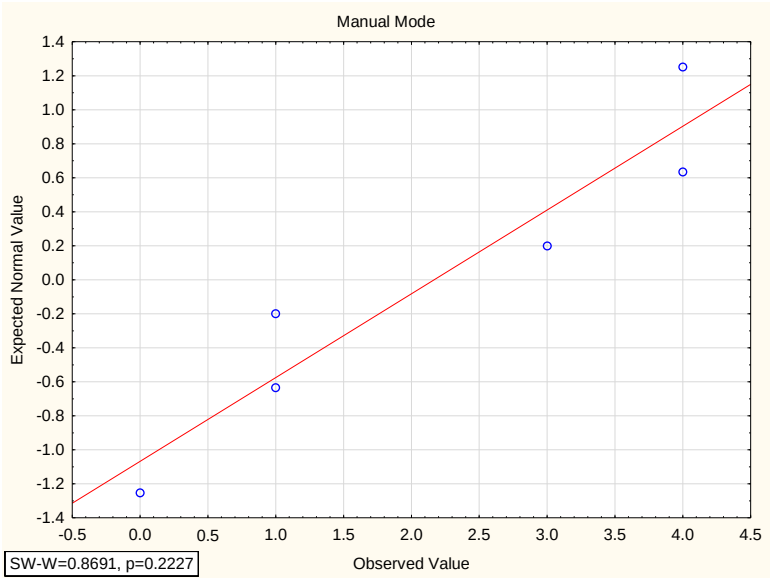

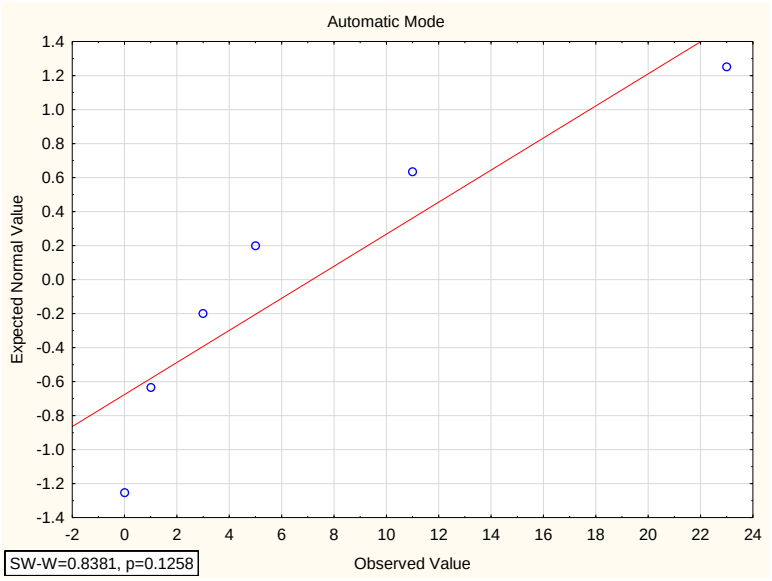

Appendix B8: normal probability plots with Shapiro-Wilk Test Results of the mean duration of episodes where SpO_2 > 99% per 1-hour (Subject II)

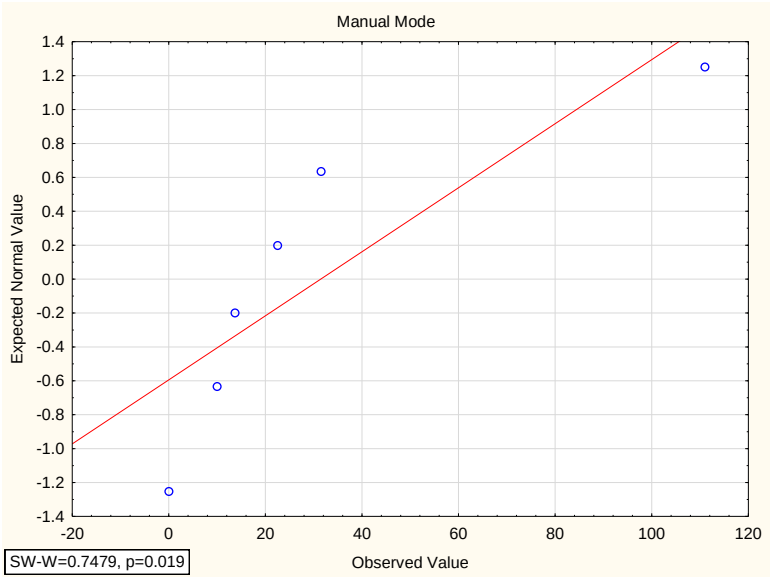

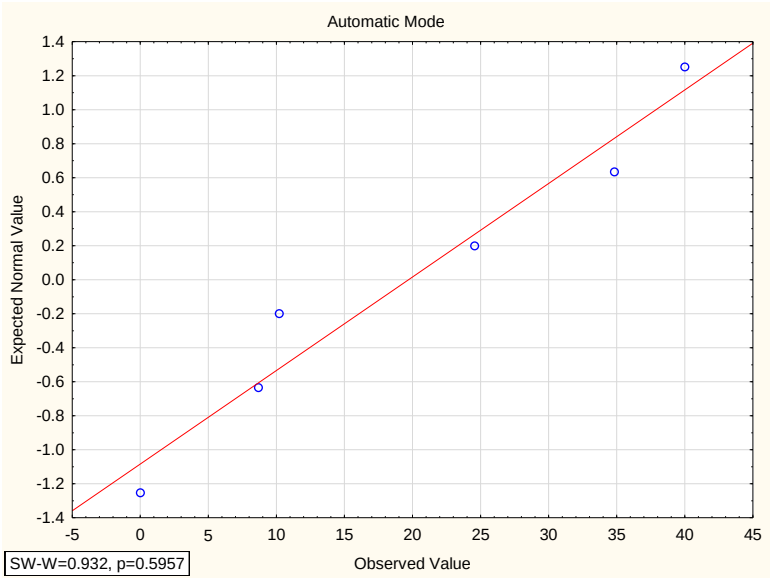

Appendix B9: normal probability plots with Shapiro-Wilk Test Results of the hypoxemic episodes (duration < 60 s) per 1-hr (Subject I)

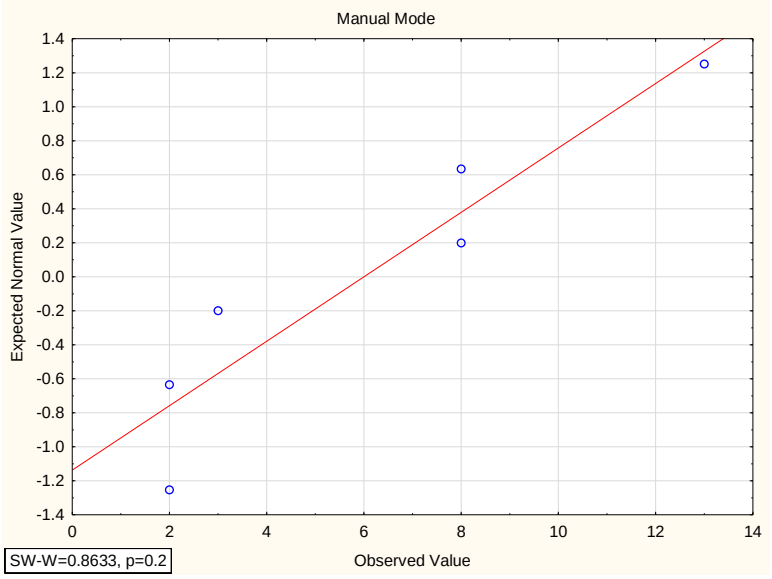

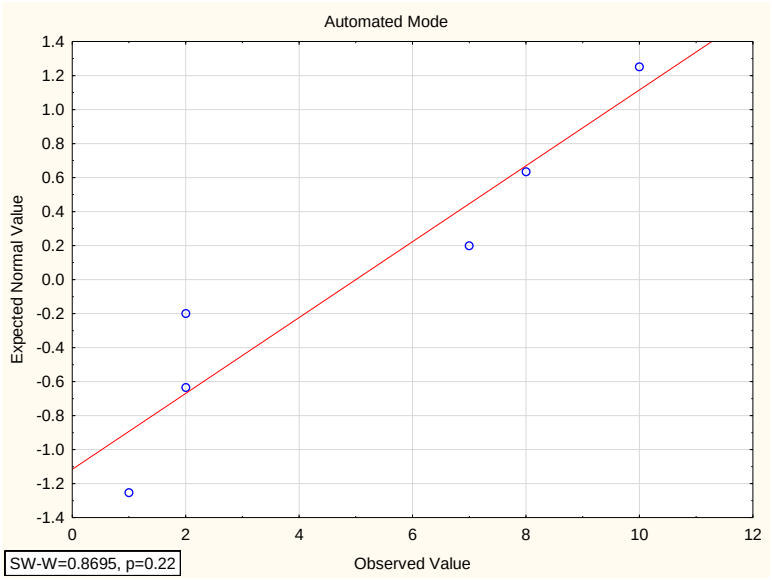

Appendix B10: normal probability plots with Shapiro-Wilk Test Results of the hypoxemic episodes (duration ≥ 60 s) per 1-hr (Subject I)

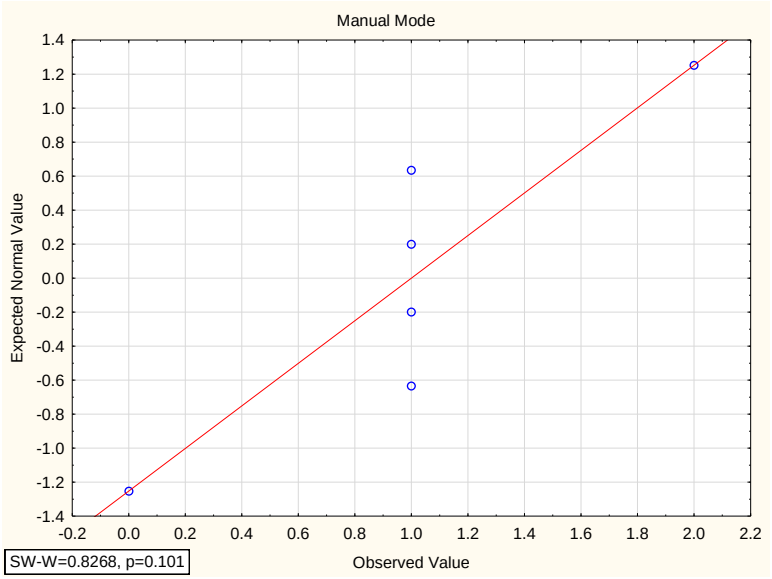

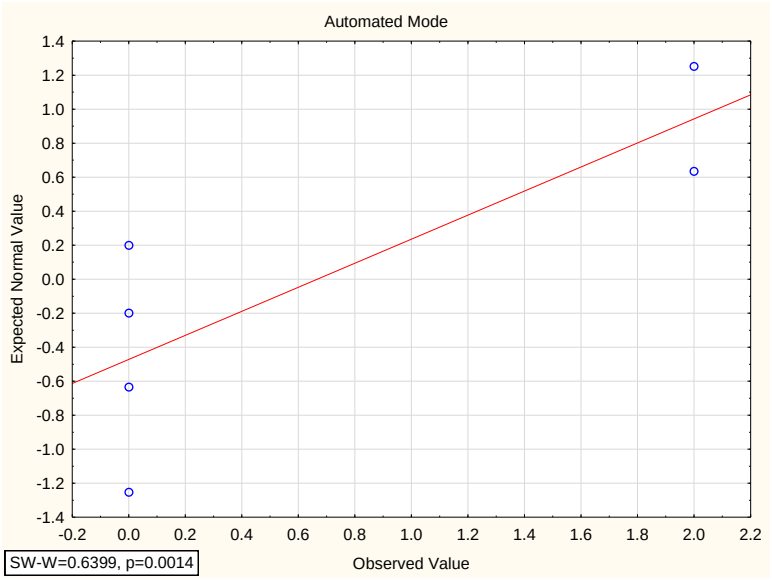

Appendix B11: normal probability plots with Shapiro-Wilk Test Results of the hyperoxaemic episodes (duration < 60 s) per 1-hr (Subject I)

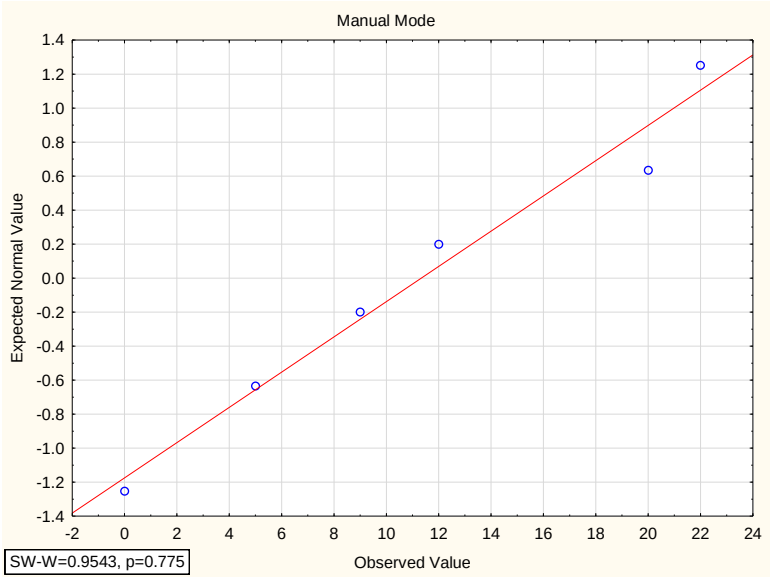

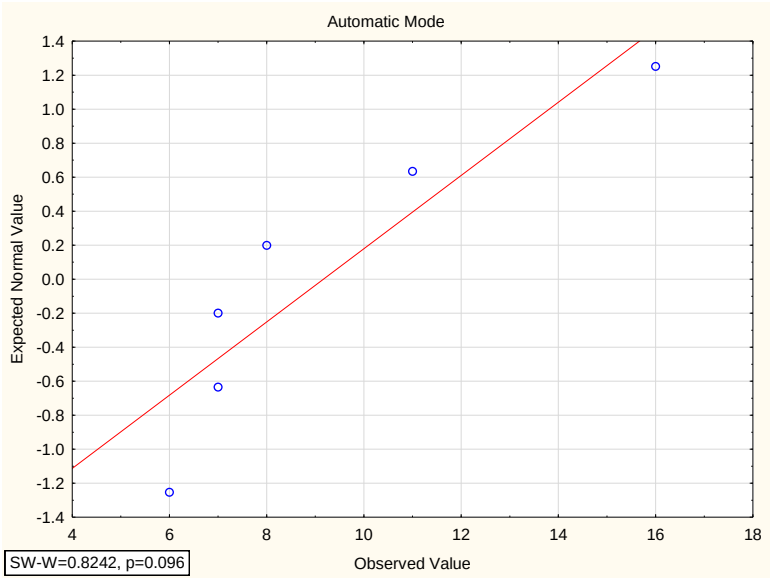

Appendix B12: normal probability plots with Shapiro-Wilk Test Results of the hyperoxaemic episodes (duration ≥ 60 s) per 1-hr (Subject I)

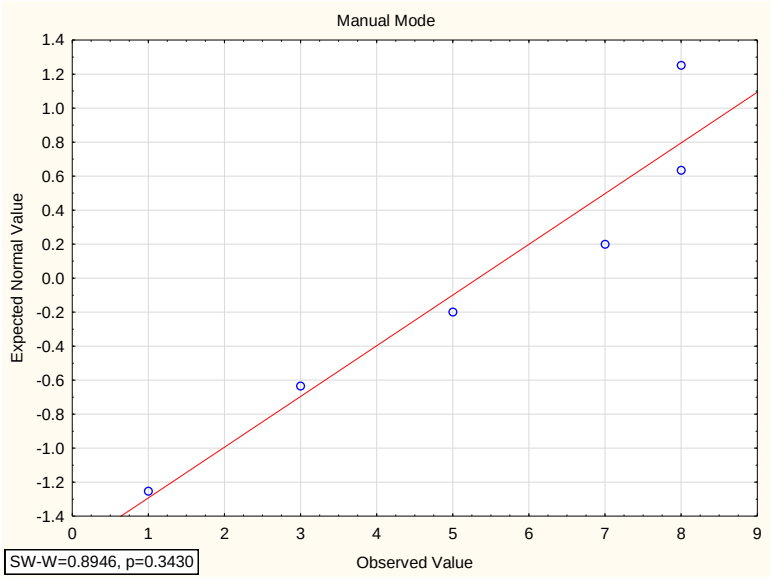

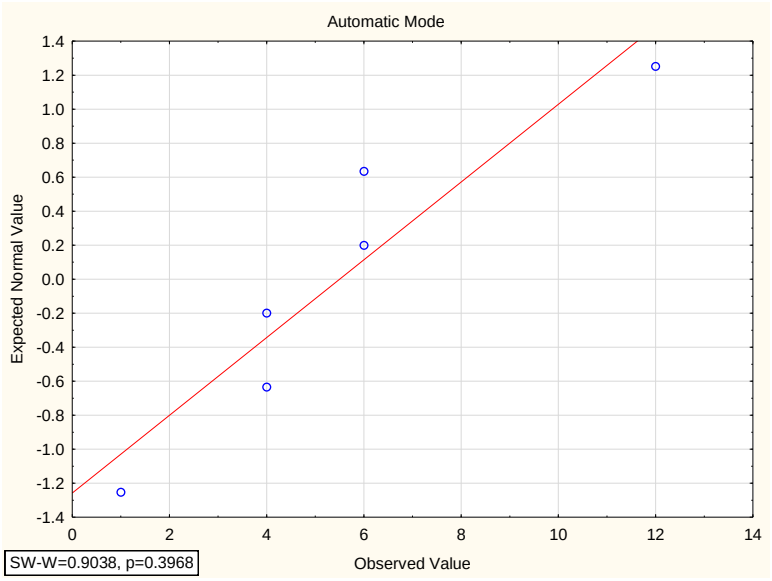

Appendix B13: normal probability plots with Shapiro-Wilk Test Results of the overshoot episodes per 1-hr (Subject I)

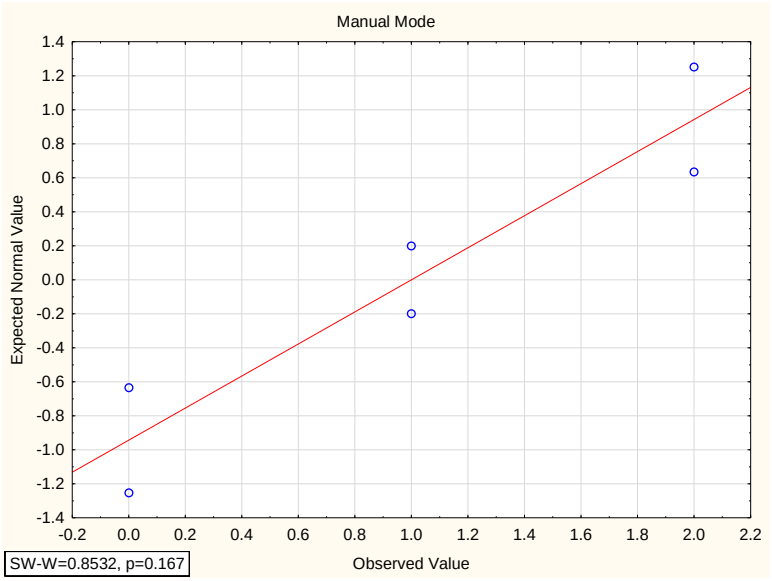

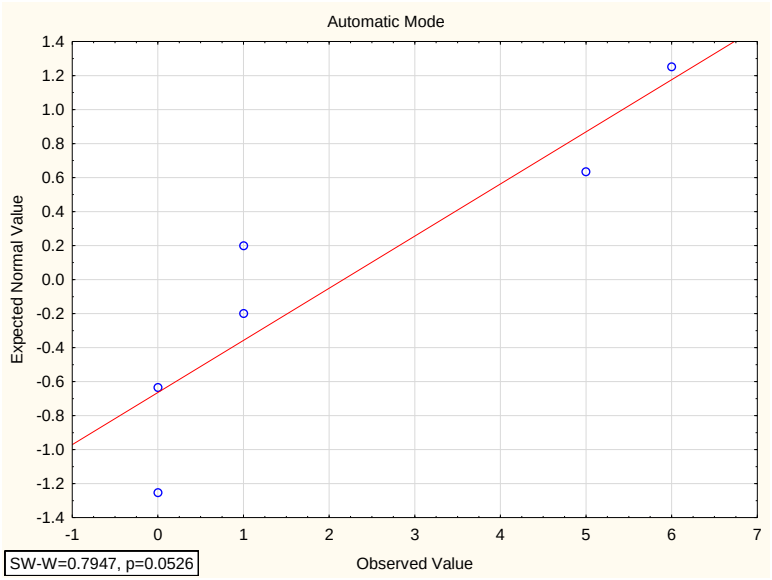

Appendix B14: normal probability plots with Shapiro-Wilk Test Results of the hypoxemic episodes (duration < 60 s) per 1-hr (Subject II)

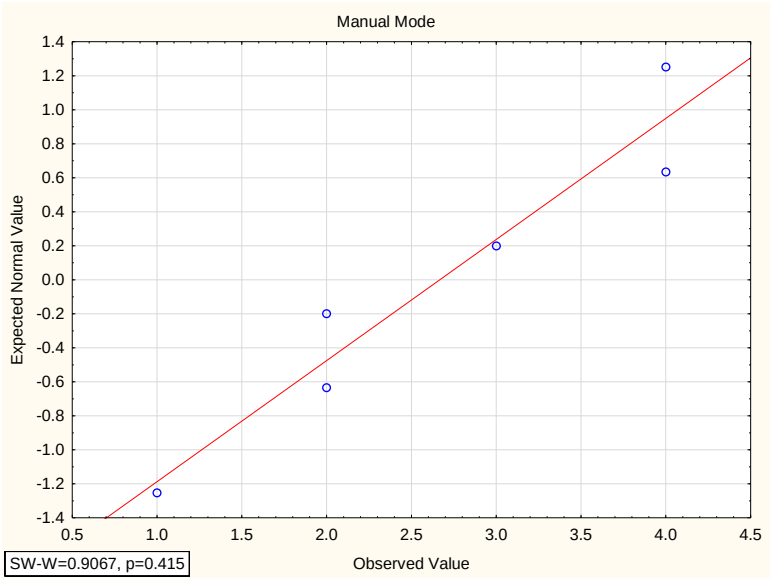

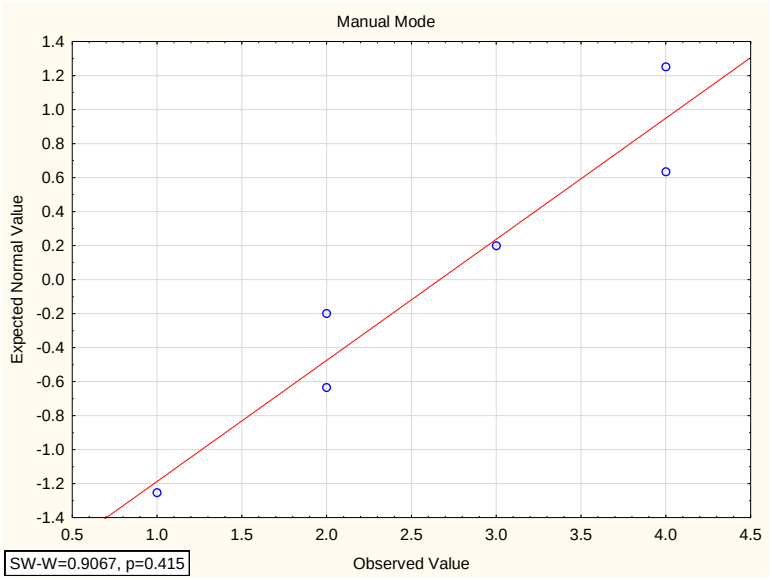

Appendix B15: normal probability plots with Shapiro-Wilk Test Results of the hypoxemic episodes (duration ≥ 60 s) per 1-hr (Subject II)

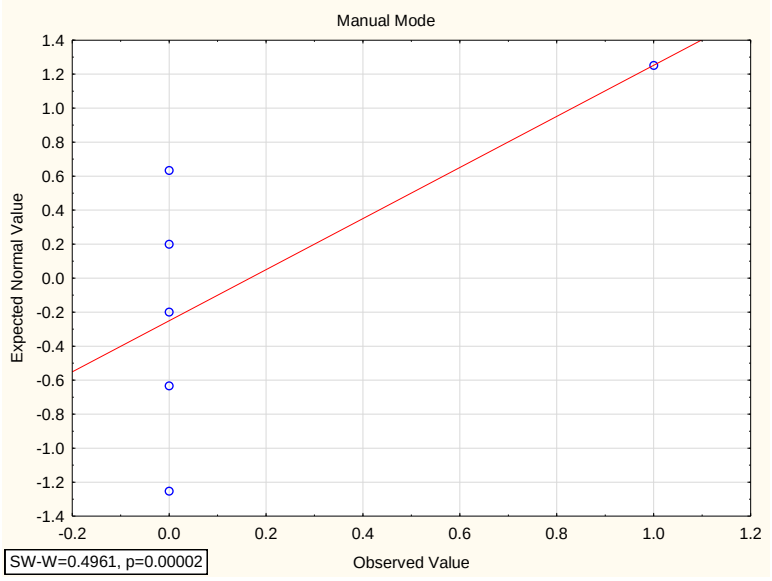

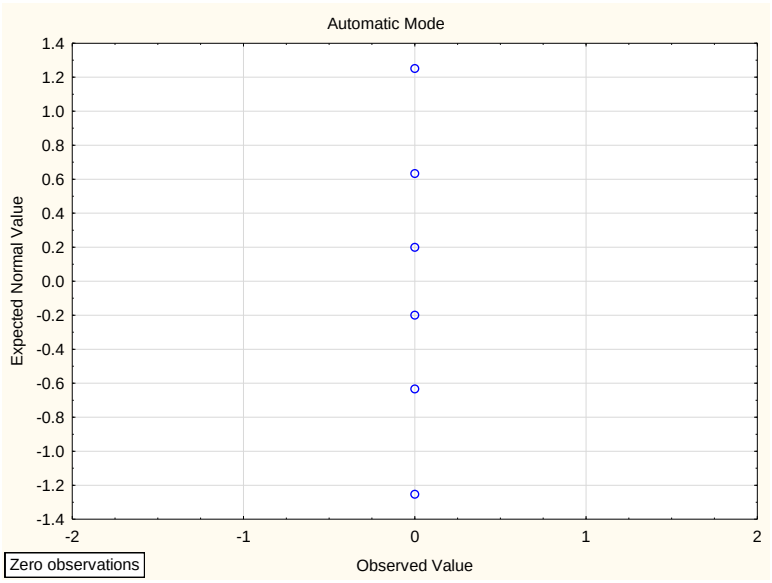

Appendix B16: normal probability plots with Shapiro-Wilk Test Results of the hyperoxaemic episodes (duration < 60 s) per 1-hr (Subject II)

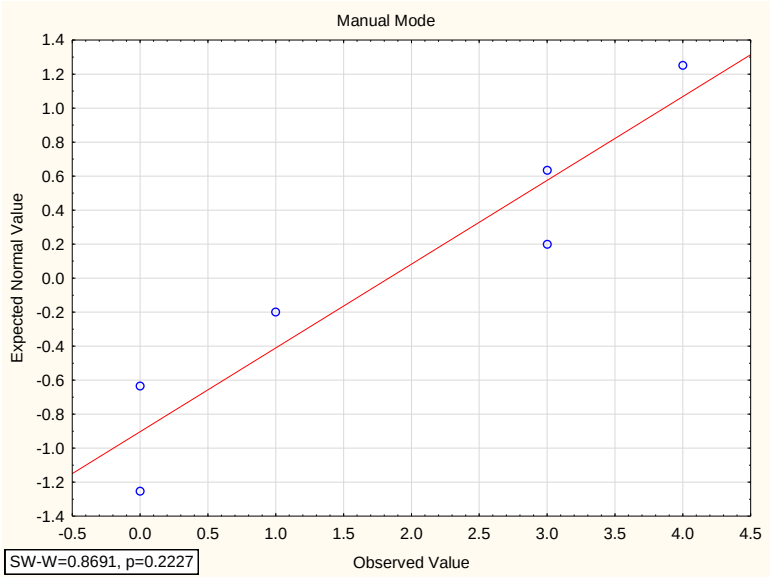

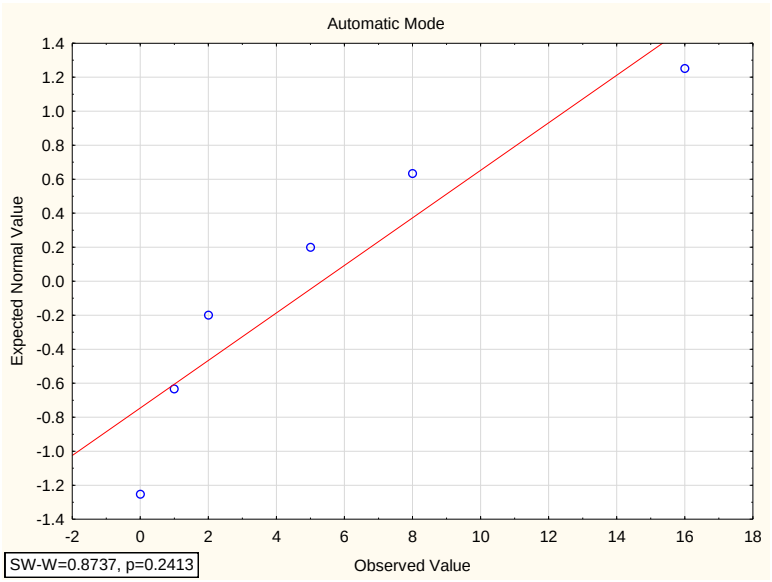

Appendix B17: normal probability plots with Shapiro-Wilk Test Results of the hyperoxaemic episodes (duration ≥ 60 s) per 1-hr (Subject II)

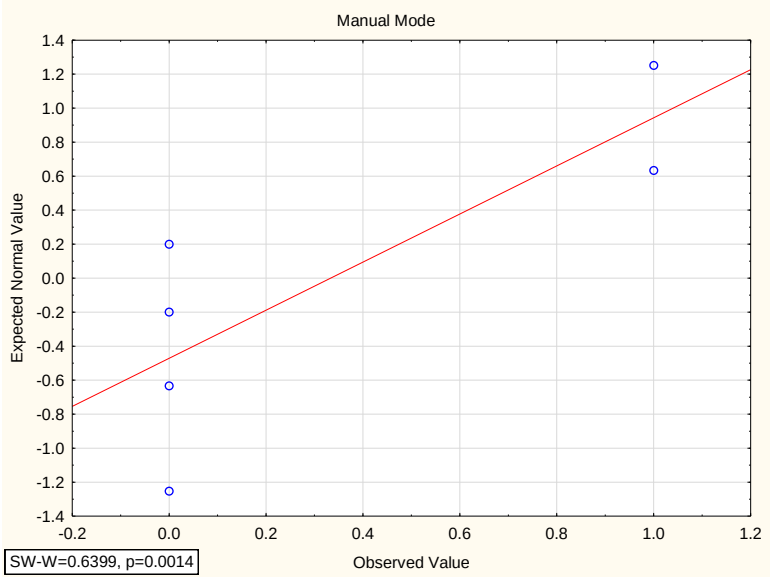

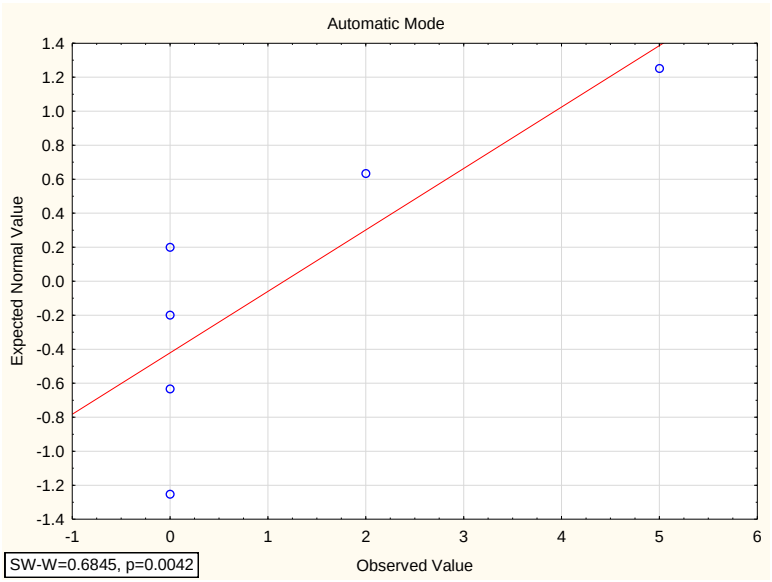

Appendix B18: normal probability plots with Shapiro-Wilk Test Results of the overshoot episodes per 1-hr (Subject II)

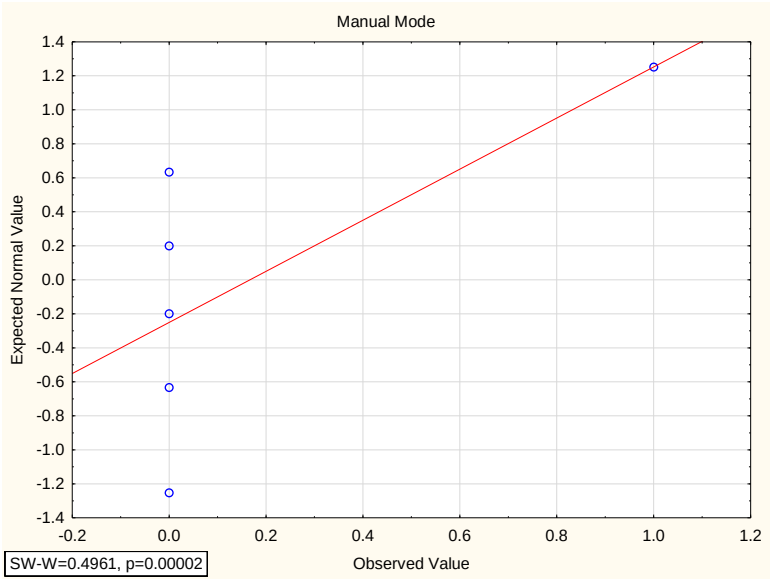

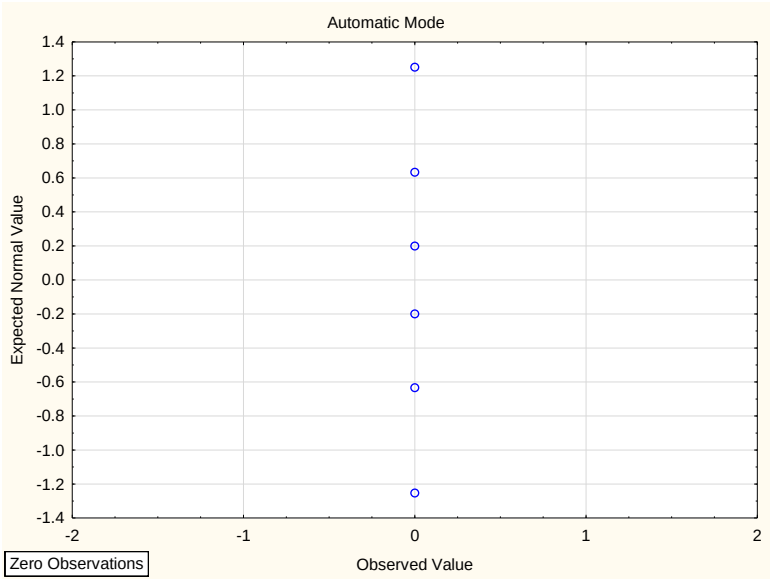

Appendix C: Chart of Required Sample Size (N) versus Power Goal (Subject I)

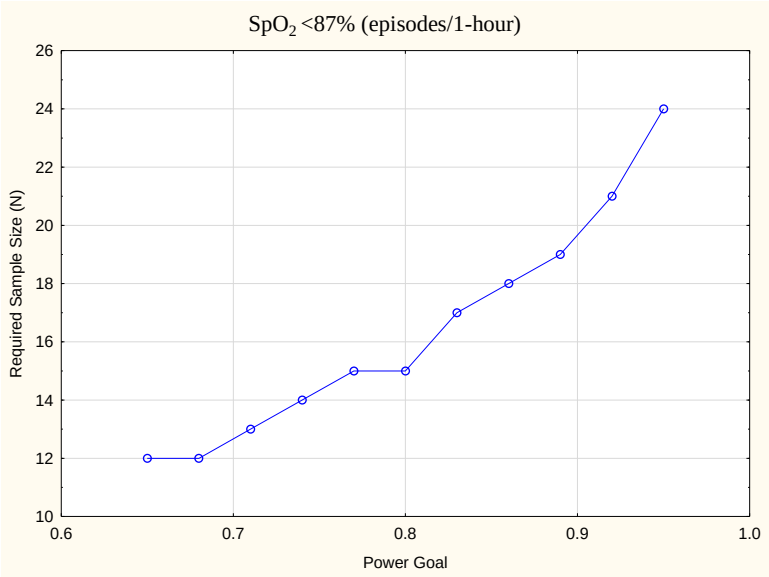

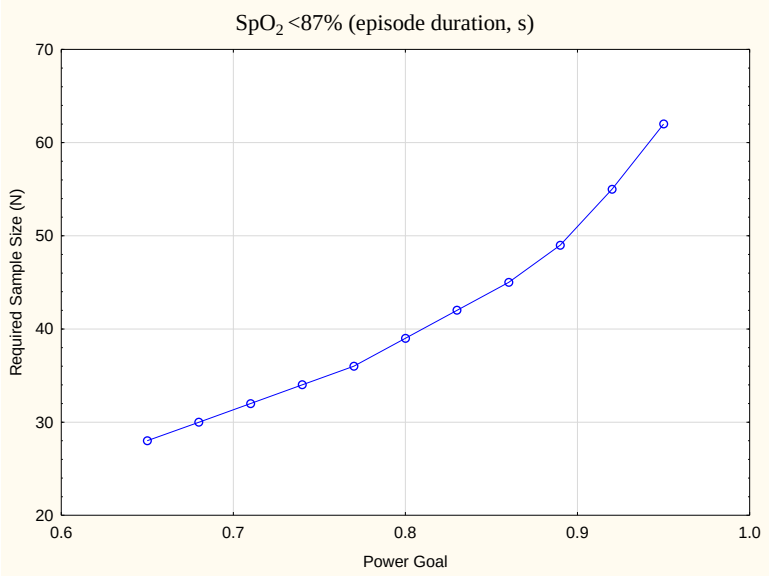

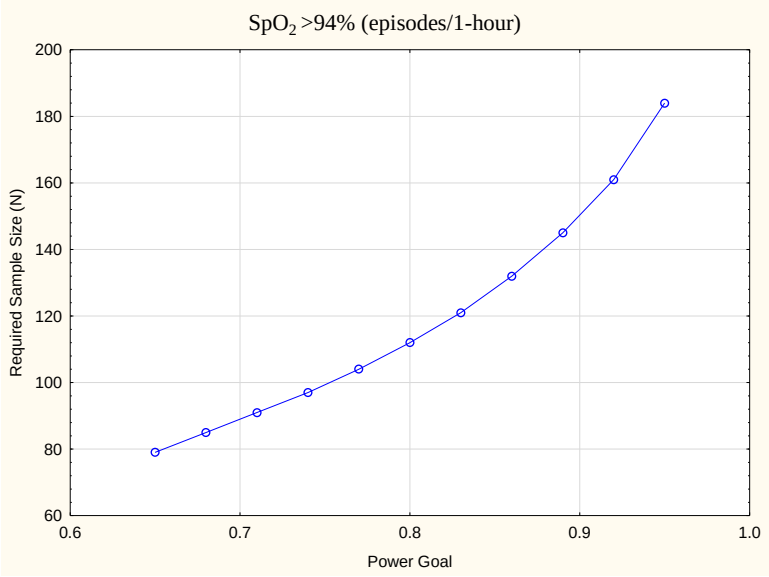
SpO2 >94% (episodes/1-hour)
Required Sample Size (N)
200
180
160
140
120
100
80
60
0.6
0.7
0.8
0.9
1.0
Power Goal

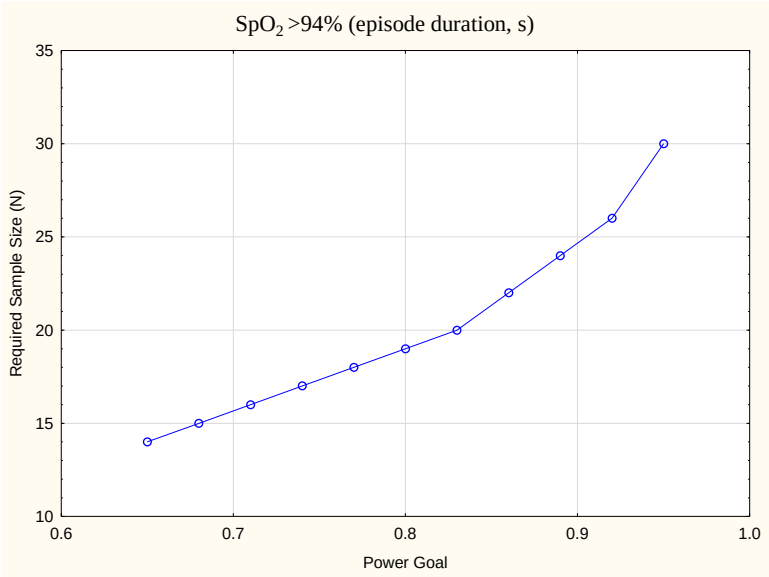
SpO2 >94% (episode duration, s)
Required Sample Size (N)
35
30
25
20
15
10
0.6
0.7
0.8
0.9
1.0
Power Goal

Appendix D: Chart of Required Sample Size (N) versus Power Goal (Subject II)

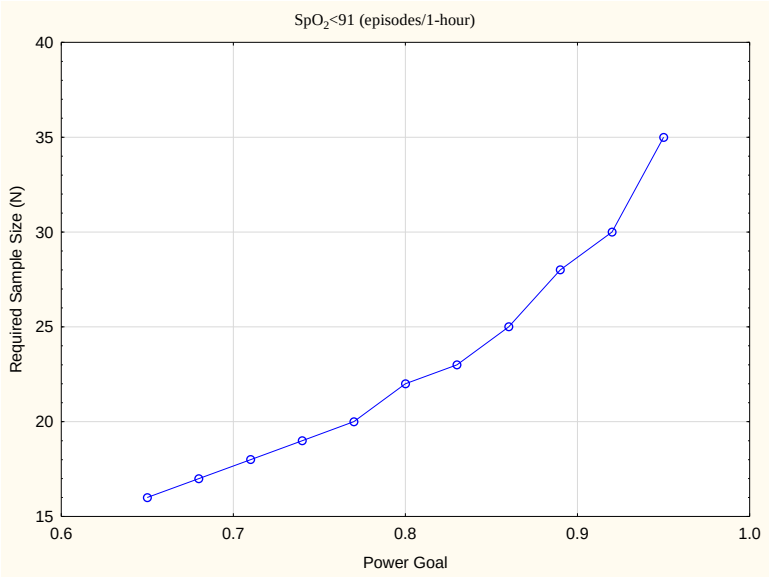

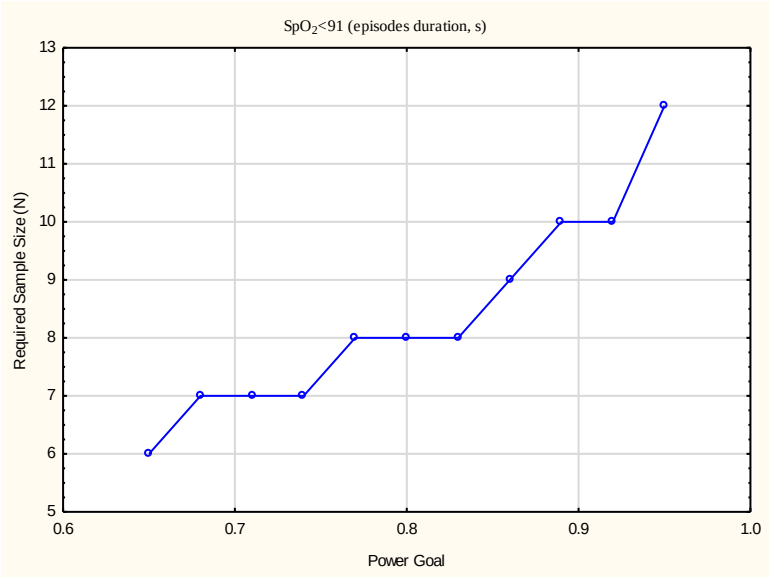

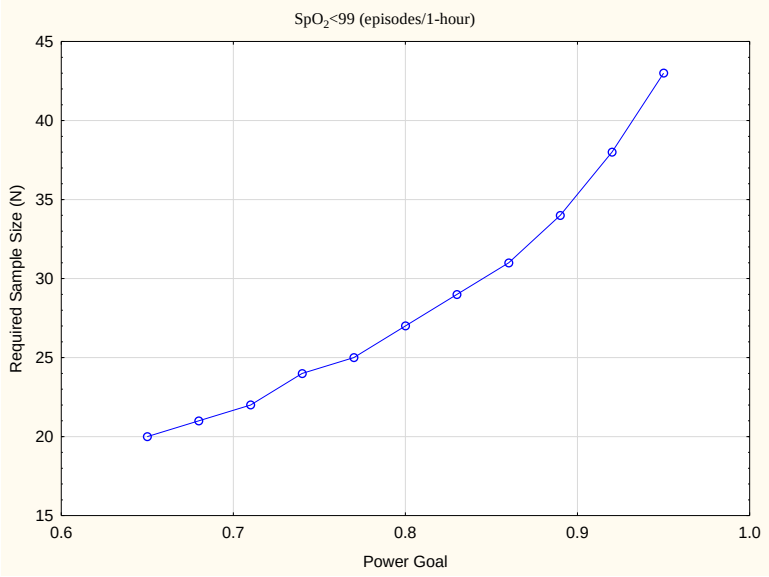
SpO2<99 (episodes/1-hour)
Required Sample Size (N)
45
40
35
30
25
20
15
0.6
0.7
0.8
0.9
1.0
Power Goal

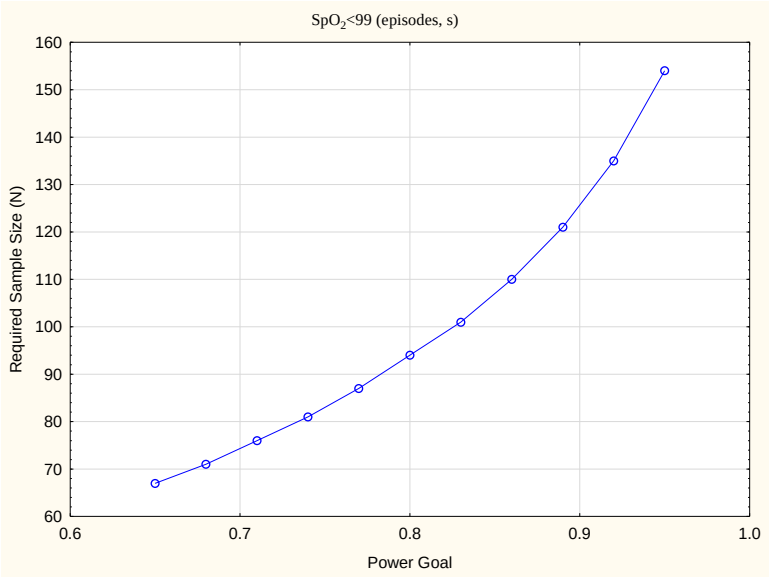
SpO2<99 (episodes, s)
Required Sample Size (N)
160
150
140
130
120
110
100
90
80
70
60
0.6
0.7
0.8
0.9
1.0
Power Goal

VITA

Akram Ahmad A. Faqeeh was born on September 30, 1985, in Makkah, Saudi Arabia. He accomplished his elementary, secondary, and high school in Makkah. He earned an Associate of Science degree in Mechanical Engineering Technology from Yanbu Industrial College, at Yanbu, Saudi Arabia in 2007. He obtained a Bachelor of Science degree in Mechanical Engineering Technology in 2010 from the same college. Immediately after he graduated on February 8, 2010, he worked as inspection & corrosion engineer in SABIC (Saudi Basic Industrial Corporation) in Al-Jubail, Saudi Arabia for five months. At the end of 2010, he started to work as iterant & students' Clubs supervisor in Yanbu Industrial College.

In June 2011, he got a scholarship from Yanbu Industrial College to continue his mechanical engineering studies in the United States. In August 2011, he arrived at Columbia, Missouri, where he enrolled in intensive English program in University of Missouri-Columbia. In the fall semester of 2012, he enrolled in Master's program in the Department of Mechanical and Aerospace Engineering of the same university. He started to work as teaching assistant in August 2013. He obtained his master degree in May 2014. The title of his master thesis is "Investigation of the effect of tool materials and process parameters on dry drilling of Ti-6Al-4V Alloy" [100]. He published a research paper that demonstrates part of the main works of his master thesis at SAE International Journal of Materials and Manufacturing [101]. Upon graduation (fall semester of 2014), he started his Ph.D. studies. He earned his Ph.D. degree in May 2018.